Studies on dihydrolipoamide dehydrogenase of *Leishmania donovani* and its biochemical functions

A Thesis
Submitted in Partial
Fulfillment of the Requirements for the Degree of

DOCTOR OF PHILOSOPHY

By

Adarsh Kumar Chiranjivi

Department of Biosciences and Bioengineering
Indian Institute of Technology Guwahati
Guwahati-781039, Assam, India

July 2019

Studies on dihydrolipoamide dehydrogenase of *Leishmania donovani* and its biochemical functions

A Thesis Submitted

By

Adarsh Kumar Chiranjivi
(Roll No. 146106019)

In Partial Fulfillment of the Requirements
Of the Degree of

Doctor of Philosophy

Department of Biosciences and Bioengineering
Indian Institute of Technology Guwahati
Guwahati-781039, Assam, India

July 2019

Dedicated to
My ever amazing parents, inspiring mentors
and curious researchers

INDIAN INSTITUTE OF TECHNOLOGY GUWAHATI

DEPARTMENT OF BIOSCIENCES AND BIOENGINEERING

STATEMENT

I hereby declare that the matter embodied in this thesis titled **"Studies on dihydrolipoamide dehydrogenase of *Leishmania donovani* and its biochemical functions"** is the result of investigations carried out by me in the Department of Biosciences and Bioengineering, Indian Institute of Technology Guwahati, Assam, India under the supervision of **Prof. Vikash Kumar Dubey and Dr. Pranjal Chandra**.

In keeping with the general practice of reporting scientific observations, due acknowledgements have been made wherever the work of other investigators are referred. Further the data in the thesis are collected by me. I certify that there is no fabrication or manipulation of data in the thesis.

Adarsh Kr. Chiranjivi

Date: July, 2019

Adarsh Kumar Chiranjivi
(146106019)

INDIAN INSTITUTE OF TECHNOLOGY GUWAHATI

DEPARTMENT OF BIOSCIENCES AND BIOENGINEERING

CERTIFICATE

It is certified that the work described in this thesis **"Studies on dihydrolipoamide dehydrogenase of *Leishmania donovani* and its biochemical function''** by **Mr. Adarsh Kumar Chiranjivi** (Roll No. 146106019), submitted to Indian Institute of Technology Guwahati, India for the award of degree of Doctor of Philosophy, is an authentic record of results obtained from the research work carried out under my supervision at the Department of Biosciences and Bioengineering, Indian Institute of Technology Guwahati, India and this work has not been submitted elsewhere for a degree.

Prof. Vikash Kumar Dubey
(Thesis Supervisor)

Dr. Pranjal Chandra
(Co-supervisor)

Acknowledgement

I feel delighted to present the dissertation on "Studies on dihydrolipoamide dehydrogenase of Leishmania donovani and its biochemical functions". This thesis would not have seen the light of day without the constant support of my thesis advisor Prof. Vikash Kumar Dubey and Dr. Pranjal Chandra. His constant motivation and supervision has led me to travel the treacherous path of research and to reach this version of work. Calling him just a thesis advisor would not do justice to the role he has played during my PhD. He was more like a guardian too me whose caring nature has made this journey a special one during my fruitful years spent at this prestigious institute. His disciplined nature, sincerity, hard work and an ambition of academic excellence has steered me to reach where I am today. He's been an overall inspiration to me in my all academic pursuits.

I would also like to extend my heartfelt thanks to my Doctoral committee members. Prof. Kannan Pakshirajan (Chairman, Doctoral committee), Prof. Tharmalingam Punniyamurthy and Dr. Shankar Prasad Kanaujia. Their constant support and constructive criticism that has helped me to progress in my research work. They have always motivated me to prove my mettle.

I would also thank present Head of Department Prof. Latha Rangan and past HoD's Prof. Kannan Pakshirajan, under whose able administration I was able to carry out my research work in a collegial environment. Central Instrumentation Facility of IIT Guwahati is also acknowledged.

Also big heartfelt thanks goes to the current lab members Kamalesh and Gundappa. Also past lab members Dr. Mousumi Das, Dr. Shalini Singh, Dr. Ruchika Bhardwaj, Dr. Ritesh Kumar, Dr. Jay Prakash, Dr. Sunita Yadav, Dr. Suresh Kumar, Ekta, Sona, Prachi, Pratyajit, Sudipta, and Bijoy. The lab has always been a fun filled experience; every one of them has made my stay in the campus a memorable one, it was another home away from home. Each and every part of this thesis bears the constant and endless efforts of all lab members, their intense discussions, and constructive criticisms have helped me to stretch my capabilities. The late lab night outs, tea at bani mandir, snacks at faculty gate and endless gossips has what made this a cherishable journey.

Also mentionable are my friends Amit Rohilan, Balwant Singh and Anil Bidkar for making me believe in me. The serene and charming campus of IIT Guwahati has provided a perfect environment to think and innovate.

And last but not the least my parents. I always feel short of words to describe what they mean to me. They are my guiding light. Their illuminated presence has always motivated to do something special. Many thanks to them for their unwavering support in me. For instilling a fighters spirit in me. For being with my side in all times.

Whatever good have been done and whatever good is too be done from my side will always be a reflection of my parents and peers. As always this work is also not free from errors. I hope peers will forgive me for this. This is what I was able to do with my limited capacities. Finally I seek blessings from my parents and peers and dedicate this work to them.

Adarsh Kumar Chiranjivi
July, 2019

ABBREVIATIONS

DLDH	:	Dihydrolipoamide dehydrogenase
WHO	:	World Health Organization
NTD	:	Neglected tropical disease
CL	:	Cutaneous leishmaniasis
MCL	:	Mucocutaneous leishmaniasis
VL	:	Visceral leishmaniasis
PKDL	:	Post Kala-azar dermal leishmaniasis
AIDS	:	Acquired Immune Deficiency Syndrome
HIV	:	Human immunodeficiency virus
FNAC	:	Fine needle aspiration cytology
FCS	:	Fetal calf serum
CCIEP	:	Counter current immunoelectrophoresis
IHA	:	Indirect haemagglutination
HRP	:	Horseradish peroxidase
DAT	:	Direct agglutination test
FAST	:	Fast agglutination screening test
ELISA	:	Enzyme linked immunosorbent assay
LST	:	Leishmanin skin test
PCR	:	Polymerase chain reaction
TDR1	:	Thiol-dependent reductase
ROS	:	Reactive oxygen species
SAG	:	Sodium antimony gluconate
PI	:	Phosphatidyl Inositol
DHFR-TS	:	Dihydrofolate reductase-thymidylate synthetase
LPS	:	Lipopolysaccharides
PDH	:	Pyruvate dehydrogenase complex
α-KGDH	:	α-ketoglutarate dehydrogenase complex
GCC	:	Glycine cleavage complex
TCA	:	Tricarboxylic acid cyle
ThDP	:	Thiamine diphosphate
PDK	:	Pyruvate dehydrogenase kinase
PDP	:	Pyruvate dehydrogenase phosphatase
PSBD	:	Peripheral subunit-binding domain
E3BP	:	E3- Binding protein
DLD	:	Dihydrolipoamide
LA	:	Lipoamide
TPP	:	Thiamine pyrophosphate
HNE	:	4-hydroxy-2-nonenal
SHMT	:	Serine hydroxymethyltransferase
SIDER	:	Short interspersed degenerate retroelement
UTR	:	Untranslated region
*Ld*DLDH	:	*Leishmania donovani* dihydrolipoamide dehydrogenase
Ni-NTA	:	Nickel-nitrilotriacetic acid
DCPIP	:	2, 6-dichlorophenolindophenol
MTT	:	Thiazolyl blue tetrazolium bromide
FAD	:	Flavin adenine diphosphate
FMN	:	Flavin mononucleotide
BCAAT	:	Branched chain 2-oxo acid dehydrogenase
NBT	:	Nitro blue tetrazolium
FBS	:	Fetal bovine serum

EDTA	:	Ethylenediaminetetraacetic acid
LB	:	Luria-Bertani
IPTG	:	Isopropyl β-D-1-thiogalactopyranoside
HPLC	:	High-performance liquid chromatography
BLAST	:	Basic Local Alignment Search Tool
SDS-PAGE	:	sodium dodecyl sulfate polyacrylamide gel electrophoresis
*Ld*DLDH_Variant1	:	LdBPK291950.1
*Ld*DLDH_Variant1	:	LdBPK323510.1
GR	:	Glutathione reductase
TR	:	Trypanothione reductase
TdR	:	Thioredoxin reductase
DTT	:	Dithiothreitol
SDM	:	Site directed mutagenesis
LADH	:	Lipoamide dehydrogenase
PDB	:	Protein data bank

LIST OF FIGURES

LIST OF TABLES

CONTENTS

CHAPTER I

Leishmaniasis: An introduction about its types, therapeutics, Current and future prospective*

1.1 ABSTRACT*

Leishmaniasis is a parasitic disease, caused by 20 species of human pathogenic parasite belonging to genus *Leishmania*. Many species of the insect vector, 30 out of 500 known Phlebotomine sand-fly (2-3mm size) transmits disease leishmaniasis. The vector phlebotomine sand-fly is found throughout the inter-tropical and temperate regions of the world. The disease is recognized as a most neglected disease by WHO which affects mainly the people belonging to below poverty line. This is the main cause that this disease is mainly ignored by the media, government and pharmaceutical companies. The disease leishmaniasis is having usually three types of clinical forms based on causative agents and clinical manifestations such as cutaneous, mucocutaneous and visceral leishmaniasis. Out of these three clinical manifestations the visceral form is most lethal. Visceral leishmaniasis commonly known as kala-azar affects Indian people and Bihar is the state where 90% of the cases were found. The current drug perspective is not good due to high toxicity, high price, low efficacy, and the most important key factor is the increasing drug resistance. The only most effective drug is miltefosine till now whose mode of administration is not painful (oral) but developing drug resistance is the main issue. Hence, the search of new and efficient drug with their effective target whose mode of administration is not painful is the continuing area of research. Drug discovery needs optimum drug target and unique drug candidate.

**** Part of the literature review is submitted for publication***

1.2. INTRODUCTION

Many communicable diseases prevalent in tropical and subtropical areas are characterized by WHO (https://www.who.in) as neglected tropical disease (NTD). Leishmaniasis is one of the identified most neglected disease by WHO after malaria.

1.2.1 History of leishmaniasis

The existence of first fossils of *Leishmania*-like parasite in pre-historical time was found in extinct blood filled female sand-fly *Palaeomyia burmitis*. The sand-fly was isolated about 100 million years ago from old Cretaceous Burmese amber (Steverding 2017). Evidence of *Leishmania*-like species were also found from fossils of genus *Paleoleishmania*. Presence of promastigote, paramastigotes, and amastigotes indicate that sand-fly takes the parasite from vertebrate during a blood meal. A blood sample taken from fossils subsequently was identified as of reptiles (Poinar and Poinar 2004). The other evidence of *Leishmania*-like fossils was shown as *Paleoleishmania neotropicum* in the extinct sand-fly *Lutzomyia adiketis*. Fossils of sand-fly *Lutzomyia adiketis* was taken from 20-30 million year old Dominican amber (Steverding 2017). In the mid-Oligocene to early-Miocene era, Neotropical sandflies were the vector of *Leishmania*-like parasite. In 1756, Alexander Russell a Scottish physician published details of dry and wet oriental sore. He described the oriental sore into wet zoonotic cutaneous leishmaniasis (CL) and dry anthroponotic CL caused by *Leishmania major* and *Leishmania tropica*. He also explained the development of lesions and their self-healing activity within 8 months to 1 year. The first evidence of mucocutaneous leishmaniasis (MCL) was given by Pedro Pizarro in 1571 (Lainson 2010). The earliest evidence in context to visceral leishmaniasis (VL) was given by military surgeon William Twining. He published an article in 1827 and mentioned about the patient in Bengal, India who suffered from VL, showed symptoms like the enlarged spleen, intermittent fever and acute anemia (Twining 1827). They also discussed about the detailed symptom of kala-azar such as dry and scaly up of the skin in an article published in 1892. In 1824/25 first outbreak of kala-azar was recorded in the village Mahomedpore in lower Bengal, India (Gibson 1983). In 1860s disease spread westwards and reached to Burdwan in Bengal. Now disease becomes endemic and spread to the north of Bengal to Assam in subsequent years. The word kala-azar was coined in the late 19th century means “black disease”. Name given as kala-azar due to greyish discoloration of the skin in the patient during the infection. In 1885 David Douglas

Cunningham a Scottish doctor saw parasite but did not able to recognize as *Leishmania* (Cunningham 1885). Subsequently, Peter Borovsky (1863-1932) a Russian army doctor first observed that parasite present in lesions were protozoans (Hoare 1938). A Scottish pathologist William Boog Leishman (**Figure 1.1A**) in November 1900 observed ovoid bodies in smear taken from the spleen of a soldier who died from splenomegaly at Dum Dum, a station near Calcutta (Leishman 1903). After few weeks a professor of Physiology at Madras Medical College namely Charles Donovan (Iris doctor) (**Figure 1.2B**) published a paper reporting the presence of similar bodies in the splenic sample of Indians suffering from enlarged spleen and remittent fever (Donovan 1903). In 1903 Ronald Ross a British doctor (**Figure 1.2C**) published an article commented that ovoid bodies in spleen pulp represent by Leisman and Donovan has not degenerated trypanosomes but a new protozoan parasite whose clinical symptom similar to kala-azar and named protozoan parasite as *Leishmania donovani*. The Cathoire and Laveran identified similar parasite in children suffering from infantile splenic anemia and named *Leishmania infantum* by Nicolle. The U.N Brahmachari in 1922 described post kala-azar dermal leishmaniasis (PKDL) and told it is dermatologic manifestation usually develops after few months of cure of visceral leishmaniasis (VL) (Mondal et al., 2010).

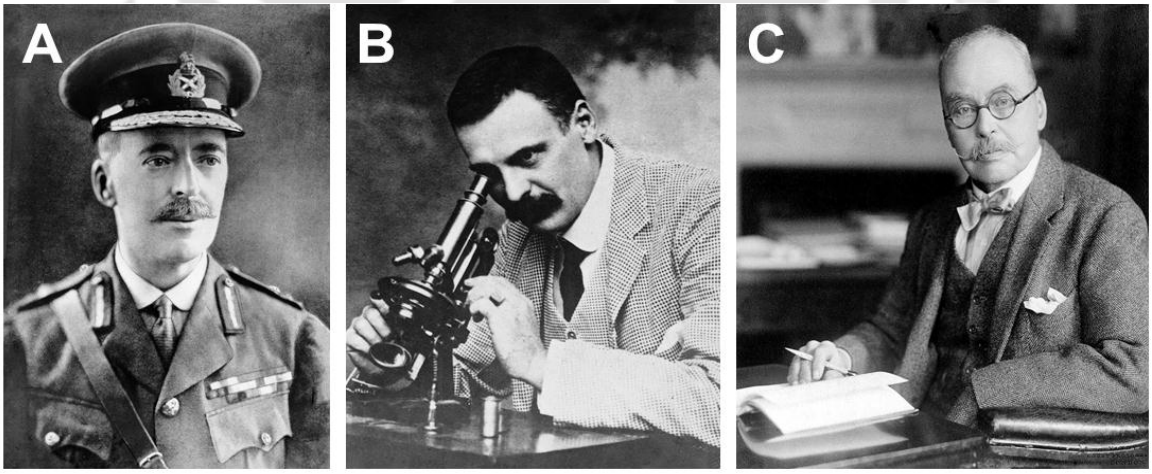

Figure 1.1: Fore fathers of leishmaniasis. SirWilliam Boog Leishman (A), Charles Donovan (B) and Ronald Ross (C), are the godfather of *Leishmania* discovery. Leishman and Donovan first observed the parasite in splenic sample. Credit to give name *Leishmaniadonovani* by Ronal Ross in honor to Leishman and Donovan. **[*Source of Images*:** Figure A and B fromSteverding 2017, C from Wikipedia**]**

1.2.2 Leishmania: Structure and morphological form

The *Leishmania* have two developmental forms based on their host and their morphological structure. The promastigote form resides in sand-fly host (Leptomonad form). It is long, slender and spindle in shape (15-20 µm length and 1-2 µm diameter) (**Figure 1.2A**). A fully developed promastigote resides in the mid gut of sand-fly and originated from amastigote transformation. A single nucleus lies at the central region and kinetoplast present at the anterior end. Front of kinetoplast is surrounded by eosinophilic vacuoles upon which flagellum root runs. A long flagella originates from the basal body which is similar in length as a parasite.

Other forms of *Leishmania*, amastigote present in the reticuloendothelial system of the mammalian host. This form is non-flagellated, intracellular and oval in shape (2-5 µm in length and 1-2.5 µm breadth). The amastigote form of parasite contains a central nucleus (< 1 µm diameter) and kinetoplast at the right angle of the nucleus. The kinetoplast is a special type of cell organelle contains DNA and mitochondria (**Figure 1.2B**). Due to their presence *Leishmania* belongs to Kinetoplastidae family. A delicate filamentous structure originated from the margin of the amastigote body called axoneme. The structure axoneme, a root of the flagella is surrounded by the vacuoles.

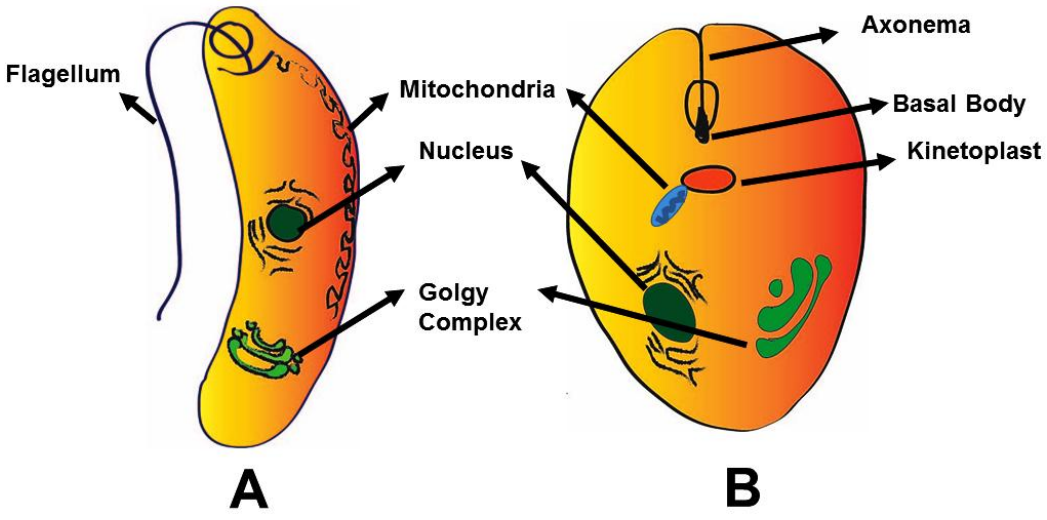

Figure 1.2: Two morphological form of *Leishmania* based on morphology and host specificity. (A) Promastigote form, spindle and slender shape resides in midgut of sand-fly. It has flagella at the exterior end for locomotion. (B) Amastigote, ovoid aflagellated form present in reticulo-endothelial system of mammalian host.

1.2.3 Vectors and their host

The vectors of leishmaniasis belong to Order: Diptera; Family: Psychodidae; and Phylum: Arthropoda (Maroli et al., 2013). The disease is transmitted by the bite of female sand-fly infected with the parasite. *Phlebotomus* (**Figure 1.3A**) spread the disease in the Old World and *Lutzomyia* (**Figure 1.3B**) in the New World (central and South America). Otherwise, both the sand-fly resembles each other in their morphology and the way of disease transmission. Sometimes name sand-fly is very confusing as this name used for other species as well. The genus *Phlebotomus* of sand-fly is also a carrier of other diseases like Carrion's disease (oroyo fever) in South America caused by bacteria *Bartonella bacilliformis*. In Asia and North Africa, it is the vector for viral agent Pappataci (arbovirus) that spread Pappataci fever as well as leishmaniasis (*Leishmania* spp.). Out of 600 species of sand-fly only 10% are known for the disease transmission. Infauna of India subzone has a total of 46 species of sand-fly in which 11 of them are *Phlebotomus* and rest are *Sergentomyia* species. The *Phlebotomus argentipes* is the well-known vector for kala-azar in the Indian subcontinent. Some animals such as dogs, rodents, pigs, sloths, bat, fox, etc. are the animal reservoir of the parasite.

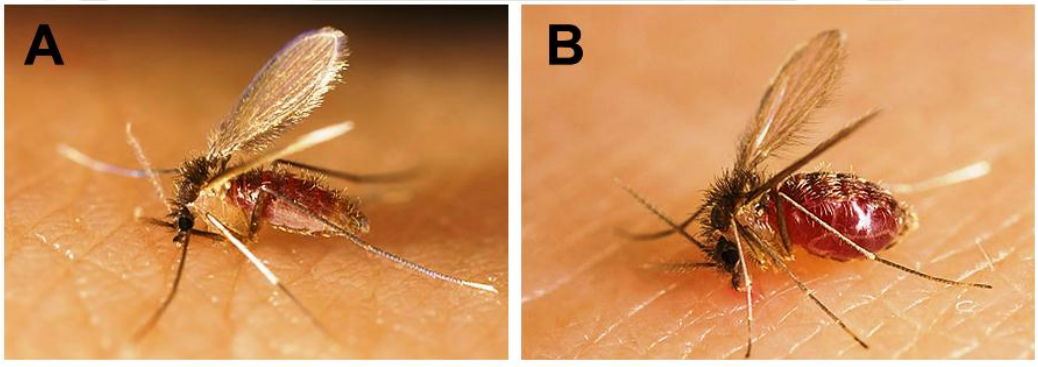

Figure 1.3: New and old world sand-fly a vector of leishmaniasis. (A) *Phlebotomus argentipes* (B) *Lutzomyia longipalpis* are the two sand-fly that transmits disease leishmaniasis in the old world (Middle East Asia and Africa) and new world (Central and South America). *Phlebotomus argentipes* the well-known vector for kala-azar.

[**Source:**http://www.raywilsonbirdphotography.co.uk/Galleries/Invertebrates/vectors/sand_fly.html]

1.2.4 Types of Leishmaniasis

Leishmaniasis has a wide range of clinical manifestation from less severe cutaneous form to most lethal visceral and most disfigured muco-cutaneous form. It is broadly classified into three types of clinical form based on symptoms and causative agent.

1.2.4.1 Cutaneous Leishmaniasis (CL): This form is usually known as oriental sore. The causative agents of CL are *L.tropica, L.major, L.mexicana, L.infantum*in the old world countries and *L.chagasi, L.naiffi, L.amazonensis, L.mexicana, L.guyanensis, L.braziliensis* in the new world. Most of the old world *Leishmania* cause self-healing lesions whereas new world parasite causes a syndrome called American tegumentaryleishmaniasis comprising CL with some other clinical manifestations like MCL (Martins et al., 2014). Normally lesion develops on the exposed portion of the body such as arms, legs, and face (**Figure 1.4A**). The number of lesions can be varied from person to person. Infection is mild and lesion healed spontaneously after treatment.

1.2.4.2. Muco-cutaneous Leishmaniasis (MCL): TheMCL develops when CL lesions expand to the mucosal region (nose, mouth, throat cavities) through metastasis. It doesn't develop after month or year of cure of CL whereas it is a gradual development of lesions. The initial symptom of MCL is similar to CL but produce severe deformity (**Figure 1.4B**). Respiratory tract mucosal region is also affected during MCL cause numerous respiratory issue. *L.braziliensis* is the main causative agents that spread MCL. Approximately 90% of the MCL cases were observed in Brazil, Bolivia, and Peru (Palumbo 2010).

1.2.4.3. Visceral Leishmaniasis (VL): The *Leishmania infantum* and *Leishmania donovani* are the main causative agent of most lethal form VL. Kala-azar is the other name of VL in the Indian subcontinent. In patient VL develop symptoms includes splenomegaly, anemia, irregular fevers, pancytopenia, weakness and weight loss (**Figure 1.4C**). Mostly person suffering from this disease dies within a month if untreated (fatality rate is 100% within 2 years without treatment). The disease VL found usually in remote, poor and politically unstable areas where the patient have limited source and access to medications (Sundar and Rai 2002).

1.2.4.4. Post-Kala-azar Dermal Leishmaniasis (PKDL): PKDL is the complex or advanced form of VL, showed symptoms like nodular, macular and maculopapular rashes in the patient (**Figure1.4D**). It is usually developed after 0-6 month or 2-3 years treatment of VL. Usually rash starts developing around the mouth and spread to other parts also. Hence this is mostly restricted to the parasite *L.donovani*. PKDL usually heals spontaneously in Sudan but not in an Indian patient. Therefore this stage is known as the reservoir of the parasite. The patient suffers from PKDL shows a high level of

immunosuppressive cytokines (IL-10) and low IFNγ in the peripheral blood (Zijlstra et al., 2003).

1.2.5 Life cycle of *Leishmania* parasite

The Life cycle of *Leishmania* complete in two stage means parasite having a digenetic life cycle. It has two hosts one is human and other is sand-fly. When sand-fly takes a blood as meal from the infected human individual, amastigote forms reached to the sand-fly midgut through the proboscis. Only female sand-fly takes a blood meal and spread the disease. Afterward, amastigote form divides into procyclic and from procyclic to more infective metacyclic form. Conversion of amastigote to infective promastigote form occurs in a particular cyclic form. In the first stage, the division of amastigote occurs in the midgut in the environment of blood meal results nectomonad promastigotes are formed. The nectomonad stage responsible for anterio migration of parasite in the midgut. Further, this stage is transformed into a leptomonad stage which triggers the second developmental stage. Subsequently, Leptomonad stage is, in turn, transform into non dividing metacyclic promastigote. This whole process takes 24-48 h in the sand-fly (Ortigao et al, 2010). Afterward, when infected sand-fly again takes a blood meal will inject metacyclic form into the skin, where macrophage takes the promastigote stage through phagocytosis and surrounds into phagolysosomes. Within 12-24 hours of ingestion by the skin macrophages, the promastigote transforms into amastigote form. Subsequently, amastigote starts multiplying and after certain population macrophage become burst. Released amastigote again infects other macrophages. This stage of the parasite is chronic in nature and may present month or year without any symptoms and sign, depending on the host immune susceptibility. As in case of CL, infected macrophage may be localized in the host skin results lesion formation or may transport to the other organ in VL or to the mucosal region in MCL. A further transmission of disease from an infected host to an uninfected individual occurs through sand-fly. In CL, sand-fly takes a parasite easily by biting to the infected host. The sand-fly penetrates 2-3 mm skin and sucks the oozed blood that having parasite. Whereas in VL, parasite mainly concentrated into visceral organ so some of the sand-fly

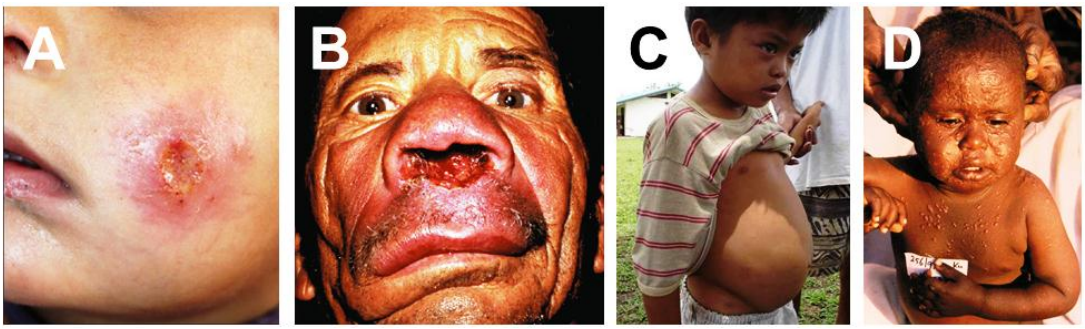

Figure 1.4: Four major types of leishmaniasis.(A) Cutaneous leishmaniasis isthecommon clinical form shows symptom like lesions on exposed portion of skin. (B) Muco-cutaneous leishmaniasis is the advanced form of CL affects mucus region of body. (C) Visceral leishmaniasis is the most sever and lethal form infects spleen, liver and bone marrow. (D) PKDL (Post Kala-azar Dermal Leishmaniasis) is mostly appears after month or years treatment of VL. It shows symptoms like nodular, macular and maculopapular rashes. [**Source of Images: Wikipedia**]

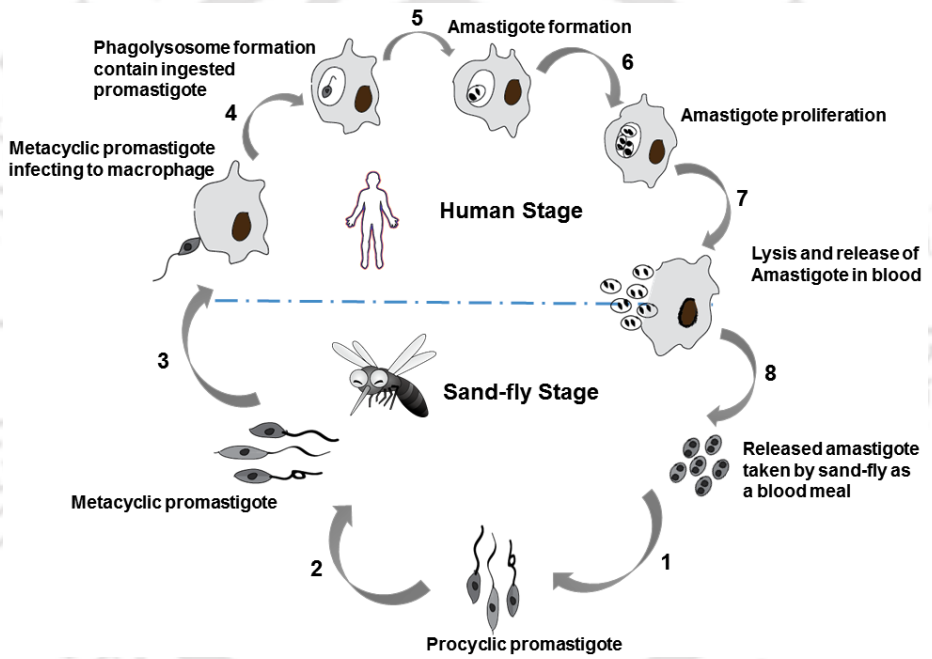

Figure 1.5: The digenetic lifecycle of *Leishmania* parasite. The life cycle is distributed into two hosts, sand-fly and human. Sand-fly and some animals are the reservoirs of this parasite. Amastigote stage present in human and promastigote in sand-fly. Conversion of promastigote to amastigote occurs in macrophage and amastigote to promastigote in the midgut of the sand-fly. In disease transmission, sand-fly takes a blood meal as an amastigote form (1). These forms reach the sand-fly midgut through the proboscis, where amastigote form converted into infectious procyclic promastigote and metacyclic promastigote from (flagellated stage) (2). When further sand-fly bites to an uninfected individual, it injects metacyclic promastigote in the skin where this stage is taken by skin-resident macrophage (3). Subsequently, these metacyclic form surrounded by phagolysosomes and convert into amastigote form (aflagellated stage) (4, 5). Finally, the amastigote form starts dividing which form many numbers of amastigotes (6, 7). When amastigote number reaches the threshold, macrophage becomes burst and release amastigote into the peripheral blood (8).

only took parasite depends on opportunity. The overall lifecycle of *Leishmania* parasite depicted in **figure 1.5**. Animals are also the reservoirs of the parasite includes canines and rodents. Transmission cycle occurs along with animal to animal, animal to man and man to man. In the Indian subcontinent, *Phleobotomus argentipes* proven to transfer the parasite form man-to-man (Kendrick 1990).

1.2.6 Geographical distribution of Leishmaniasis

Leishmaniasis is distributed worldwide across 88 tropical, subtropical and temperate countries with 350 million peoples are at risk of infection. Approximately, 12 million peoples are suffering from leishmaniasis along with 0.2-0.4 million of new cases of VL and 0.7-1.2 million for CL cases per year (Ivar et al., 2012). Normally, this disease mainly affects Asia, Africa, and Latin America due to malnutrition, poor residence condition, population migration, lack of resources and weak immune responses (Alvar et al., 2006). Specifically, maximum cases of VL (approximately 90%) occurs in Brazil, Bangladesh, India, Ethiopia, and Sudan. The CL cases are distributed across America, western Asian and The Mediterranean basin. Total 75% incidence of CL occurs in Algeria, Afghanistan, Brazil, Colombia, Ethiopia, Costa Rica, Peru, Iran, Syria, and North Sudan. The advanced form of cutaneous leishmaniasis, MCL (90% cases) prevalent in South America mostly in Paraguay, Brazil, Bolivia, Ecuador, Venezuela, and Colombia. As for the WHO report in 2017, 20,792 out of 22,145 new cases occurred around seven countries include Brazil, India, Ethiopia, Kenya, Somalia, South Sudan, and Sudan. In the South-East Asia Region, Kala-azar elimination programme went satisfactory and only 255 and 192 new cases in 2016 and 2017 from 9000 cases in 2006 was observed respectively (https://www.who.int/leishmaniasis/burden/en/). The detailed distribution of all the three clinical forms at the geographical scale represented in **figure 1.6** and **table 1.1.**VL has appeared as an opportunistic infection of HIV. Normally, VL co-infection was found in the endemic area of HIV infection. Most of the Southern European population infected with VL (70%) were developed HIV infection. *Leishmania* and HIV co-infection is prevalent in some countries like France, Portugal, Italy, and Spain observed during the last 30 years (Jarvis and Lockwood 2013). Generally, in certain countries such as India and Brazil, it was found that VL affecting HIV infected individual (Alvar et al., 2008).

Table 1.1: Geographical distribution of three different forms of leishmaniasis and prevalent causative agents.

Species	Region	Geographical Area	Clinical Form
Leishmania major	Old world	Africa, Asia, Middle East	CL
Leishmania tropica	Old world	Mediterranean basin	CL
Leishmania donovani	Old world	Africa, India, Arabian Peninsula	VL
Leishmania infantum	Old world	Mediterranean basin	VL
Leishmania aethiopia	Old world	Ethiopia and Kenya	CL/MCL
Leishmania Mexicana	New world	South America	CL
Leishmania amazonensis	New world	North, Central and South America	CL
Leishmania chagasi	New world	Central and South America	VL
Leishmania braziliensis	New world	South America	CL/MCL

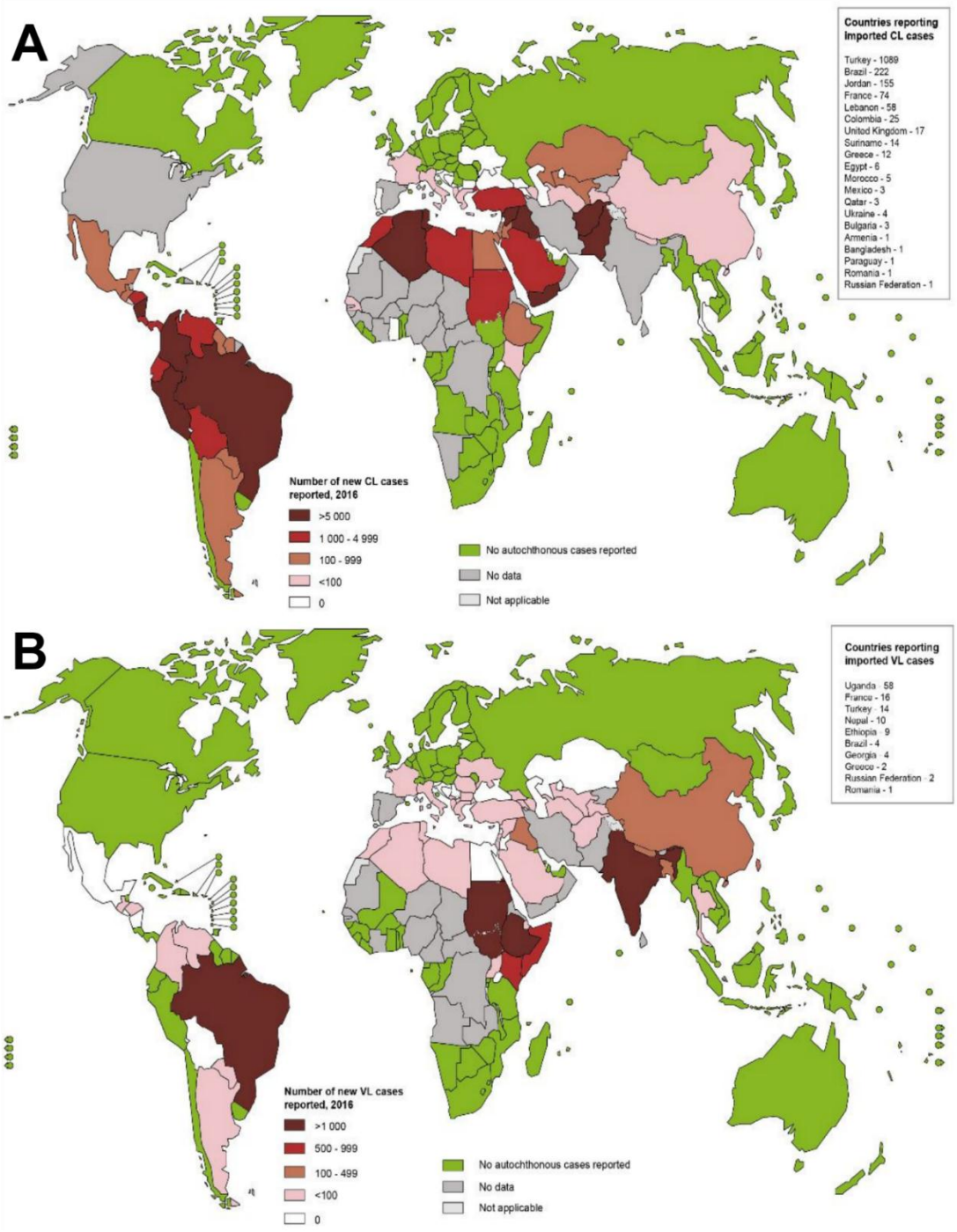

Figure 1.6: Geographical distribution of three major clinical forms of leishmaniasis. (A) Cutaneous (B) visceral leishmaniasis. The disease is endemic in a different part of the world like India, Africa, China, Southern Europe, America, and Russia. The total number of CL and VL cases reported in 2016 is shown in figure A and B. As for the current survey of the WHO, more than 5000 cases for CL/MCL and 1000 cases for VL has been reported.[**Source of Images**: https://www.who.int/leishmaniasis/burden/en**]**

1.2.7 Diagnosis of Leishmaniasis

1.2.7.1 Spleen aspirate and biopsy: In the case of VL, a splenic sample is best for diagnosis. Practitioner's take spleen aspirates through capsule by using a very fine needle (21-gauge, 0.8 mm). Before that, they confirmed the patient platelet counts (>40,000/ml) and optimum prothrombin concentration. Bleeding should not occur at the time of aspirate collection that may cause fatal hemorrhage. Some part of aspirate can be used for smear preparation to perform staining and microscopic observation and remaining should be cultured for further studies.

1.2.7.2 Liver biopsy: Parasite visualization in liver aspirates and biopsies can also be utilized for diagnosis. Normally a liver biopsy is less sensitive (40%) for diagnosis due to less availability of the parasite in the liver (Hag et al., 1994). However, during infection, if most of the parasite is localized in liver kuffer cells then sensitivity may be increased.Similar precaution should be taken as spleen aspirate collection like bleeding should not occur during aspirate suction.

1.2.7.3 Bone marrow aspiration: Bone marrow aspirates can be obtained from sternal iliac crest but it is painful. From bone marrow aspirates, direct staining sensitivity is 76-85% but with the cultured cell it is 85% (Singh and Sivakumar 200578).

1.2.7.4 Blood buffy coat: In very rare cases Practitioners demonstrate parasite in peripheral buffy coat. In a certain condition like during immunosuppressive therapy and in AIDS buffy coat can be utilized for parasite diagnosis but the efficiency is less up to 56% (Delgado et al., 1998).

1.2.7.5 Lymph node fine needle aspiration cytology (FNAC) and biopsy: Any lymph gland can be punctured and utilized for parasite confirmation. This technique can be utilized for both kala-azar and CL but sensitivity (for kala-azar 40-50% and 58.6% for CL) was found different for both of them as for study carried in Brazil (Romero et al., 1999).

1.2.7.6 Tegumentary leishmaniasis: The diagnosis of CL is performed by visualization of skin smear taken from the lesion area and culture of dermal cell or biopsy of skin section. To perform diagnosis 3-5 aspirates are taken from a different portion of skin. It is collected

by application of saline in the lesion portion. Different size of gauge needle has been used for ulcerative and facial lesion for aspirate collection (Mimori et al., 2002).

1.2.7.7 Culture examination: Thecells taken from different causative agents and characterize it at species or genotype level are the most suitable criteria to diagnose. The promastigote from the different causative sample can be cultured in a specific media such as solid NNN-media with 20-30% rabbit blood or liquid Schneider's insect media. In VL cases, most of the times promastigote grow in their liver and splenic aspirates. Other media like M199, Tobies media with FCS can also be used for promastigote culture (Singh et al., 2000). For MCL, the culture based investigation have less sensitivity due to an insufficient number of the parasite in the patient to perform culture (Singh et al., 2000; Weigle et al., 1987).

1.2.7.8 Isolation in experimental animals: It is the alternative method to isolate the parasite from an infected patient. In this technique, the parasite taken from infected individuals is injected through footpad in hamster and in susceptible mouse BALB/c. This technique increases the yield of the parasites. In most of the cases, it was found that to use of experimental animals is a better way of diagnosis compared to the microscopic method (Weigle et al., 1987; Shatry et al., 1988).

The sufferers of VL possess hyperimmunoglobulinaemia as the most specific criteria to diagnose. Similarly, in CL and MCL, low humoral immune response or B-cell response is the hallmark criteria to diagnose. Many serological tests are available for diagnosis of VL which are grouped as nonspecific and specific tests, on the basis of specificity and sensitivity. Nonspecific tests were used in the past but are rarely used in practice these days which include counter current immunoelectrophoresis (CCIEP), indirect haemagglutination (IHA), and immunodiffusion (ID). Non-specificity of the techniques most likely due to the cross-reactivity of antibodies with multiple antigens from other organism's (Schallig et al., 2001; Iqbal et al., 2002; Boelaert et al., 2004). Hence,a positive test by nonspecific methods doesn't confirm the disease as leishmaniasis (Boelaert et al., 2004).

1.2.7.9 Fluorescent antibody test: For the antigen detection in tissue section or smear, fluorescent antibody (direct fluorescent test) or HRP labeled antibody can be used. In case

of direct fluorescence detection, microscopic observation is required but no such observation is required for HRP conjugated antibody and slide can be stored for a very long period of time (Boelaert et al., 2004).

1.2.7.10 Direct agglutination test (DAT): In DAT, the sample can be either plasma and serum, that can be performed by serially diluted samples. The Coomb's reagent has been employed on the serum that contains antibody against human globulin. If agglutination will happen then test will be positive otherwise negative. Apart from advantages like specificity and sensitivity, it has a major disadvantage of the relatively high incubation period (18 h) (Abdallah et al., 2004). Another similar technique, a fast agglutination screening test (FAST) were discovered, which detects the *anti-Leishmania* antibody in the serum or blood sample in very less incubation time (3 hrs) with single dilution (Schoone et al., 2001).

1.2.7.11 Enzyme linked immunosorbent assay (ELISA): ELISA is one of the important techniques for the serological test of VL. It can be utilized for various antigens like fucose-mannose, synthetic peptides, soluble antigens and recombinant proteins (Palantnik-de-Sousa et al., 2001; Maalej et al., 2003). Type of antigen can influence the sensitivity and specificity of ELISA. Many ELISA test has been performed with range of different antigen such as hydrophilic protein (geneB protein, rGBP) (Jensen et al., 1999), gp63 (Singh et al., 2005), rK39 (Singh et al., 2002), rK26, rK9 and rKE16 (Bhatia et al., 1999) of *Leishmania* and it has own sensitivity and specificity during diagnosis. The antigen rK39 based ELISA have very high sensitivity and it produces very high titers of antibody in VL patient. Now antigen is commercially available in the form of strips (rK39 impregnated on nitrocellulose paper) for the detection of VL (Singh 2005).

1.2.7.12 Rapid antibody detection methods: It contains two rapid tests that is developed by InBios (USA) and Sapn Diagnostic Limited (India). This test is based upon antigen Lc-rK39 and Ld-rKE16 respectively (Singh 2005).

1.2.7.13 Leishmanin skin test (LST): Delayed-type of hypersensitivity is a hallmark of cutaneous leishmaniasis and measured by LST. This test doesn't show cross-reaction with Chagas' disease but shows with glandular tuberculosis and lepromatous leprosy. LST is used for CL and MCL in human as well as in animal but not sensitive for kala-azar

infection. It is due to negligible cell-mediated response (Liarte et al., 2001). Leishmanin test is not commercially utilized for leishmaniasis diagnosis in the Indian subcontinent.

In spite of a large number of serological test, not a single one can be used for CL and MCL diagnosis due to poor humoral response (Ahluwalia et al., 2004). As for specificity, a molecular method is most reliable which is based upon detection of parasite-specific DNA and RNA. However, In the case of molecular method, information about genetic materials (DNA and RNA) are required.

1.2.7.14 Polymerase chain reaction (PCR): PCR based approach in diagnosis is proven to be more sensitive and specific. By this technique of diagnosis basically conserved region of DNA or RNA has been targeted. Conserved gene targets are small subunit rRNA, 18S-rRNA, β-tubulin, mini-exon gene repeats, gp63 gene, microsatellite DNA, internal transcribed spacer (ITS) regions and kinetoplast DNA (da Silva et al., 2004; Pizzuto et al., 2001; Wortman et al; 2001; Gangneux et al., 2003).

1.2.8. Treatment of Leishmaniasis

There are many drugs available commercially and each one having own advantages and disadvantages.

1.2.8.1 Pentavalent antimonials: Antimony based drug comes under first-line treatment. It came in the market in 1945 and still the first choice of treatment for CL and VL in many countries. The Pentavalent antimonials include sodium stibogluconate (USA) (**Figure 1.7A**) and meglumineantimoniate (in French-speaking countries and in some part of Latin America) are some antimony based drugs used to treat leishmaniasis. These compounds are the inhibitor of bioenergetics processes such as fatty acid oxidation and glycolytic pathways. However, resistance gained by the parasite reduces the effectiveness of first line treatment. Apart from the resistance, the drug is also associated with some toxicity such as anorexia, abdominal pain, vomiting, headache, nausea, and lethargy. In one of the studies on 103 patient of CL in Peru infected with *Leishmania* (Viannia) *guyanensis* (23.3%), *Leishmania*(Viannia) *peruviana*(47.6%) and *Leishmania* (Viannia) *braziliensis* (22.3%) showed no effect of antimony based drug on parasite means clue of parasite resistance towards first line treatments (Tiuman et al., 2011). Drug administration is painful and given intravenous or intramuscular. The drug is rapidly absorbed and eliminated within three days. Mode of action of antimonial drug is not well known. Even it is not clear about the active form of antimony either Sb (V) or Sb (III). Many models

have been proposed to define the mode of action (Govard et al., 2003; Marquis et al., 2005).

The first model is Prodrug model, in which pentavalent antimony Sb (V) acts as a prodrug which undergoes reduction to form active trivalent antimony Sb (III) that shows anti-leishmanial activity. Conversion of pentavalent to trivalent antimony occurs only in amastigote, not in promastigote, represents their more susceptibility towards amastigote (Shaked-Mishant et al., 2001; Goyard et al., 2003). Other reports suggest that the conversion also takes place in macrophage but quantity is very less. Pentavalent antimonial concentration even at 25 µg/mL only kills 50% of THP1 macrophage cell (Wyllie and Fairlamb 2006) so parasite plays a major role in the accumulation of toxic trivalent antimonial Sb (III) compare to macrophage. Many literatures suggests the role of thiol compound in the conversion of Sb (V) to Sb (III) both in mammals and in the parasite (Fr´ezard et al., 2001; Dos Santod Ferreira et al., 2003; Yan et al., 2003). Mammalian thiol that involves in the conversion includes cysteine (Cys), glutathione (GSH) and cysteinyl-glycine (Cys-Gly). In parasite, trypanothione [T(SH)2] made up by the association of spermidine and glutathione play a crucial role in this conversion as well as a large amount of accumulation of toxic Sb (III) (Fairlamb and Cerami 1992). Some of the studies suggest the enzymatic conversion of Sb (V) occurs in presence of thiol. Two enzymes, thiol-dependent reductase (TDR1) and arsenate reductase play a key involvement in the reduction process by utilizing GSH as the reductant (Denton et al., 2004; Zhou et al., 2004). Trypanothione reductase and zinc finger proteins are the main targets of Sb (III) (Wyllie et al., 2004). Trivalent antimonial Sb (III) treatment induce apoptosis in parasitic cells through increase the oxidative stress or ROS level and intracellular calcium level (Mukherjee et al., 2002; Sudhandiran and shaha 2003).

Next is intrinsic anti-leishmanial activity model, as for this model pentavalent Sb (V) itself involve in inhibition of key metabolic enzyme of glycolytic and fatty acid oxidation pathways (Berman et al., 1987). However, the specific target of these pathways is not clearly known. Another target of Sb (V) is DNA topoisomerase I in amastigote that inhibits the action of winding and unwinding of the DNA (Walker and Saravia 2004). In one hypothesis Sb (V) binds to adenine nucleoside and form complex that may interfere with the transport of purine. In other hypotheses these complexes may accumulate in the parasite where it may face a surrounding neutral environment that retards the dissociation of these complexes and behave like a purine analog, results interfere in the purine salvage pathways (Marr 1991; Roberts et al., 1995).

Another model is the Host immune activation model, in which sodium stibogluconate activate the host immune response such as innate and adaptive immunity to increase the clearance of the parasite. This activation is performed by the induction of ROS and NO generation in the reticuloendothelial system (Raise et al., 2000). As for some literature, a functional T-cell requirement is essential for the anti-leishmanial effect of the drug. During infection IL-2, IL-4 and IL-12 influence the effect of drug action (Alexander et al., 2000; Murray et al., 2000). In some cases, the involvement of cytotoxic T-lymphocyte in antileishmanial activity was also measured and their role was confirmed by expression analysis of MHCI and MHCII (Smith et al., 1991).

Sodium antimony gluconate (SAG) activate ROS generation in macrophage through phosphorylation of ERK via PI3K/Akt pathway. This pathway facilitates the production of NO through p38MAPK. It is the downstream intermediate of the PI3K/Akt pathway (Basu et al., 2006). SAG also increase the expression of IFNγ receptor in both uninfected and *Leishmania* infected THPI cells whichrepresent their role as antileishmanial through altering IFNγ expression and modulating immune response (Dasgupta et al., 2003).

1.2.8.2 Amphotericin B: It belongs to the polyene macrolide group of antibiotics, discovered as an antifungal drug to fight for systemic fungal infection (**Figure 1.7B**) (Fr´ezard et al., 2009). Apart from the antifungal activity it has antimicrobial, antiparasitic (Singh and Sivakumar 2004; Berman 1988; Estes 1989) and antiviral activity also. Amphotericin B performs its biological activity by forming a channel in the cell membrane. Channel cause release of cellular component potassium ions that leads to cell death (Peters 1981; Aikat et al., 1979). As for sterol hypothesis, the drug amphotericin B specifically target sterols (Brahmachari 1989; Shortt 1945). Out of many sterols, amphotericin B specifically acts on ergosterol which is present in parasite or microbial system but absent in mammalian part. However, the application of amphotericin B is limited as for medical purpose is due to their toxic effect include vomiting, nausea, fever, rigors, hypoxia, RBC lysis, hypotension, hypertension, and nephrotoxicity. To improve the drug selectivity and reduction of toxicity, two different methods has been employed which includes:

I) Modification of existing drug or principal drug (Rosen 2002; Brochu et al., 2003). Preclinical studies suggested that L-histidine methyl ester derivative of amphotericin has better selectivity and safety (Antillon et al., 2016).

II) Delivery of drug through some carriers like lipid formulations, liposome (Shaked-Mishant et al., 2001; Goyard et al., 2003) and nanoparticles (Fr´ezard et al., 2001). Due to the lipophilic property of amphotericin B, it can be encapsulated in liposome to increase the efficacy and safety. Three commercially available lipid formulations of amphotericin B includes a lipid complex, a liposomal preparation, and a colloidal dispersion. These formulations differ in their lipid shape, composition, clinical effect, and pharmacokinetic behavior. The toxicity associated with amphotericin B was found to be low by the use of lipid formulations (Herbrecht et al., 2003). The nanotechnology-based drug delivery system also gives promising result as nanoparticles have the ability of targeted delivery. Another advantage of using nanoparticle-based drug delivery approach includes prolonged drug release profile that led to a longer period of contacts between parasite and the drug (Zaioncz et al., 2017).

1.2.8.3 Miltefosine: Theactivity of miltefosine was first tested as an anticancerous drug but later it was also approved by WHO in 2011 as an essential medicine to treat leishmaniasis (**Figure 1.7C**) (Croft and Engle 2006). It is the only orally administrated drug used by different countries such as South America, India, and Germany since 2002. In terms of selectivity, stability and safety issue, miltefosine is one of the best drugs for leishmaniasis treatment. Cure potential of this drug is 97% for *Leishmania donovani* infection in India, 53% for *L. mexicana* and *L. braziliensis* in Guatemala, 71.4% for *L. guyanensis* and 75% for *L. beaziliensis* (Soto et al., 2004; Machado et al., 2010; Chrusciak-Talhari et al., 2011). It is structurally similar to phospholipid so can easily cross the protozoan cell membrane and affect many metabolic processes (Huang et al., 2005; Marco et al., 2009). Literature gives evidence for their selectivity towards membrane component sterol (Rakomanga et al., 2004). Miltefosine has less toxicity and side effects compare to pentavalent antimonial based therapy that make it more beneficial to treat leishmaniasis. In the context of the pharmacokinetic activity, it is easily absorbed orally and is distributed rapidly throughout the body parts. Miltefosine accumulates in visceral organ and metabolizes slowly by liver phospholipase (Agrawal 2006). Drug require to prolong treatment and having a long half-life (proximately 150 hrs) (Perez-Victoria et al. 2006).

1.2.8.4. Paromomycin: Paromomycin belongs to the aminoglycoside group of antibiotics (**Figure 1.7D**) which was tried over anti-leishmanial activity either alone or in combination with other drugs (Mishra et al., 2007). It has been used for a long term treatment of CL and VL which gave the promising result. The mode of administration for this drug is intramuscular (Thakur et al., 1992; Sundar et al., 2007). The selectivity of this drug towards its anti-bacterial or anti-leishmanial activity is through inhibitory action against dissociation of ribosome subunits and other concept is to specifically bind to small rRNA that leads to mistranslation errors (Fourmy et al., 1996; Wimberly et al., 2000). The multistep model has been given to explain their anti-bacterial as well as anti-leishmanial activity. As for the model, inhibition of chain elongation process leads to mistranslation then damage of membrane and finally ribosome blocked for translation process (Davis et al., 1986; Marisa et al., 2011).

1.2.8.5. Pentamidine: It is an aromatic diamidine utilized for the cure of *Pneumocystic jiroveci* (pneumonia), *Trypanosoma brucei*, and *Leishmania donovani* infection (**Figure 1.7E**) while the mode of actionis not completely known.Although, the role of pentamidine has been reported in the interference of glycolysis (Goodman and Gilman 1965). Robins in 1967 has suggested the role of pentamidine in the inhibition of folic acid metabolism and reported the requirement of folic acid administration together with pentamidine treatment (Robbins, 1967). However, folic acid administration together with pentamidine therapy in rat did not affect the efficacy of the drug (Frenkel et al., 1966). During pentamidine treatment in eight year old girl suffering from a disease, hypogammaglobinemia showed megaloblastic changes in the bone marrow (Robbins et al., 1965).The pentamidine treatment especially reduces the folic acid level that impairs DNA synthesis. These symptoms are similar to the drug against DNA such as 5-fluorouracil, hydroxyurea, and methotrexate. The common toxic effect includes severe hypo glycemia, diabetes mellitus, and shock myocarditis. In *Leshmania*, pentamidine migration occurs through unknown transporter (Vercesi and Docampo 1992). It has been reported the action as a competitive type of inhibition of arginine transport as well as noncompetitive inhibition of putrescine and spermidine (D'Silva and Daunes 2000).

1.2.8.6. Sitamaquine: The sitamaquine an analog of 8-aminoquinoline (**Figure 1.7F**) developed by GlaxoSmith-Kline gave promising result in India and Kenya during Phase II clinical trials. Mode of administration is oral as miltefosine but not active against topical

route treatment of CL (Jha et al., 2005; Garnier et al., 2006). Advantage of sitamaquine (26 h) over miltefosine includes less half-life (Miltefosine half-life: 150-200 h). It has been investigated that sitamaquine action was diminished when medium protein was increased indicating their activities related to interaction with protein (Duenas-Romero et al., 2007). A possible target of this drug has been confirmed as phosphatidylglycerol or phosphatidylinositol (PI) (Coimbra et al., 2010).

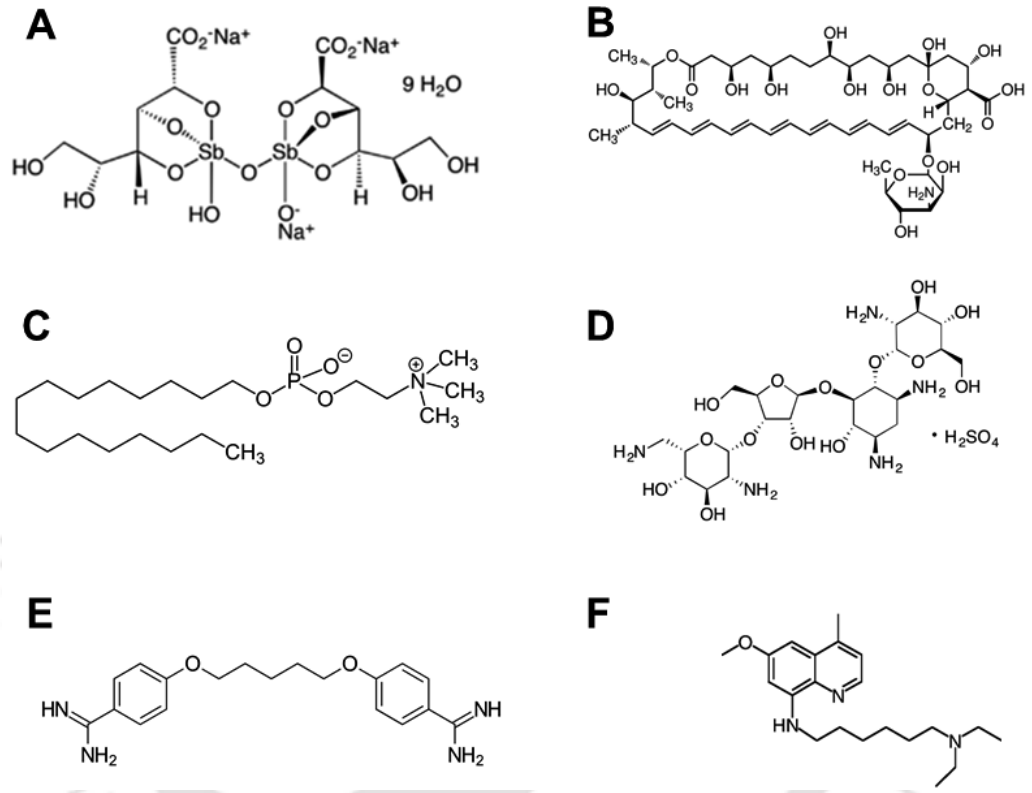

Figure 1.7: Existing drugs for the treatment of leishmaniasis. (A) Sodium antimony gluconate, consider under first line treatment. (B) Amphotericin B, a polyene macrolide group of antibiotics discovered as an antifungal drug but it has ant-parasitic activity also. (C) Miltefosine, comes under second line treatment. First oral drug against leishmaniasis. (D) Paromomycin, belongs to aminoglycoside group of antibiotic. It showed effective against cutaneous and visceral leishmaniasis. (E) Pentamidine, an aromatic diamidine also used for the cure of leishmaniasis. (F) Sitamaquine, an analogue of 8-aminoquinoline under Phase II clinical trials. Like miltefosine, its mode of administration is oral.

1.2.9 Vaccine against Leishmaniasis

Not a single vaccine in routine use against leishmaniasis in the whole world. Most of the vaccines are in the advanced stage of trials.

1.2.9.1 Killed Vaccine: Many vaccination trials with a cocktail of five killed *Leishmania* stock were performed in Brazil and Ecuador gave promising results with significant protection from natural infection (Marzochi et al., 1998; Armijos et al., 1998; Luca et al., 1999). However, immunized individual gave a long lasting T-cell response (Th1) represent their role as a protector during infection (Castes et al., 1994; Mendonca et al., 1995). In South America, a combination of the strain of *L.brazilliensis* or *L.mexicana* with *M.bovis*was tried in severely infected leishmaniasis patient gave high cure percentage. The protective mechanism was confirmed by the development of Th1-type response with concomitant production of IFNγ with reduction of IL-4 level (Cabrera et al., 2000; Castes et al., 1989). In other studies, a mixture of BCG-*L.major* killed vaccine was applied in the Iranian leishmaniasis patient gave better result than BCG alone, suggesting their transient immune response (Momeni et al., 1999; Sharifi et al., 1998). Hence, it may have multiple doses with prolong use to give optimum immune protection. In one of the experiment, monkey's model of CL was taken for a vaccine trial in which killed *L.amazonensis* was given together with IL12 as an adjuvant gave significant protective mechanism (Rivier et al., 1992; Aebischer et al., 2000).

1.2.9.2 Live attenuated Vaccine:

Live attenuated vaccines are those in which avirulent parasite used as a prophylactic vaccination. In one of the early experiment, parasite cloned directly from skin lesion found avirulent suggested the heterogeneous population of the virulent and avirulent parasite in the lesions (parasite killed by the host itself and act as an antigen). As for literature the most interesting thing is mainly avirulent parasite take part in immune response generation (Handman et al., 1983). Other data showed that macrophage presents only dead parasite to the T-cells although, it engulfs live parasite (Overath and Aebischer 1999). However, without knowledge of the clear genetic structure of avirulent parasite, their use as a human vaccination would be risky due to the chance of reversal of virulence. One of the experiment strongly suggested the role of attenuated vaccination in immune response generation in which mice were injected with the irradiated parasite and got evoked an immune response (Rivier et al., 1999). In recent advancement of vaccine development include the knockout of the essential gene from the parasite to make it nonvirulent. In one of the study, parasite *L.amazonensis* having an absence of dihydrofolate reductase-thymidylate synthetase (DHFR-TS) gene was injected in the mouse model. In that case,

parasite underwent a certain cycle of replication without generating any disease and protected against infection of two parasite strain *L.amazonensis* or *L.major* (Veras et al., 1999; Titus et al., 1995).

1.2.9.3 Recombinant and Synthetic Vaccines: TheRecombinant and synthetic vaccines include any DNA derived protein or peptides. This DNA derived antigen may be of growth specific or equally shared by promastigote and amastigote and others are conserved among many species of *Leishmania.* Normally, T-cell recognize antigen from antigen presenting cell by MHCI and MHCII. MHCI only attached with cytosolic protein but MHCII presents only protein comes through lysosomes it suggests that any protein part of the parasite can acts as an antigen, regardless of their location. Hence, recombinant protein as well as naked DNA can be delivered directly to the parasite. In other case targeted delivery of protein or DNA in a specific cell such as Langerhans or dendritic cells, which are essential to generate the primary T-cell response. Injection of naked DNA have unique advantage such as it acts as an adjuvant and generate continuously immune response through antigen presenting cells (Matzinger 1998).

1.2.9.4. Synthetic Peptides: In the early 1980s, a wave was blown to use synthetic peptide that can be presented by antigen presenting cells and recognize by T-cell to use as a vaccine (Jardim et al., 1990; Russo et al., 1993; Spitzer et al., 1999). This wave has been slowed down in recent years and moved towards DNA encoding polypeptides and to naked DNA. Many disadvantages of the use of peptide antigen make it less attractive to work as a vaccine like less induced T-cell memory, failure to give a response by all individuals in the population and high production cost. Other additional disadvantages include the peptides are not processed and presented by the MHC molecule in the individual due to failure of cleavage, processing, transport or deletion of a T-cell specific region (Howard 1993). Despite the limitations, *Leishmania* gp63 peptides were tested in animal models and produced long lasting host protection and T-cell memory response (Spitzer et al., 1999). Use of subunit vaccine based upon recombinant protein is affected by many factors such as correct folding and post-translation modification. A polypeptide PSA-2 to processed by the immune machinery require correct folded or native conformation that may not be done by using *E.coli* as a host for protein expression. This problem can only be overcome by expressing the protein in their native host *Leishmania* itself or similar organism like *Crithidia*. Peptides or protein expressed in the native host will be properly

folded and glycosylated (Pfeffer et al., 1990; Constant et al., 1994; Moody et al., 2000). Other reason for the failure of peptide vaccine includes low immunogen capacity.

1.2.9.5 Non-protein based Antigens: Early literature tells that *Leishmania* lipophosphoglycan (LPS) a glycolipid give good protection against the disease (McConville 1987; Russell et al., 1988). Use or delivery of LPS or any other molecule depends on adjuvants like liposome and molecule for stability or integrity. At the time when the work was published related to immunity induced by glycolipid as an antigen, the mechanism to recognize glycolipid by T-cell was not known. Nowadays, it is completely accepted that some of the non-protein molecules include mycobacterium glycolipids are presented to T-cell by MHCI protein (CD1 molecule) (Sugita et al., 1998; Sieling et al., 2000).

1.2.9.6 Naked DNA Vaccine: Immunization by naked DNA to use as a vaccine candidate is a novel approach. In that case gene coding vaccine candidate cloned in specific plasmid can be transferred into human muscles or skin. Further, these genes reach to the nucleus and form a protein that provokes an immune response. The Skin and muscles cell, will not itself present antigen to the T-cell but are presented by MHC class I and class II molecule of antigen presenting cells (Hasan et al., 1999). Both CD4 and CD8 positive immune response generates during the use of DNA vaccine make it attractive to use as a *Leishmania* vaccine (Pardoll and Beckerleg 1995). Apart from a good immune response, this strategy also provides proper folded polypeptide, long persistence of antigen in the system and absence of a requirement of adjuvant. It has been proven that vaccination by different gene encoding *Leishmania* protein gp63, PSA-2 and LACK, protected the genetically susceptible mice against *L. major* infection (Gurunathan et al., 1997; Siolander et al., 1998; Walker et al., 1907). Although the efficiency of plasmid DNA taken by the cells is low but that amount of plasmids and their expression is enough to generate appropriate B and T cell response (Hasan et al., 1999; Gurunathan et al., 2000).

1.2.10. Organizational control of leishmaniasis

An organization WHO which controls leishmaniasis through certain control measures. As for WHO the transmission of leishmaniasis goes through complex biological system include sand-fly, parasite, and their human and animal reservoir. Key strategies to prevent

leishmaniasis are as follows (**Source:**https://www.who.int/news-room/fact-sheets/detail/leishmaniasis):

1.2.10.1 Early diagnosis and effective prompt treatment: Several medicine available commercially for the treatment and prevention of death from this deadly disease. Effective medicine reduces disease transmission and monitors the spread and burden of the disease. Although, the leishmaniasis mostly affect the poor population so, WHO provides effective medicine through WHO-negotiated price scheme and drugs donation program.

1.2.10.2 Vector control: Other safety measure taken by WHO to reduce the disease transmission by decreasing the number of sand-fly. Control strategies include use of the insecticide-treated net, a spray of insecticide, personal protection and environmental management.

1.3.20.3 Effective disease surveillance: As for this prevention strategies, deceased individual should be promptly monitored and take necessary action during the epidemic and high fatality condition during treatment.

1.3.10.4 Control of animal reservoir host: To control the animal which is the reservoir of the parasite is one of the key strategies to control leishmaniasis.

1.3.10.5 Social mobilization and strengthening partnerships: To educate the population regarding disease behavior and symptom is also require. Partnership with various stakeholders and other vector-borne disease elimination program is essential.

Most of the drugs have specific target means they are synthesized against particular molecules or pathways. Currently available therapeutics for anti-leishmanial effect associated with toxicity, high cost and unsatisfactory route of administration. Another most important issue is resistance towards the first and second line drugs so there is an immense need for discovery of new target and drug against them. A multi-enzyme complex is a group of enzymes that coordinately regulate a special type of reaction. It is the part of many major biosynthetic pathways that plays a major role in the energy flow in the system. Like Pyruvate dehydrogenase complex (PDH) and α-ketoglutarate dehydrogenase complex (α-KGDH), both are associated with respiratory pathways.

Another multi-enzyme complex is glycine cleavage complex (GCC), it provides important intermediate N^5, N^{10}-methylene H4-folate for the DNA synthesis. Hence, the use of multi-enzyme complex enzymes as a drug target may be a good choice for the drug candidate.

1.2.11 Pyruvate Dehydrogenase (PDH) Complex

Glycolysis and Krebs cycle are the two major biosynthetic pathways that involve in the generation of essential intermediates that actively participate in the yield of energy in the form of NADH, $FADH_2$, GTP, and ATP. Glycolysis occurs in the cell cytoplasm and Krebs cycle (TCA) in the mitochondria.Through glycolysis, glucose converted into key intermediate pyruvate. Pyruvate destines to transport into the mitochondrial matrix where all the Krebs cycle enzyme resides. The mitochondrial outer membrane is permeable for small molecules so pyruvate crosses through the outer membrane. However, inner membrane is not permeable thus it translocates through specific transporter protein called pyruvate translocase in symport with H^+. PDH complex connects glycolysis to Krebs cycle present in the mitochondrial matrix. It is a multi-enzyme complex that maintains glucose homeostasis in the mammalian system. PDH comprises of three catalytic residues: E1 (pyruvate dehydrogenase), E2 (dihydrolipoamide acetyltransferase) and E3 (dihydrolipoamide dehydrogenase). All three enzymes work together to perform a cycle reaction to convert pyruvate into acetyl-CoA with the generation of NADH as an energy source. E1 and E2 convert pyruvate into acetyl-coenzyme A, CO_2 and NADH (H^+) by decarboxylation. E3 component performs the recycling of dihydrolipoamide by utilizing FAD and NAD^+. The overall mechanism of the catalysis by the PDH complex is depicted in **Figure1.8.** PDH is posttranslationally regulated by phosphorylation through kinases and dephosphorylation by phosphatase. PDH of the bacterial cell is the simplest form of complex that can be compared to mammalian PDH in context to the regulation. In many diseases such as obesity, neurological disease, type II diabetes and cancer, PDH is the main causative agent (Imbard et al., 2011; Patel et al., 2012; Kaplon et al., 2013; Jeoung et al., 2014).

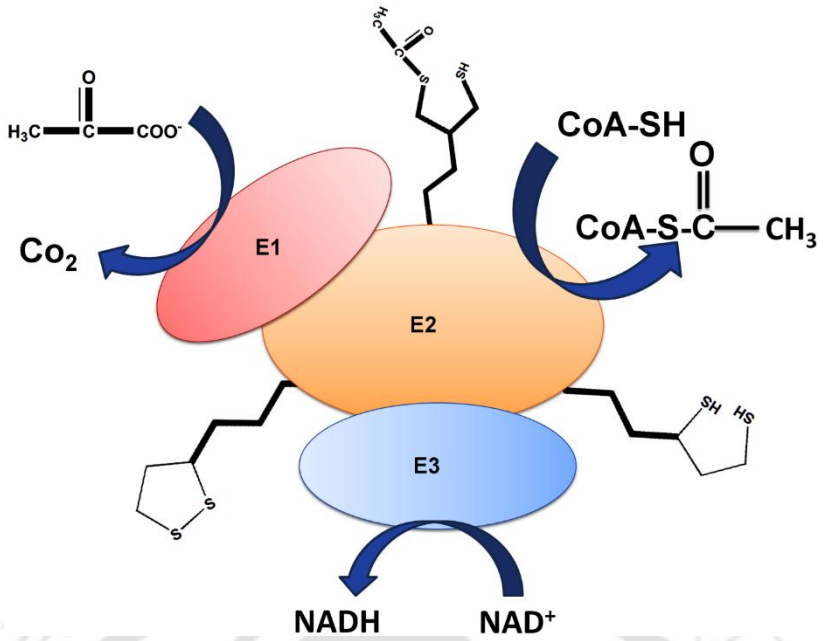

Figure 1.8. Schematic representation of PDH complex. The PDH complex decarboxylate the pyruvate intermediate by E1-enzyme. E2-enzyme having a lipoate arm catalyze transfer of decarboxylated acetyl moiety to lipoate arm. Finally acetyl group reacts with CoA-SH to form acetyl-CoA and leave the lipoate arm in reduced form. E3-enzyme acts as dehydrogenase so oxidize the reduced lipoate arm into oxidized lipoamide. E1, α-ketoglutarate dehydrogenase; E2, dihydrolipoamide acetyl transferase; E3, dihydrolipoamide dehydrogenase; ThDP, thiamine diphosphate.

1.2.11.1 PDH structural Organization and their Regulation: In PDH, three catalytic enzymes (E1, E2 & E3) work coordinately to regulate carbon influx in the TCA cycle. It performs oxidative decarboxylation of pyruvate into acetyl CoA, CO_2, and NADH. E1 enzyme having cofactor thiamine diphosphate (ThDP) perform decarboxylation of pyruvate. It transfers acetyl moiety to the lipoyl domain of E2 enzyme generate acetyl lipoyl intermediate. In higher eukaryotes like human have two isoforms of E1- enzyme (PDHA1 and PDHA2) which coded by two different genes. E2 enzyme finally transfers acetyl group to the CoA-SH forms acetyl-CoA and leave lipoyl domain in the reduced form. N-terminal of E2-enzyme have 1-3 lipoyl domains. It varies organism to organism. Human has two lipoyl domain (L1 and L2) and *E.coli* (L1, L2, and L3) (**Figure 1.11**). E2 also having peripheral subunit binding domain (PSBD) through which E1 and E3 binds. It has a large C-terminal catalytic domain that makes a dodecahedral structure. E3-enzyme transfer electron from lipoyl moiety to FAD and at the end to NAD^+. PDH in higher eukaryotes has an additional E3- binding protein (E3BP). E3BP is composed of E3 binding domain and C-terminal domain (Marcucci& Lindsay 1985; Harris et al., 1997). Pyruvate dehydrogenase kinase (PDK) [four isoforms in human] (Roche et al., 2001) and pyruvate

dehydrogenase phosphatase (PDP) [two human isoform] (Huang et al., 1998; Harris et al., 2002; Roche et al., 2003) regulate PDH coordinately by phosphorylation and dephosphorylation. PDK recruits to lipoyl domain (L1, L2) of E2 and L3 of E3BP. PDH of prokaryotic cells is simpler than the eukaryotes. In *E.coli,* 24 copies of E2 is present as a cubic core. E1 (12) and E3 dimers (6) bound non-covalently with PSBD of E2 core, collectively exhibit octahedral symmetry (Reed and Hachert 1990). In mammalian PDH, E2-E3BP assembly proposed by two models: "addition" model where E2-E3BP assembled by 60 and 12 copies of E2 (for human) and E3BP, respectively (Sanderson et al., 1996). Other model is "substitution" model where either 48 and 12 copies or 40 and 20 copies of E2 and E3BP forms E2-E3BP core assembly (Hiromasa et al., 2004). Heterotetramer of E1 ($\alpha_2\beta_2$) binds to PSBD of E2 and E3 homodimer bind to E3 binding domain of E3BP. Homodimer of pyruvate dehydrogenase kinase (PDK) and heterodimer of pyruvate dehydrogenase phosphate (PDP) binds to lipoyl arm of E2 and E3BP. Mammalian PDH has icosahedral symmetry which shows greater complexity in context to structure and function with *E.coli*.

1.2.11.2 E1 Component: structural and functional studies: E1 component of PDH complex have thiamine diphosphate as a cofactor that performs decarboxylation of pyruvate residue. E1 component from the *E.coli* has mainly three types of 2-oxoacid dehydrogenase enzymes such as α_2-homodimer and $\alpha_2\beta_2$-heterotetramer. In mammals, $\alpha_2\beta_2$ form is regulated by kinase and phosphatase. In *E.coli* α_2-homodimer of E1 component is the best characterized quaternary structure. *Pyrobaculum aerophilus* E1β subunit crystal structure was reported by Eisenberg and his collaborator belongs to $\alpha_2\beta_2$ class (Kleiger et al., 2001). E1β subunit has no activity without α subunit counterpart because, in absence of α, E1β subunit can't be able to bind with cofactor hence inhibit appropriate quaternary structure assembly. This structure doesn't provide the active site and catalytic information but gives information about helix-helix packing around β- subunit interface. *E.coli* E1-subunit structure shows as a tightly bind homodimer having a molecular weight of 200 kDa and 886 amino acid residues. Its catalytic activity depends on cofactor ThDP and Mg^{2+}. The tightly bound dimer forms a symmetrical active site at the dimer interface as observed in other known ThDP-dependent enzymes. Dimer area is around 103 x 95 A^o wide and 71 A^o thick. The structure has three functional domains: residues less than 470 amino acid belongs to N-terminal domain whereas greater than 470 belongs to middle domain made by other subunit and remaining part is C-terminal domain (**Figure 1.9A**).

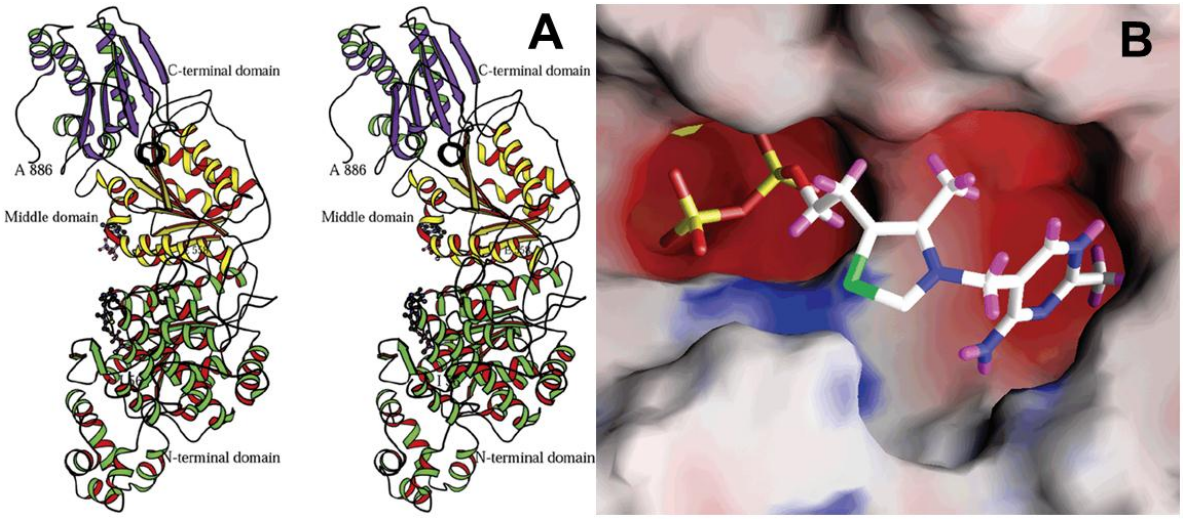

Figure 1.9: Diagrammatic representation of PDH E1- protein with their cofactor binding cleft. (A) Ribbon diagram of E1-enzyme have three regions includes C-terminal domain, middle domain, and N-terminal domain.Normally N-terminal domain is larger than other two domains. ThDP cofactors represented in a ball and stick form. (B) Binding cleft for ThDP cofactor. Stick structure shown ThDP. Some residues of cofactor has been removed for better visibility. (Kraulis 1991; Arjunan et al., 2002).

Dimer interface made by the interaction of all the three domain. The active site of E1-component in *E.coli* is 18 x 8 x 21 A^o wide and having a deep cleft. Residues around the cleft contain His106, Ser109, Gln140, His142, Tyr177, Met194, Asp230, Glu235, Asn260, Leu264 and Lys392 from one subunit and Asp521, Glu522, Ile569, Glu571, Tyr599, Phe602, Glu636 and His640 from other subunits. The key residues responsible for binding for cofactors are likely to be engaged in catalysis and substrate binding also. The residues His106, His142, and His640 help to interact with negatively charged pyruvate around thiazolium ring of ThDP cofactor. Glu522 in E1-component present around the positively charged region of thiazolium ring to neutralize the overall charge and also may be responsible for proper orientation of the substrate. Residue His142 showed interaction with cofactor diphosphate. Other residues His640, His106, and Glu522 take part in the exchange of proton between substrate as well as stabilize the intermediate formed between substrate and ThDP. Asp521 directed towards active site cleft might indirectly utilize in reaction catalysis by interaction with Glu522 (Arjunan et al, 2002).

Comparative study of the crystal structure of ThDP-dependent enzyme from a different organism such as *Lactobacillus plantarum* pyruvate oxidase, yeast pyruvate decarboxylase and transketolase reveals about cofactor ThDP binding in the hydrophobic zone called ThDP-fold that forms at the dimer interface (Muller et al., 1993). Diphosphate arm of cofactor binds to N-terminal residues of one subunit and amino-pyridine end binds to middle domain residues of other subunits. Diphosphate end of Cofactor interacts with

protein part either by hydrogen bonding or through coordinate interaction to Mg^{2+} ion. The cofactor Mg^{2+} associated with protein through interaction by Asp-230, Asn-260, and Gln-262 (Arjunan et al, 2002).

ThDP resides in the hydrophobic zone of protein active site. These hydrophobic areas ThDP-fold has conserved 30 amino acid residues consisting of G (229) DG and terminates by N (258) CN. This binding motif was found conserved in almost hundreds of ThDP-dependent enzyme (Hawkins et al., 1989). Importance of ThDP-fold in the regulation of enzyme activity in *E.coli* has confirmed by site-directed mutagenesis (Yi et al., 1996).Jordan groups performed single amino acid mutation in ThDP-motif and found significantly diminishing binding of ThDP cofactor. Mutational studies performed at Gly-231 and Asn-258 reveals that these residues involved in activation process by ThDP. Other substitution C259N showed less critical in cofactor binding and behaved more similar to parental complex (Jizu et al. 1996). Scientist found lag phase in the activation of multi-enzyme complex and that was due to the association of E1 to E2-E3 complex whereas, lag phase was independent on ThDP cofactor (Bisswanagar 1974). Association and dissociation constant for ThDP binding and lag phase depend on the concentration of pyruvate, reported in PDH for pig heart (Sümegi and Alkonyi 1983).

As E1-component of *E.coli*, human E1-protein performs ThDP mediated decarboxylation of pyruvate and acetylation to lipoyl arm containing E2 and E3BP. E2 component of PDH in human is heterotetrameric ($\alpha_2\beta_2$) and regulated by PDK isoform by phosphorylation at three serine residues (Ser264-α site 1; Ser271- α site 2; and Ser203- α site 3) (Sale and Randle 1981; Yeaman et al. 1978). Site 1 and 2 of the E1 component present in conserved phosphorylation loop A (residues: 259-282 α subunit) (Ciszak et al. 2003). Phosphorylation loop A forms at one side of active site wall which anchors ThDP. Site 3 is located in short arm of other phosphorylation loop B (198-205 α subunit) present adjacent to Phosphorylation loop A anchors Mg^{2+} through coordinated by ThDP. Phosphorylation at these three sites inactivates E1 component of PDH. Site 1 is more rapidly phosphorylated and site 3 least (Korotchkina and Patel. 1995). Different PDKs have different site specificity for phosphorylation. All PDKs phosphorylates at site 1 and 2 except PDK1 that phosphorylates at site 3 (Korotchkina and Patel, 2001; Kolobova et al. 2001). Phosphorylation at Ser264-α prevents the cofactor binding due to steric clash between phosphorylated site 1 and Ser266-α (Kato et al. 2008).

1.2.11.3 E2 Component: structural and functional studies: The E2-component (Dihydrolipoyl acetyltransferase) of PDH makes the core of complex which perform noncovalent interaction with E1 and E3 component. The *E.coli* E2-component have multi-domain trimer structure comprises of three lipoyl domain (3-lip E2, ~80 amino acid), a peripheral subunit binding domain (PSBD, ~45 amino acid) and center core have acetyltransferase domain (Bleile et al., 1979; Stephens et al., 1983). The E2 has E1 recognition domain for E1 binding whereas, E3 have recognition domain that makes interaction with E2-component through E3BP in higher eukaryotes (Patel and Roche 1990; Patel et al., 2009; Patel and Korotchkina 2003). In *E.coli* PSBD shows interaction with E1 and E3 component in place of E3BP as in higher eukaryotes (Toyoda et al., 1998). The N-terminal of the E1 component interacts with E2 component electrostatically through PSBD. This terminal is rich in acidic and PSBD in basic amino acid. Interaction study between E1 and E3 component with E2 was confirmed through a mutational approach (Lys191 and Arg202) at the catalytic site. Point mutation of R129E, R150E, R150A, R150K and R202E in E2 showed 10% less activity than parental E2 protein. The multi-substituted E2 (G144A, G146A, and G149A) component showed only 3% activity. The *E.coli* E2-component catalytic activity depends on proximity residues around highly conserved amino acid H602 and S550 at the catalytic center, present at the junction of two subunits. For the *E.coli*, point mutation of H602C didn't show significant PDH or E2 (acetyltransferase) activity. Other substitutions such as S550A cause drastically reduced PDH activity but not affected the binding of E1 and E3 component to E2 and reductive acetylation of lipoyl domain of E1 component (Nemeria et al., 1998). Based on X-ray crystallographic and kinetic studies of *A. vinelandii* E2-component in complex with CoA and dihydrolipoamide were also suggested that histidine and serine at catalytic center play a crucial role in acetyltransferase activity (Kale et al., 2007). The highly conserved residue S550 involved in CoA binding and stabilization of negatively charged intermediate of acetyltransferase during the reaction at catalytic center. Binding of dihydrolipoamide substrate to the catalytic center of E2 component promotes flipping of the D606 side chain to make electrostatic interaction with H602 (**Figure 1.10B**) (Steiert et al., 1990; Mattevi et al., 1991).

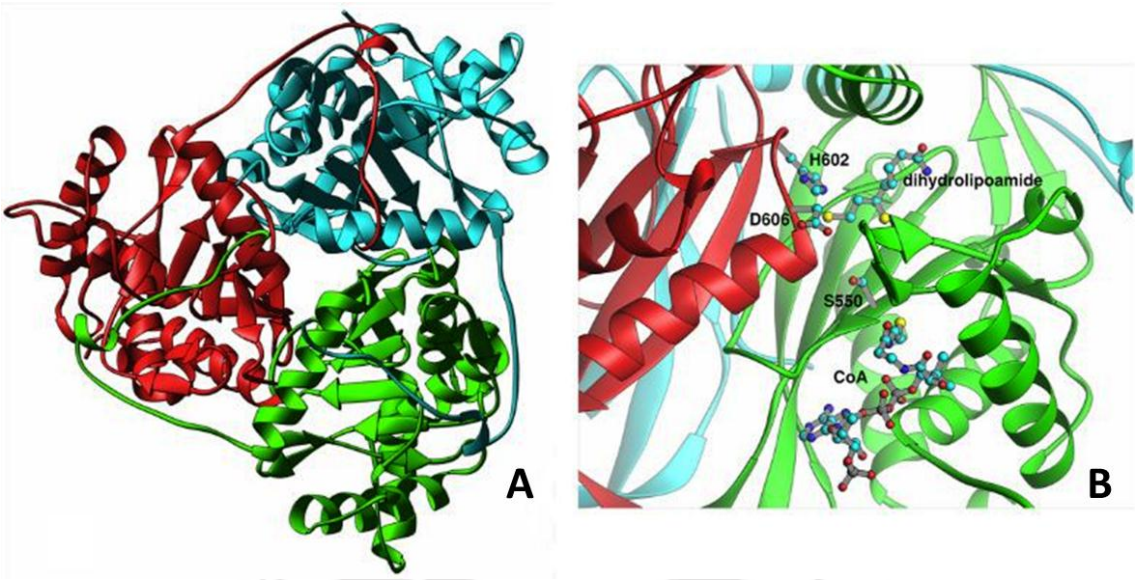

Figure 1.10: Diagram of E2-component and their active site (*A. vinelandii*). (A)Ribbonlike structure represent trimeric form of E2-component where each subunit shown in different color code (red, green, and cyan). (B) Active site shown at interface of two subunits within the trimeric structure. Main residues depicted at the interface are H602, D606 and S550. The substrate (dihydrolipoamide and CoA) shown in a ball and stick form (Mattevi et al., 1993).

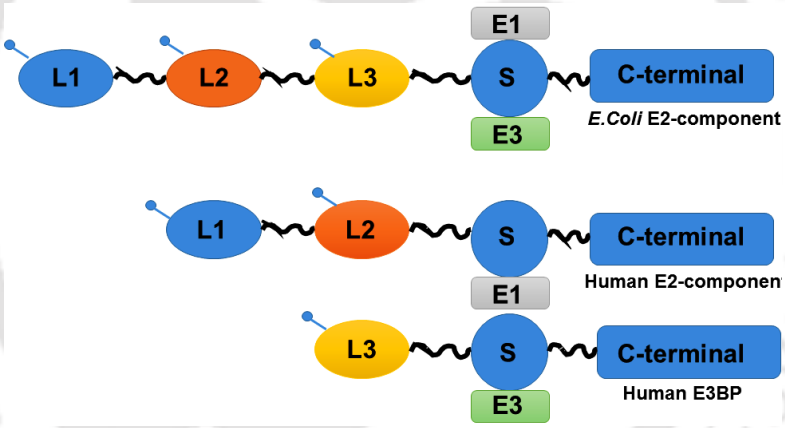

Figure 1.11: Schematic illustration of lipoyl domain in *E.coli* and Human. In *E.coli* E2-component have three lipoyl domain (L1, L2 and L3) present towards N-terminal whereas, human have only two (L1 and L2) domain. Human having extra E3BP (E3-binding protein) from which one lipoyl domain (L3) attached along N-terminal.

In many reports, it has been demonstrated that E2 as well as independently expressed catalytic domain of E2 component perform reaction by transferring acetyl residue from acetyl-CoA to the acetyl acceptor DL-dihydrolipoamide that replaces dihydrolipoyl moiety from lipoyl domain in a reversible manner (Mattevi et al., 1993). Acetyltransferase activity of E2 component was demonstrated by a coupled reaction catalyzed by the enzyme phosphotransacetylase. Formation of thioester derivative (S-acetyl-dihydrolipoamide) can be monitored at 240 nm (Mattevi et al., 1991) or by radioactive detection method by labeling [1-^{14}C] acetyl-CoA (Mathews 1968; Adams et al., 2010). In human, E2-E3BP

provide the site for the proper binding of E1-component through interaction by subunit binding motif of human protein E2. A model system of *Bacillus stearothermophilus* was employed to investigate the binding site of Human E1-component to E2 where the interaction of E1/E3 with E2-enzyme was compared. The E1 ($\alpha_2\beta_2$) subunit of *Bacillus stearo thermophilus*make interaction with E2 by C-terminal of β-subunits. Investigation on β-subunits interaction of human E1-component with E2 revealed the electrostatic interaction (salt bridge formation) between Asp289 (E1) and Lys276 (E2) (Patel et al., 2009). The E2-E3BP provide the binding site for the attachment of human E3-component. Complex E2-E3BP binds at the interface of two E3-subunits through electrostatic and hydrophobic interaction but doesn't perturb between subunits (Cizak et al., 2006; Brautigam et al., 2006). Mutational studies were employed to know the essential residue involved in the interaction of human E3BP (Ile157) and E3 (Tyr438) (Park and Patel 2010).

1.2.11.4 E3 Component: structural and functional studies: Dihydrolipoamide dehydrogenase (EC 1.8.1.4) (E3-enzyme) is the third component of multi-enzyme complexes serves to oxidize the lipoic acid attached to lysyl residue of E2-component of three α-oxo acid dehydrogenase complex as well as to the L-protein in glycine cleavage complex by reducing the NAD^+ through FAD cofactor (Randle et al., 1978; Reed 1981, Feigenbaum and Robinson et al. 1993). It belongs to flavo enzyme family means enzyme requires FAD as a cofactor for their catalytic activity. The E3-enzyme is also the member of the pyridine nucleotide-disulfide oxidoreductase family so perform oxidation reduction reaction. Other members of this family include glutathione reductase, thioredoxin reductase, mercuric reductase, and trypanothione reductase. All these enzymes are the key regulator of redox metabolism in the biological system and establish homeostasis.

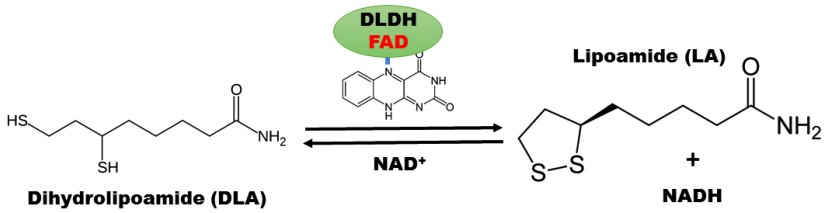

Figure 1.12: Reaction catalyzed by dihydrolipoamide dehydrogenase (DLDH). DLDH contains FAD as a cofactor that mediate electron and proton transfer between DLA, protein Disulfide Bridge and NAD^+. During oxidation process, DLA becomes oxidize in presence of NAD^+ into LA where NAD^+ undergoes reduction to from NADH.

Active site prediction of human E3- enzyme were performed by comparing the sequence with other families of pyridine nucleotide-disulfide oxidoreductase of different organism (glutathione reductase of human and *Azotobacter vinelandii*) (Schierbeek et al, 1989). Site-specific mutants of human-E3 were made and characterized to confirm the catalytic residues (Kim and Patel, 1992). The catalytic mechanism of pyridine nucleotide-disulfide reductase family is almost similar and regulated by disulfide residues. Similarly in the human E3-enzyme Cys-45 and Cys-50 forms the disulfide bridges to perform oxidation-reduction process (Jentoft et al, 1992). Disulfide bond breaks and forms intermediate with the substrate to regulate the reaction. In *Azotobactervinelandii*, disulfide bond shows unusual shorter C^{α}-C^{α} bond than normal (Mattevi et al, 1991). Sequence alignment from different organisms has been reported that sequence around disulfide forming cysteine is conserved. The aligned sequences from different organisms are shown in table 1 (Kim 2002). This conservation may have role in generation of strain in disulfide bond during catalytic process (reduction of disulfide bond). The consensus sequences in E3-enzyme in most of the organism is suggested as GG (TV) CLN (VX) GCIP (Kim 2002). However, some of the amino acid was mutated at the consensus region to confirm their role in the catalytic process. Thr-44 in human as well as in other organism is conserved which involved in bonding with FAD residue by –OH group. Apart from this conservation in some organism Thr-44 is also absent in some organism which is replaced by Val. Hence, in one of the study Thr-44 was substituted with Val and found 2.2 fold decrease of E3 activity. Decrease of activity might be due to a slight change of microenvironment around FAD-binding region (Kim 2002). Eukaryotic organism bears mitochondrial 2-oxo acid dehydrogenase complex and glycine cleavage complex. However, some eukaryotes have absence of functional mitochondria. The causative agent of African sleeping sickness (*Trypanosoma brucei*) have an absence of functional mitochondria in bloodstream form so parasite fully dependent on glycolysis for their energy production. Thus it transports glucose and metabolized to pyruvate which is then excreted out (Fairlamb 1982). In such bloodstream form, DLDH is associated with plasma membrane for the hexose transport (Danson et al, 1987). In an experiment, ithas been tried to confirm that DLDH association with the plasma membrane is also present in an organism that having functional mitochondria. For that plasma membrane was prepared from rat adipocyte cells and confirmed the associated DLDH activity. On the basis of above experiment, scientist has suggested that DLDH have two locations, one inside the mitochondria and the other in the extra mitochondrial region. The function of membrane-associated DLDH is primarily the

transport of sugar and lipid soluble substrate lipoamide (substrate of DLDH). In another study, *E.coli* supplemented with a media deprived of lipoic acid resulted in reduced transport of ribose, galactose, and maltose. When lipoic acid is supplied with growth media, lipoic acid-dependent transport was inhibited by the dithiol-specific arsenite (Inhibitor) (Richarme, 1985).

Table2: Comparision of amino acid residues present around disulfide Cys-45 and Cys-50 at active site of human-E3 with other organisms (Kim 2002).

Source	Amino acid sequence
Homo sapiens (Human)	GGTCLNVGCIP
Sus scrofa (Pig)	GGTCLNVGCIP
Canis familiaris (Dog)	GGTCLNVGCIP
Mus musculus (Mouse)	GGTCLNVGCIP
Trypanosoma brucei	GGTCLNVGCIP
Trypanosoma cruzi	GGTCLNVGCIP
Pisum sativum (Garden pea)	GGTCLNVGCIP
Manduca sexta (Tobacco hawk moth)	GGTCLNVGCIP
Saccharomyces cerevisiae (Yeast)	GGTCLNVGCIP
Schizosaccharomyces pombe (Fission Yeast)	GGTCLNVGCIP
Pseudomonas putida (lpdg)	GGTCLNVGCIP
Pseudomonas putida (lpd3)	GGTCLNVGCMP
Pseudomonas fluorescens	GGTCLNVGCIP
Azotobacter vinelandii	GGTCLNVGCIP
Rhodobacter capsulatus	GGTCLNVGCIP
Alcaligenes eutrophus	GGTCLNVGCIP
Pseudomonas putida (lpdv)	GGTCLNIGCIP
Chlamydia trachomatis	GGTCLNRGCIP
Chlamydia pneumoniae	GGTCLNRGCIP
Halobacterium volcanii	GGTCLNYGCIP
Bacillus subtilis (acol)	GGTCLNEGCIP
Bacillus subtilis (bfmbc)	GGTCLHKGCIP
Synechocytis sp.	GGTCVNRGCIP
Escherichia coli	GGVCLNVGCIP
Bacillus stearothermophilus	GGVCLNVGCIP
Bacillus subtilis	GGVCLNVGCIP
Staphylococcus aureus	GGVCLNVGCIP
Vibrio parahaemolyticus	GGVCLNVGCIP
Mycoplasma pneumoniae	GGVCLNVGCIP
Mycoplasma genitalium	GGVCLNVGCIP
Haemophilus influenzae	GGVCLNVGCIP
Chlorobium vibrioforme	GGVCVNWGCIP
Acholeplasma laidlawii	GGICLNHGCIP
Zymomonas mobilis	GGICLNWGCIP

Hence, it clearly explains the regulation of transport of sugar by disulfide-containing protein. The *E.coli* deficient of even *lpd*gene code for dihydrolipoamide dehydrogenase component of 2-oxo acid dehydrogenase complexes had activity. The activity was 15% of the parental strain was stimulated by galactose and maltose. The experiment clearly explains the presence of two different types of DLDH in the system (Richarme and Heine 1986). Other evidence linked with the presence of plasma membrane-linked transport function by Frost and Lane (1985) has examined that the phenyl arsine oxide and tetravalent arsenicals turn off insulin-stimulated hexose transport by adipocytes. The site of modification has not been cleared but the specificity of reagent and reversal of their effect by 2, 3-dimercaptopropanol have represented the involvement of a pair of dithiols. Dithiol function in the signal transduction process starts when insulin phosphorylates the protein. Due to phosphorylation of the receptor, there was interconversion of hydrodynamic form to other by the involvement of disulfide-thiol results biological function of insulin (Maturo et al; 1983). After the discovery of the association of DLDH with the plasma membrane, other question came whether or not the interchange of disulfide-thiol occurs through cofactor lipoamide. To confirm this puzzle gas liquid chromatography-mass spectroscopy experiment was utilized to detect the lipoic acid in oxidized lipoate methyl ester. The sample was the first acid hydrolyzed to remove any protein attached with lipoic acid then extracted through dried benzene. Subsequently, hydrolysate was reduced by $NaBH_4$ to get reduced dihydrolipoamide from lipoic acid. Subsequently, the hydrolysate was passed through arsenical immobilized agarose column. These columns have the capacity to bind with any thiol-bearing residue. Bound dihydrolipoamide to the column is then eluted by 2, 3-dimercaptopropane sulhonic acid. This method confirmed the presence of lipoic acid cofactor in the vicinity of the receptor associated with DLDH that probably involvedin downstream signal processing of transport (Danson 1988).

1.2.12 α-keto glutarate dehydrogenase Complex (α-KGDH)

α-KGDH is one of the key multi-enzymes that regulates metabolic flux and catalyze non - equilibrium reaction. The complex converts α-ketoglutarate, CoA-SH, and NAD^+ into succinyl-CoA, NADH and CO_2 by utilizing thiamine pyrophosphate as a cofactor. The complex is regulated by ATP/ADP ratio, NADH/NAD^+ ratio, $Ca^{2+,}$ and availability of substrate in the mitochondria (Hansford 1980; Tretter and Adam 2005). α-KGDH complex comprises of multiple copies of three subunits (**Figure 1.13**) includes thiamine

pyrophosphate-dependent dehydrogenase (E1), dihydrolipoamidesuccinyltransferase (E2) and dihydrolipoamide dehydrogenase (E3). These enzymes perform catalytic reaction coordinately in a cyclic manner (Koike & Koike 1976).

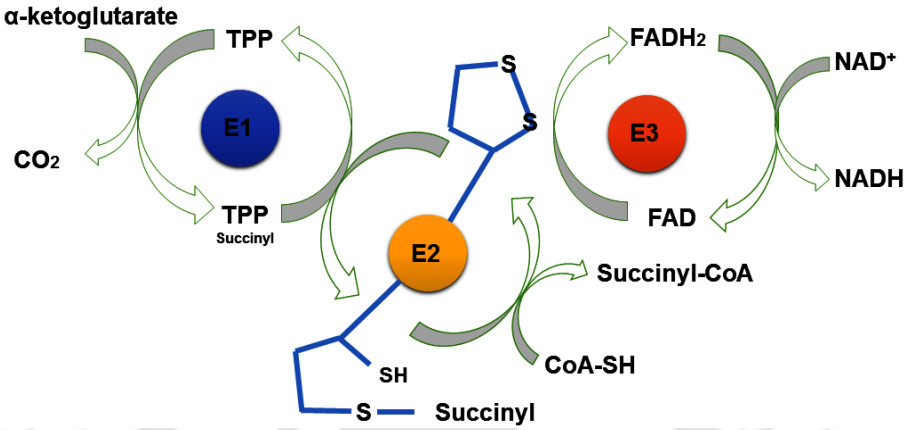

Figure 1.13: Schematic representation of α-KGDH complex. E1-enzyme (Thiamine pyrophosphate dependent dehydrogenase) perform decarboxylation of α-ketoglutarate. E2-enzyme (dihydrolipoamidesuccinyltransferase) transfer succinyl residue to CoA-SH. E3-enzyme (dihydrolipoamide dehydrogenase) catalyze reoxidation of reduced lipoate arm by using FAD cofactor.

1.2.12.1 Reaction catalyzed by E1-enzyme: The E1-enzyme performs decarboxylation reaction by utilizing TPP (thiamine pyrophosphate). It decarboxylates the α-ketoglutarate and transfers succinyl group to the reduced lipoate arm of E2-enzyme. TPP acts as a carrier between E1 and E2 enzyme. Other name of Vitamin B1 is thiamine, Aneurin and thiamin which is made of two ring thiazole and pyrimidine ring interconnected by a carbon atom. The nitrogen resides at the third position of thiazol ring have a positive charge that can accept electron in TPP dependent catalytic reaction. The biological active form of thiamine is thiamine pyrophosphate and thiamine diphosphate (TDP). Single hydroxyl (–OH) group at thiamine accept phosphate residue (**Figure1.14**).

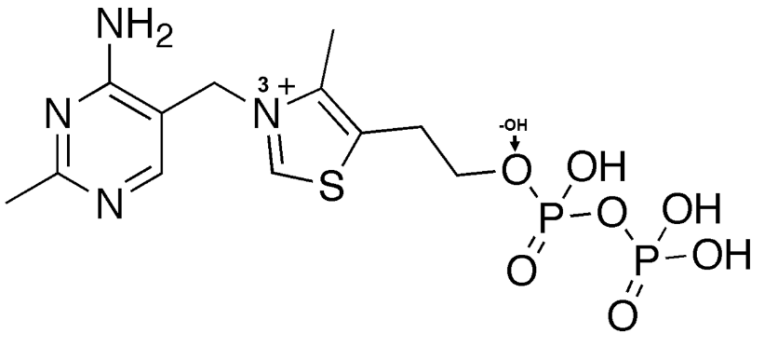

Figure 1.14: Molecular structure of Thiamine pyrophosphate (TPP). It resides as a cofactor in the E1-enzyme (Thiamine pyrophosphate dependent dehydrogenase) of α-KGDH. TPP involve in transfer process of decarboxylated substrate.

1.2.12.2 Reaction performed by E2-enzyme: E2-enzyme is substrate carrier protein (lipoic acid) that undergo oxidation-reduction events. E2-enzyme in the oxidized state take succinyl group and transfer it to the CoA-SH to form succinyl-CoA and left lipoate arm into the reduced state. This reduced intermediate is dihydrolipoamide that can be taken by the E3 enzyme for further processing.

1.2.12.3 Reaction performed by E3- enzyme: E3-enzyme keep lipoate arm of E2-enzyme in the oxidized state. The reduced form of lipoic acid (dihydrolipoamide) transform into oxidized form by converting a molecule of NAD^+ into NADH. Released NADH can be taken by the electron transport system in mitochondria to produce high energy for the cell. E3-enzyme belongs to flavo group means apo-E3-enzyme requires FAD as a cofactor for their proper folding and activity, reported in *E.coli* (Lindsay et al., 2000). FAD acts as a carrier for electron and proton exchange which acts as mediator between E3 and E2 enzymes. Now oxidized form of lipoate arm of E2-protein can further act as a substrate for next round of the cycle.

1.2.12.4 ROS generation mechanism by α-KGDH: Some studies suggest that dehydrogenase of the different multi-enzyme complex take part in ROS generation in mitochondria. Hence, concept behind the main source of ROS generation by respiratory chain has been challenged (Starkov et al., 2004; Tretter and Adam-Vizi 2004). As for the earlier report, dehydrogenase belongs to flavoprotein is the main source of activation of oxygen which forms hydrogen peroxide and superoxide (Massey 1994; Zhang et al., 1998). It has been reported that purified lipoamide dehydrogenase generates hydrogen peroxide in the presence of NADH (Gazaryan et al., 2002). The lipoamide dehydrogenase catalyzed reaction not only produce hydrogen peroxide but also less quantity of superoxide

in the ratio of 1:9 (Bando & Aki 1991). A metal ion Zn^{2+} inhibits the α-KGDH activity but enhance the oxidase activity of lipoamide dehydrogenase to induce ROS production (Sensi et al., 1999). In some studies, it has been suggested that the ratio of NADH/NAD^+ is an important regulator of ROS production through *α*-KGDH. Presence of NAD^+ can able to inhibit H_2O_2 generation by α-KGDH by 80%. Increased ratio of NADH/ NAD^+ favors the oxidase activity of lipoamide dehydrogenase so produce peroxide and superoxide (Tretter& Adam-Vizi 2004).

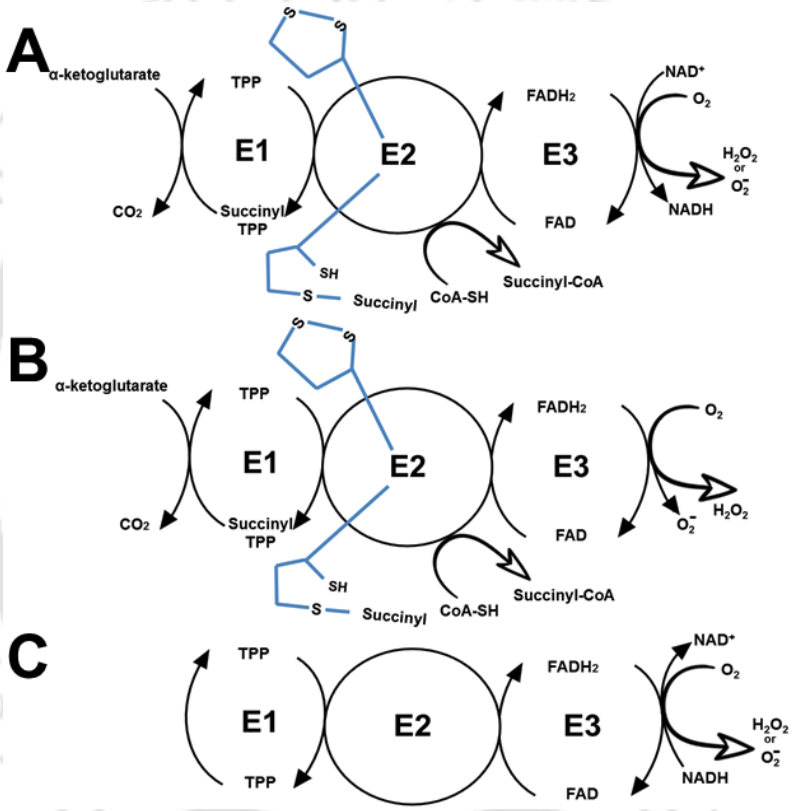

Figure 1.15. Diagram representing formation of ROS by α-KGDH complex. (A) ROS generation by α-KGDH in presence of all the component like coenzyme, cofactor and oxygen. (B) Increased ROS generation in absence of NAD^+ by α-KGDH. (C) ROS generated by α-KGDH in absence of substrate. Here NADH acts as electron and proton donor for radical (Oxygen) formation. E1, α-ketoglutarate dehydrogenase; E2, dihydrolipoamidesuccinyl transferase; E3, dihydrolipoamide dehydrogenase; TPP, thiamine pyrophosphate;

ROS generation can be favored in the absence of physiological electron acceptor NAD^+as well as α-ketoglutarate and CoA. For stimulation of ROS generation, no substrate is required, only NADH is enough to produce ROS. It clearly represents the active participation of ROS generation by lipoamide dehydrogenase upon the whole complex (Tretter& Adam-Vizi 2004).

1.2.12.5 Regulation of α-KGDH multienzyme complex: α-KGDH can be regulated by many factors includes metal ions, substrate or byproduct. There are reports that calcium ion (Ca^{2+}) even at 0.1-10 µM range plays a major role in the activation of the three mitochondrial dehydrogenases such as pyruvate dehydrogenase (PDH), isocitrate dehydrogenase and α-KGDH by regulating the rate of metabolism (Denton et al, 1978, Denton & McCormack 1979). The first evidence for the involvement of increased Ca^{2+} ion to activate the mitochondrial dehydrogenase that increases in level of cellular NADH was provided by Duchen et al. (1992). Regulation by Ca^{2+} is different for the different mitochondrial complexes. For α-KGDH, it mainly decreases the apparent $K_m$for α-ketoglutarate and dephosphorylates the enzyme in PDH (Denton et al, 1972; Pettit et al. 1972). Ca^{2+} at high concentration (100 µM) inhibits all the complexes instead of activation hence it shows the deleterious effect on neurons (Lai & Cooper 1986; Bulos et al, 1984; Sheu et al, 1985). Reactive oxygen species (ROS) is a crucial target of α-KGDH in the cell which is one of the regulatory sites in the mitochondrial metabolism. α-KGDH is not only the scavenger of ROS but also produce ROS and exert oxidative stress to the cell. During oxidative stress, ROS production became increase together with the decrease in their elimination. These stress cause cell damage by trauma, ischaemia, aging and several other neurodegenerative diseases (Olanow 1993; Siesjo et al.1995). Generally, ROS have toxicity towards many parts of the cell wheras, membrane is highly sensitive due to the presence of lipid. Polyunsaturated fatty acid present in the cell membrane is more sensitive towards peroxidation. Lipid peroxidation product is highly reactive that produce toxic aldehyde. One of the aldehyde, 4-hydroxy-2-nonenal (HNE) is the most reactive and toxic for the cell (Esterbauer et al. 1991). When cardiac mitochondria were exposed to HNE aldehyde, results in a decrease of α-KGDH activity. Apart from α-KGDH, PDH is also sensitive to HNE but remaining other mitochondrial dehydrogenase complex is insensitive. Investigation on the effect of HNE on the decrease of activity of α-KGDH and PDH is due to inhibition of lipoic acid bound E2-enzyme (Humphries and Szweda 1998). The electron transport system is also a rich source of ROS generation. Inhibition studies on electron transport enzyme reveal that complex I (NADH ubiquinone oxidoreductase) and Q-cycle (Starkov and Fiskov 2001; Turrens and Boveris 1980) is the main ROS generator. Other reports tell that α-KGDH activity in the brain mitochondria having lowest K_m among all other body parts thus α-KGDH acts as rate limiting step (Lai et al., 1977; Hansford 1980). Even in the brain, α-KGDH activity is not uniform everywhere. The

activity was found highest in cerebral cortex and lowest in the older part of the brain. The properties of enzyme in the neural system (brain) completely differ from the non-neural part. The neural part is highly sensitive to ammonia but non-neural part is less sensitive. Lai and Cooper 1986 found less sensitivity of α-KGDH isolated from rat heart or bovine heart. Some α-KGDH inhibitors of the bovine heart such as β-methylene- D, L-aspartate or D, L-vinyl glycine don't affect the brain mitochondria α-KGDH but L-aspartate significantly affects the brain mitochondrial α-KGDH but not bovine heart mitochondrial α-KGDH (Lai and Cooper 1986). Hence, the sensitivity of α-KGDH not only different for different byproduct but also it is position dependent.

1.2.13 Glycine Cleavage Complex (GCC)

Glycine is the simplest amino acid undergoes decarboxylation process to generate CO_2, $NH4^+$, and methylene ($-CH_2-$) residue. The product form by glycine catabolism is taken by H4-folate (tetrahydrofolate) by glycine synthase. During the catalysis coenzyme NAD^+ takes electron and proton to form NADH. Since GCC complex found in mitochondria so NADH can directly be utilized by electron transport system for high energy yield. GCC complex was originally reported in 1961 in an anaerobic bacteria *Diplococcuss glycinophilus*which was used for the fermentation of glycine into acetate, CO_2, and ammonia (Sagers and Gunsalus 1961). In one of the reports, a similar type of reaction was also mentioned by Richert and his colleagues in the homogenate of duck, pigeon and Chicken liver. They found an increased yield of CO_2 from the carboxylic group of glycine rather than α-carbon of glycine. The maximum number of the α-carbon reacted with another molecule of glycine to synthesize serine (Richert et al., 1962). An enzyme apart from GCC, serine hydroxymethyltransferase (SHMT) is also involved in serine formation. In 1966, Kawasaki et al. performed an experiment on rat liver mitochondria. They found that rat liver mitochondria is not only take part in glycine degradation but also in the formation of two glycine molecules from a single molecule of serine, bicarbonate, and ammonia (Kawasaki et al., 1966). The experiment performed by mitochondrial extract *in vitro* by taking different constituent of glycine synthesis and degradation revealed their reversible mode of reaction in all vertebrates livers and other parts body system. Hence, GCC is the most crucial pathways for any organism not only for glycine synthesis but also for serine degradation (Yoshida and Kikuchi 1973).

1.2.13.1 Reaction mechanism: The GCC includes three proteins and one carrier protein together perform three partial reactions to the inner side of the mitochondrial membrane (Motokawa and Kikuchi 1969). The four enzymes of GCC includes P-protein (Contains pyridoxal phosphate) or glycine dehydrogenase (perform decarboxylation reaction) (EC1.4.4.2), T-protein or aminomethyltransferase (EC2.1.2.10), L-protein or dihydrolipoamide dehydrogenase (EC1.8.1.4) and H-protein (lipoic acid carrier protein). The overall reaction mechanism is shown by GCC complex represented in **figure 1.16**.

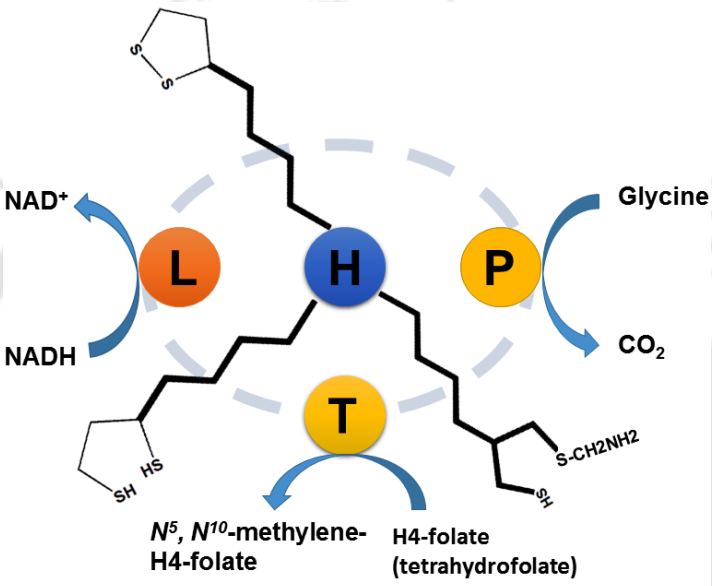

Figure 1.16: Schematic representation of GCC complex. P-protein (Glycine dehydrogenase), perform glycine decarboxylation; T-protein (Amino methyltransferase), transfer amino methyl group from glycine to reduced lipoate arm of H-protein; L-protein (dihydrolipoamide dehydrogenase), oxidation of lipoate arm; H-protein (carrier of lipoic acid cofactor) bear substrate dihydrolipoamide in bound stage.

1.2.13.2 Reaction performed by P-protein: P-protein having a molecular weight of 200 kDa is a homodimer (human, pea, chicken and *E.coli*) or a dimer of heterodimer [$(\alpha\beta)_2$] (*Eubacteriumacidaminophilus* and *Thermusthermophilus*) (Kume et al., 1991; Turner et al., 1992; Okamura-Ikeda et al., 1993). The cofactor pyridoxal phosphate attaches specifically to P-protein by lysine residue (Lys-704 in chicken P-protein) (Fujiwara et al., 1984). The first half reaction is decarboxylation performed by P-protein by utilizing H-protein as a co-substrate. In sequential step, first glycine carboxylic group release CO_2 then remaining part transferred to the sulfhydryl group of lipoate arm attached to H-protein. The intermediate formed between the lipoate arm and decarboxylated glycine can be recovered by gel permeation chromatography (Fujiwara et al., 1979). Attached decarboxylated glycine to the sulfhydryl can be confirmed by tracing remaining sulfhydryl

group to the lipoate intermediate and this has been confirmed by a crystallographic study in pea H-protein (Pares et al., 1994).

1.2.13.3 Reaction performed by T-protein: T-protein catalyze the cleavage and transfer of H-protein decarboxylated glycine moiety intermediate. Reaction utilizes H4-folate to give N^5, N^{10}-methylene-H_4folate, ammonia and reduced form of lipoate H-protein intermediate. This reaction can also be operated in the absence of H4-folate, formaldehyde will form as a product, instead of N^5, N^{10}-methylene-H_4-folate but the rate of the product formation will very slow (approximately 0.05%) (Fujiwara et al., 1984). The reversible reaction catalyzed by T-protein favors the formation of aminomethyllipoate intermediate by using N^5, N^{10}-methylene-H_4-folate, ammonia and reduced lipoate arm by a mechanism namely Ter-Bi. In this mechanism, H-protein first binds as a substrate than N^5, N^{10}-methylene-H4-folate, and ammonia. The order in which product release include H_4folate then intermediate decarboxylated glycine moiety loaded H-protein intermediate (Okamura-Ikeda et al., 1987). T-protein having a molecular weight of 40 kDa form complex with H-protein (Okamura-Ikeda et al., 1982). Interaction study was done through the crosslinking experiment reveals that interaction of H-protein with T-protein responsible for conformational change of T-protein. H and T-protein form complex at residue Asp43 and Lys288 in human GCC complex (Okamura-Ikeda et al., 1999). Mainly, N-terminal of T-protein interacts with H-protein for the proper function of GCC and the interaction (between H and T protein) makes the whole structure in a compact form (Okamura-Ikeda et al., 2003). Human crystal structure of humane T-protein was analyzed in free as well as in bound form with N^5-methyl-H_4folate, a similar compound as for their native product N^5, N^{10}-methylene-H_4folate (Okamura-Ikeda et al., 2005). The whole structure looks like three cloverleaf-structure in which H4-folate bound to pteridine ring resides at the central cavity. The human T-protein resembles the T-protein structure of *Termotoganaritima* (Lee et al., 2004), *Pyrococcus horikoshii* and *E. coli* (Lokanath et al., 2004). The mutational study performed on Human T-protein reveals that conserved Asp101 play a major role in the catalysis by enhancing the nucleophilic character of N^{10} atom of the substrate H4-folate (Okamura-Ikeda et al., 2005).

1.2.13.4 Reaction catalyze by L-protein: Finally, the last step of the reaction is catalyzed by L-protein. Similarly like other E3-enzyme, L-protein also belongs to flavo group and use FAD for their catalysis. It performs reoxidation (-S-S-) of H-protein attached with

reduced lipoate (-SH HS-) arm by consuming NAD^+ as a coenzyme. L-protein is similar to dihydrolipoamide dehydrogenase or E3-component of multienzyme complex (PDH, branched-chain-2-oxoacid and 2-oxoglutarate).

1.2.13.5 H-protein: H-protein, a monomeric structure having 14 kDa molecular weight which attached with lipoic acid in the core region by Lys59 in human (Fujiwara et al., 1986). The crystallographic study reveals the surface presence of lipoyl-lysine on H-protein. It acts as a shuttle for the intermediate and reduced lipoate at the active site region of GCC multienzyme complex. The mechanism is similar to 2-oxoacid dehydrogenase complexes where one substrate is converted into the product in a cyclic way (Perham et al., 2000). The lipoylation reaction on H-protein is catalyzed by two enzyme lipoate-protein ligase A (LplA) and acyltransferase (E2). The reaction is completed in two steps. In the first part, the enzyme LplA catalyze the transfer of AMP residue from ATP to lipoate and finally lipoyl-AMP to the H-protein or E2-enzyme. The crystallographic study of LplA protein showed that it has a large extended N-terminal domain as compare to C-terminal. These terminal form a pocket for binding of the substrate at their interface (Green et al., 1995; Fujiwara et al., 2005). In mammals, activation of lipoate residue performed by high-energy compound GTP in place of ATP to form lipoyl-GMP as an intermediate. Similarly, as lipoyl-AMP, lipoyl-GMP is also transferred to the H-protein or E2-enzyme (Fujiwara et al., 2001).

1.2.13.6 GCC complex in context to Trypanosomes: The GCC complex of *Leishmania* and trypanosomes resides in mitochondria as other organisms. It is also associated with three different protein and coded by three different genes includes P-protein (product of gene *GCV-P*) perform decarboxylation, T-protein (aminomethyl transferase, product of *GCV-T* gene), H-protein (carrier of dihydrolipoamide, encoded by gene *GCV-H*) and L-protein (dihydrolipoamide dehydrogenase). Several dihydrolipoamide dehydrogenases like protein have been predicted in trypanosomatidswhose metabolic function and their role needs to be established (Scott et al., 2008; Muller and Papadopoulou 2010). In one of the literature where *GCVP* (*gcvp*-) knock out was performed and found parasite sensitivity (growth retardation) towards methotrexate drug during serine limitation. This experiment suggests that *Leishmania* cannot take sufficient serine to compensate for the loss of GCC activity through an enzyme SHMT (serine hydroxyl methyltransferase). In*Leishmania*, SHMT present in both cytosol and mitochondria and involved in the synthesis of 5-CHO-H_4folate. This intermediate product is toxic to parasite so leishmania having other enzymes

namely 5-CHO-H_4folate cyclo-ligase that convert the intermediate into N^5, N^{10}-methylene-H_4-folate (Gagnon et al., 2006; Stover et al., 1993). Methylene-H4-folate is the product of three pathways and their relative contribution needs to be investigated. The enzyme SHMT present in *Leishmania* but absent in *T.brucei*so study about GCC complex in context to intermediate N^5, N^{10}-methylene-H_4-folate will be the attractive area of research (Vickers and Beverley 2011). The GCC regulation by different gene was studied by Muller and Papadoulou in 2009. They mainly focused their study on the regulation of T-protein of GCC complex. As for the study, T-protein is translated by two tandemly arranged copies of a gene that has a difference in the 3'UTR region which regulates GCVT-1 and GCVT-2 gene expression in both the morphological form of *L.infantum*. The GCVT-1 3'UTR is active during heat stress and shows higher expression in the promastigote stage. The other gene GCVT-2 3'UTR mainly interacts with SIDER (short interspersed degenerate retroelement) retroposon, which is responsible for amastigote specific expression of GCVT-2 protein. SIDER mainly involve in transcriptional regulation which present towards the 3'UTR region (Thomas et al., 2010).

1.2.14 Significance of the current work

The enzyme dihydrolipoamide dehydrogenase (DLDH) belongs to the multi-enzyme complex. These complexes include a group of the enzyme that regulates a specific metabolic step in crucial metabolic process. The major group of multi-enzyme complexes is PDH, GCC, and α-KGDH. In the present study, the biochemical importance of DLDH from *Leishmania donovani* (*Ld*DLDH) has been explored. *Ld*DLDH has two variants in the parasite LdBPK291950.1-Variant 1 and LdBPK323510.1-Variant 2. We were the first to report the less sequence similarities between variants. Hence, both the variants of the *Ld*DLDH were biochemically characterized. In the kinetic characterization, we found the difference in the K_m and V_{max} value of the variants. DLDH enzyme has two biological activities. In the first one, it can catalyze the physiological reaction by using a physiological substrate. Apart from the physiological substrate, it can also catalyze the reaction with another substrate (DCPIP, MTT) by transferring an electron to them called diaphorase activity. This activity was also observed with *Ld*DLDH variants. The enzyme belongs to flavo groups that was confirmed by HPLC. Active site residues of the variants were compared and found the absence of key residues in the first variant. The second variant active site is conserved as present in other similar groups of pyridine oxidoreductase enzyme. All the reported crystal structure have similar active site region

like the second variant but not a single study is available on variant 1 like an enzyme. The first time we recognize and reported the variation of active site residues within the *Ld*DLDH variants. These different residues around the active site were mutated and kinetic parameters were studied. Interestingly all the mutated residues showed a very large change of kinetic parameters. These studies clearly gave significant and clear cut importance of mutated residues in the catalytic reaction. Change of protein structure after the mutation was also analyzed through fluorescence study. Subcellular localization was also studied for the variants and found different compartmental localization. Our studies opened a new door of research towards variants of the enzyme.

CHAPTER II

Dihydrolipoamide dehydrogenase from *Leishmania donovani*: new insights through biochemical characterization*

2.1 ABSTRACT*

Dihydrolipoamide dehydrogenase (DLDH) regulates many crucial metabolic pathways as a multi-enzyme complex. *Leishmania donovani* dihydrolipoamide dehydrogenase (*Ld*DLDH) has two variants present on two different chromosomes with very less sequence similarities. In the current study, we cloned both the variants in pET28a (+) vector and expressed in Rosetta-gami (DE3) *E.coli* strain. Expressed proteins were finally purified from pellets using Ni-NTA (nickel-nitrilotriacetic acid) affinity chromatography. Purified enzymes were biochemically characterized and different kinetic parameters were studied. Both the variants showed maximum activity in pH range of 7.0 – 8.0 and temperature 50 ± 5 °C in the physiological direction. The estimated K_m for dihydrolipoamide (DLA) and NAD^+ were 2.7 ± 0.48 mM and 171.23 ± 11.59µM, respectively for variant 1 (LdBPK291950.1). In the case of variant 2 (LdBPK323510.1), K_m values for DLA and NAD^+ were found to be 829.85 ± 37µM and 226 ± 1.56µM, respectively. The variant 2 was more efficient in terms of activity. Apart from physiological activity, both the forms of the enzymes showed diaphorase activity as well. Calculated diaphorase activity for variant 1 for substrate 2, 6-dichlorophenolindophenol (DCPIP) and thiazolyl blue tetrazolium bromide (MTT) were 0.108 units/ml and 0.035 units/ml. However, for variant 2, diaphorase activity for DCPIP and MTT were found to be 0.054 units/ml and 0.00317 units/ml, respectively. Thereby, Variant 1 showed better diaphorase activity compare to variant 2. Sequence dissimilarities of both forms were analyzed for biological insights.

Complete work has been published in International journal of biological macromolecules. (2018), 112: 1241-1247.

2.2 INTRODUCTION

Protozoan parasites of the order kinetoplastida are the causative agents of many major neglected tropical and subtropical diseases. Leishmaniasis is one of such diseases caused by different species of *Leishmania* parasite. Different clinical manifestations of the disease, ranging from self-healing cutaneous to lethal visceral Leishmaniasis have been reported. Available drugs for the disease have severe side effects (nephrotoxicity, anemia, nausea, and vomiting), toxicity and drug resistance issues (Chappuis et al., 2007; Petiz et al., 2017; Santos et al., 2017, Andrade-Neto et al., 2018). Emergence of drug resistance presents new challenges that require new drug(s) targeting of novel unexplored enzymes/pathways. In the current work, we have investigated dihydrolipoamide dehydrogenase (*Ld*DLDH), a key metabolic enzyme of the parasite. The enzyme remains unexplored and has not been characterized extensively. *Ld*DLDH have two variants [LdBPK291950.1- Variant 1, LdBPK323510.1- Variant 2], present on two different chromosomes (29 and 32). It belongs to class-I pyridine-nucleotide disulfide oxidoreductase family that includes many other crucial redox enzymes such as trypanothione reductase and glutathione reductase. Enzyme catalyzes oxidation of dihydrolipoamide (DLA) to lipoamide (LA) by utilizing NAD^+ as an electron acceptor and FAD as an electron carrier. During oxidation DLDH transfers electron and H^+ to disulfide bridges of the enzyme. Further, FAD takes electron and H^+ to form $FADH_2$. This $FADH_2$ again transfers electron and H^+ to NAD^+ which forms final end product LA and NADH (Batista et al., 2008). The process of catalysis by DLDH is reversible in all organisms. In several organisms, the enzyme works as a multi-enzyme complex such as pyruvate dehydrogenase complex (PDH), α-ketoglutarate dehydrogenase (α-KGDH), branched-chain 2-oxo acid dehydrogenase complex (BCAAT) and glycine cleavage complex (GCC) where DLDH acts as an integral component and plays important catalytic role. LA is a substrate of DLDH covalently attached with E2-enzyme of multi-enzyme complex (PDH, GCC or BCAAT) that take part in transfer of decarboxylated intermediate in various metabolites of key metabolic pathways (Stacpoole 2017; McDonough et al., 2010; Xu et al., 2017; Scott et al., 2008). Assembly of these multi-enzyme complexes is reported to be crucial in many metabolism and energy production processes. In human, DLDH is shown to have anti-oxidative property due to the presence of FAD and NADH moieties. The substrate of the enzyme, α-Lipoic acid, is proposed as a treatment of many chronical diseases, including cancer (Dorsam and Hickerson, 2016). DLDH can also react with free DLA to form oxidized product LA. It also acts as diphorase due to the presence of flavin

moiety and oxidase activity of NADH. DLDH belongs diaphorase group of enzyme which can oxidize various dyes such as nitro blue tetrazolium (NBT), methylene blue and 2, 6-dichlorophenolindophenol (DCPIP) (Chakraborty et al., 2008). It has been reported that DLDH has the ability to transfer the electrons to variety of quinone derivatives (Roldan et al., 2011). Different antimicrobial compounds like nifuroxazide, nifuroxime and nifurprazine were used as an inhibitor against the target DLDH in *T. cruzi* and *T. brucei* and showed better efficacy as compared to the mammalian counterpart (Blumenstiel et al., 1999). In context with localization, it was found loosely associated with the inner side of the plasma membrane in bloodstream form of *Trypanosoma sps.* (Danson et al., 1987). To best of our knowledge, there is no report associated with mitochondrial DLDH in *Trypanosome sps*. The bloodstream form of *Trypanosoma* has no mitochondria and glycolysis is the only source of ATP production. Overall DLDH enzyme is crucial for different pathogenic organisms that making it a suitable target for future drug discovery efforts. In order to understand biochemical properties of the enzyme from *Leishmania donovani*, two different variants of the enzyme were cloned, expressed, purified and biochemically characterized.

2.3 MATERIAL AND METHODS

2.3.1 Strains and reagents

Leishmania donovani BHU1081 cells kindly donated by Prof. Shyam Sundar, Banaras Hindu University, India were grown in MI99 media (Sigma-Aldrich) with 15% FBS (Himedia) and cultured as reported earlier (Tiwari and Kumar 2016; Saudagar and Dubey 2011). Healthy parasites were harvested for genomic DNA isolation by Bioline genomic DNA isolation kit (Cat No. BIO-52066). Ni-NTA (Sigma-Aldrich) column was used for protein purification. DLA (Dihydrolipoic acid) and LA (DL-α-Lipoamide) were purchased from sigma-aldrich. FAD (Flavin adenine nucleotide), FMN (Flavin mono nucleotide), EDTA (Ethylenediaminetetraacetic acid), NADH (Nicotinamide adenine dinucleotide, reduced form), NAD^+ (Nicotinamide adenine dinucleotide), NaCl, K_2HPO_4 and KH_2PO_4 were purchased from Himedia. DCPIP and MTT were purchased from himedia and sigma-aldrich, respectively.

2.3.2 Sequence Analysis

The sequence of variant 1 & variant 2 was taken from geneDB (Logan-Klumpler et al., 2012) which were aligned to check the percentage similarity between them. Both the sequences were aligned by Clustal Omega (McWilliam et al., 2013). Aligned files

generated by Clustal Omega were downloaded and represented through ESpript3.0 (Robert et al., 2014) software. It represents the most similar sequence through red and gap through dotted line.

2.3.3 Cloning, expression and purification of two variants of LdDLDH

L. donovani genomic DNA was isolated through genomic DNA isolation kit from Bioline. Isolated genomic DNA was confirmed on 1% agarose gel (Sigma-Aldrich). Variant 1 (1527bp) & Variant 2 (1431bp) coding sequences was amplified from *L. donovani* genomic DNA using gene specific forward primer (Variant 1/ Variant 2 FP: AAGGATCCATGTTCCGCGAACATAG / CCGGATCCATGAAGCGCACTATCTTTG) and reverse primer (Variant 1/ Variant 2 RP: CGAAGCTTTTAGAAGTTGATCGTCTGCG / CCAAGCTTTCATTTATTGTG) synthesized from Bioserve Biotechnology Private Limited, Hyderabad India. For gene amplification, initial denaturation was performed at 95^{o}C for 3 min followed by total 30 cycles of denaturation at 95^{o}C for 30 sec, annealing at 59 ^{o}C and extension on 72 ^{o}C for 1.5 min (Variant 1). For variant 2, all other parameters were identical except annealing at 56 ^{o}C for 40 sec. The final extension were performed at 72 ^{o}C for 10 min. Amplified fragments (*Bam*HI & *Hind*III restriction site) and pET28a (+) (Novagen) vector were digested and ligated with each other through T4 DNA ligase (NEB). Ligation was done at 25 ^{o}C for 2 hrs in hot water bath followed by transformation in *E.coli* (*DH5α*). Positive clones were selected on kanamycin (Himedia) agar plate which was confirmed by amplification and digestion. Cloned plasmid pET28a (+) _Variant 1/pET28a (+) _Variant 2 were further transformed in Rosetta-gami (DE3) to over-express the protein. For expression of protein, overnight grown primary culture was used as inoculums for the secondary culture. Transformed Rosetta *E.coli* strains were selected on chloramphenicol and kanamycin (Himedia) positive LB (Luria-Bertani) media (Himedia). The conditions of protein expression were optimized after extensive optimization of parameters like temperature, IPTG concentration, and culture growth duration. Finally, the protein was expressed and purified from the pellet fraction.

2.3.4 Protein purification

Maximum expression of the protein was induced at optimized high IPTG concentration (0.5mM). Overnight grown secondary culture (2 liters) at 25^{o}C was harvested at 4000 rpm for 10 min, media was discarded and the pellet was re-suspended in lysis buffer (20 mM

Tris-HCl, 200 mM NaCl pH 8.0, 2.5% glycerol). Thereafter, the sample was sonicated with 6 on and 12 off cycle by sonicator (Sonics) followed by centrifuged on 10,000 rpm for 30 min. The supernatant was discarded and the pellet was taken for further processing. Thereafter, the pellet was solubilized in pellet solubilization buffer (Wash I: 500 mM NaCl, 20 mM Tris-HCl, 1% Triton-X-100, 2.5 mM EDTA, pH 8.0) followed by again centrifugation on 10,000 rpm for 10 min. After obtaining the washed pellet, the supernatant was discarded and the pellet was taken for further purification in a suitable buffer. Pellet was further washed in 500 mM NaCl, 20 mM Tris-HCl, 0.1% Triton-X-100 and 2.5 mM EDTA. Again centrifuged on 10,000 rpm for 10 min and the pellet was again washed with 500 mM NaCl & 20 mM Tris-HCl. Each washing was performed two times to remove undesirable protein. After third washing, finally centrifuged on 10,000 rpm for 10 min and pellet was solubilized in final optimized concentration of urea (Himedia). Maximum yield was observed at 8 M urea therefore, this concentration was used for protein solubilization. The solubilized protein was centrifuged on 10,000 rpm for 30 min and the supernatant was passed through Ni-NTA column. Purified protein was eluted in 500 mM imidazole. Finally, protein was dialyzed in 40 mM potassium phosphate buffer pH 7.5 with 300 mM NaCl and 10 µM FAD to remove imidazole and urea to refold the protein. All the condition for protein expression and folding was taken the same for both the variants of the enzyme.

2.3.5 pH and temperature optimization

Recombinant *Ld*DLDH enzyme was utilized for activity assay. The enzyme kinetic assays were performed in physiological direction. For activity assay, the enzymes (30 µg) was incubated with fix concentration of DLA and NAD^+ (2mM each) at a given pH or temperature. The mixture was incubated for 10 minutes for end point enzyme assay and increase in NADH absorbance at 340 nm was measured. The optimum conditions for pH and temperature were evaluated by doing enzyme assay at different pH and temperature range.

2.3.6 Dihydrolipoamide dehydrogenase kinetic parameters

Enzymatic assays were performed in 40 mM potassium phosphate buffer (pH 7.5 and temperature 37 °C), 1 mM EDTA with different concentrations of DLA and NAD^+. Progression of the reaction was analyzed by measuring the increasing absorbance of NADH at 340 nm in 10 minutes. For variant 1, K_m and V_{max} were performed by varying the concentration of DLA from 250 µM to 7 mM with fix NAD^+ (2 mM) concentration. Similarly, K_m and V_{max} of NAD^+ were calculated by employing a range of NAD^+

concentration 50 µM to 3mM on a fixed concentration of DLA (2 mM). Likewise, for the variant 2, K_m and V_{max} for DLA and NAD+ was calculated using concentration range of 100 µM to 7 mM and 50 µM to 3 mM keeping fixed concentration (2 mM) of NAD^+ or DLA (Loher and Krauth-Siegel 1990; Santos et al., 2016).

2.3.7 Diaphorase activity assay

Diaphorase is the ubiquitous class of flavin bound enzyme that has the ability to reduce various dyes by utilizing the reducing equivalent of NADH or NADPH. Time kinetics was performed with both the variants of the enzyme on a fixed concentration of 40 µM DCPIP and MTT with 200 µM NADH. The concentration of enzyme was taken 30 µg per reaction in a final reaction volume of 1 ml and progression of reactions was monitored by the decrease in absorbance at 340 nm in case of DCPIP or increase in absorbance at 570 nm in case of MTT on 30 ºC and pH 7.5 in variant 1. In variant 2, same concentration of DCPIP and MTT was used as variant 1 at pH 8 and at temperature 25 °C. It is worth mentioning that the diaphorase activity operated as a reverse reaction. Hence, optimum temperature and pH conditions for the same were used for the assay. One unit of *Ld*DLDH will oxidize 1 µmole of NADH or MTT per minute. For the calculation of diaphorase activity of variants, we utilized the following formula (Savage et al., 1957).

$$\textbf{Unit/ml} = \frac{(\Delta A/\text{min Test} - \Delta A/\text{min Blank})\ (\text{Total volume of assay})\ (\text{Dilution factor})}{(\text{Millmolar extinction coefficient})\ (\text{Volume of enzyme used})}$$

2.3.8 Cofactor identification

Many redox enzymes use FAD/FMN as an electron carrier to catalyze oxidation reduction reaction that comes under flavo enzyme group. DLDH is one of those flavo enzymes that catalyze redox reaction by utilizing FAD as a cofactor. The dependency of *Ld*DLDH variants on FAD cofactor was confirmed through HPLC (Ultimate 3000, Thermo Fischer scientific). For that, purified enzymes were treated at 100 °C for 10 min in dark. Thereafter, protein sample was further centrifuged on 13,000 rpm for 10 min at 4 ºC (Aliverti et al., 1999), in order to obtain FAD in supernatant for identification. Standard of 1.50 nM of FAD and test sample were run through HPLC and peaks were separated on 60% potassium phosphate buffer with 40% acetonitrile. Presence of FAD in variant was confirmed by comparing peak with standard (Absorbance was taken at 265 nm).

2.4 RESULTS

2.4.1 Sequence Analysis

Sequences of both the variants of *Ld*DLDH were analyzed (**Figure 2.1)** which showed significant differences in sequence alignment. It has been reported that about 11 amino acid (GGTCLNVGCIP) residues on active site around disulfide in DLDH are highly conserved among different organisms (Kim 2002). However, BLAST analyses showed that this sequence is not very conserved in both variants of *Leishmania donovani*. In variant 1, the conserved residues are as Thr48-Cys49-Leu50-Asn51-Val52-Cys54-Pro56 while variant 2 shows the sequence of the conserved region as Ala48-Asp49-Phe50-Trp51-Asn52-Ala54-Glu56. Interestingly, in variant 2, part of catalytic residues Cys-49 and Cys-54 (makes Disulfide Bridge) were found completely absent in variant 1. Further, the variant 1 also has a C-terminal extension region as compared to variant 1 as shown in **Figure 2.1**.

2.4.2 Cloning, expression, and purification of LdDLDH variants

Both the variants were cloned in pET28a (+) cloning vector and positive clones were confirmed by amplification through PCR and restriction digestion. Variant 1 & variant 2 positive pET28a (+) vectors were confirmed by amplification of 1,527 bp and 1,431 bp amplicon, respectively (**Figure 2.2A and 2.2B**). Further, both the variants were also confirmed by restriction digestion through the release of 1,527 and 1,431 bp fragments (**Figure 2.2C and 2.2D**). Sequence and frame of the insert was confirmed by sequencing. Finally, cloned (pET28a_Variant1/pET28a_Variant2) vector was transformed into Rosetta-gami (DE3) *E.coli* strain. Protein expression and molecular weight was confirmed by running the recombinant enzyme on 10% SDS-PAGE (**Figure 2.2E and 2.2F**). Protein bands of mass 56.3 kDa and 50.6 kDa corresponded to the molecular weight of variant 1 and variant 2 of *Ld*DLDH, respectively.

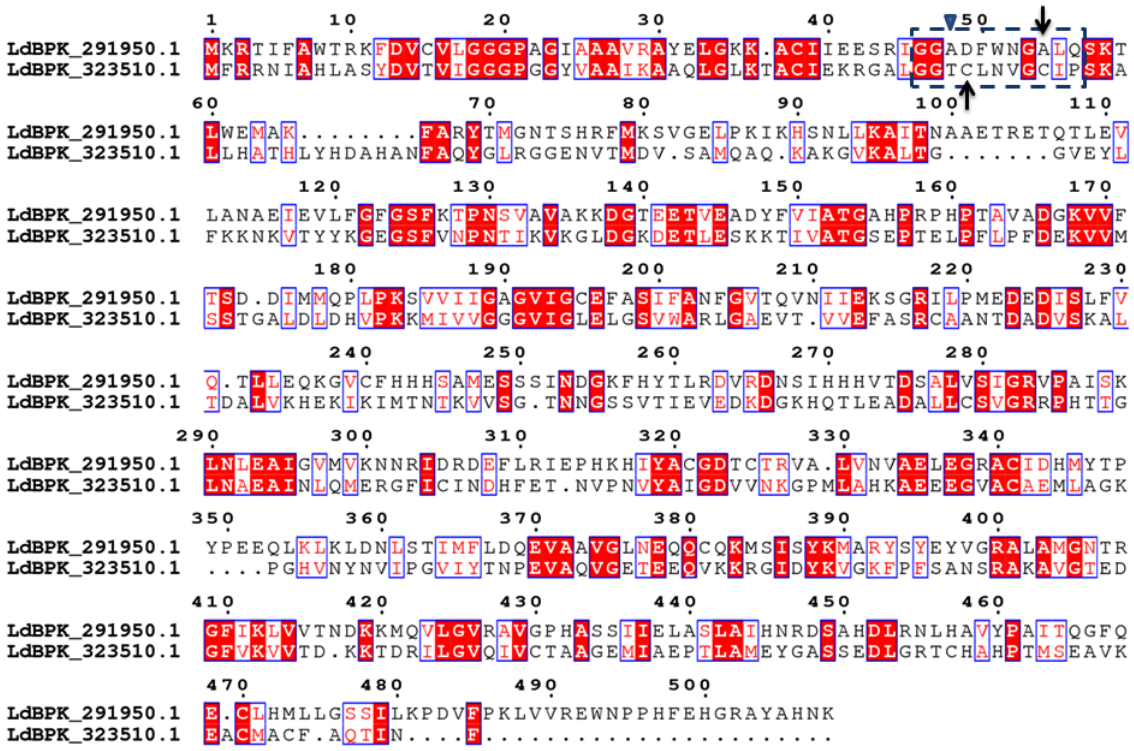

Figure 2.1: BLAST Analysis of *Ld*DLDH variant 1 (LdBPK291950.1) and Variant 2 (LdBPK323510.1). Red highlighted area representing conserved residues between variants. Black arrow represents cysteine residues on active site of variant 2 that involved disulfide bridge formation. Open rectangle shows similar type of amino acid. Dotted area represents gaps between sequences. Area surrounded by broken rectangular box (46-54) represents active site residues and blue color inverted triangle depicts important key residue threonine in variant 2 (Hakjung 2002).

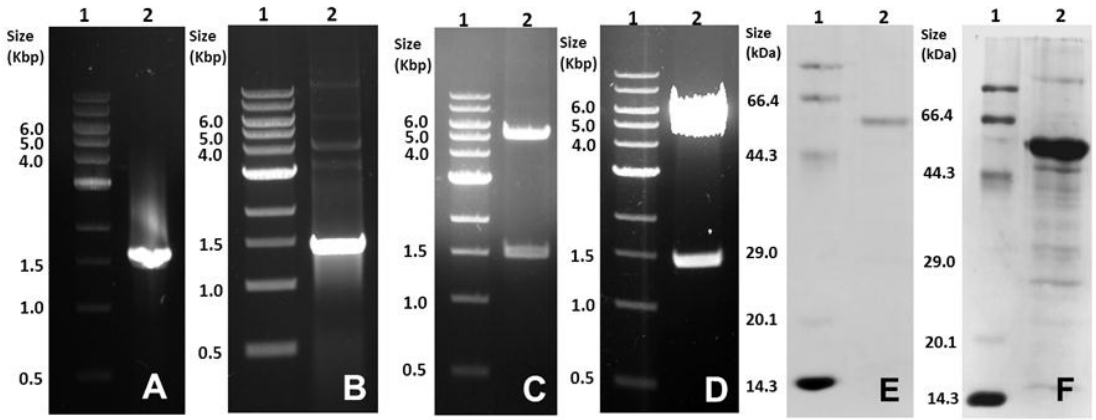

Figure 2.2: Cloning and expression of *Ld*DLDH variants. **(A)** Gene amplification of variant1 (1527 bp in lane 2) **(B)** Gene amplification of variant 2 (1431 bp in lane 2) **(C)** Clone confirmation through restriction digestion by *Bam*HI and *Hind*III and release of fragment (1527 bp in lane 2) for variant 1. **(D)** Clone confirmation through restriction digestion by *Bam*HI and *Hind*III and release of fragment (1431 bp in lane 2) for variant 2. Both clones were also confirmed by sequencing. Protein expression on 10 % SDS-PAGE **(E)** purified variant 1 of mass 56.3 kDa shown in lane 2. **(F)** Purified variant 2 of mass 50.6 kDa shown in lane 2. Lane 1 in **(A), (B), (C)** and **(D)** represents 1 kbp DNA ladder**. (E)** and **(F)** shows low range protein marker.

2.4.3 pH and temperature optimization

Conditions for enzymatic activity were optimized by utilizing a range of pH and temperature. Enzyme activities at different pH and temperature gradient were evaluated.

Variant 1 displayed the highest activity at 50 ± 5 °C (**Figure 2.3A**). Enzyme activity was also analyzed at pH range of 4.0 -10.0. Variant 1 showed maximum activity at pH 7.5 to 8.0 (**Figure 2.3B**). In reverse reaction, the highest activity of variant 1 was observed at 25 to 37°C and pH of 7.0 - 7.5 (**Figure 2.3C and 2.3D**). Similarly, optimum activity for variant 2 was evaluated in both the directions by varying temperature and pH conditions. The highest activity of second variant in the forward direction was observed at a temperature and pH of 50 °C ± 5 °C and 7.5, respectively (**Figure 2.3A and 2.3B**). Reverse kinetics showed maximum activity at pH 8.0 and temperature 25 °C, respectively (**Figure 2.3C and 2.3D**).

2.4.4 Dihydrolipoamide dehydrogenase (LdDLDH) kinetic assay

Variant 1 was characterized by employing different concentrations of DLA or NAD^+ keeping one of the substrate concentration fixed. The K_m value of DLA and NAD^+ was found to be 2.7 ± 0.48 mM and 171.23 ± 11.59 µM, respectively (**Figure 2.4A and 2.4B**). Similarly, for the Variant 2, K_m of DLA or NAD^+ was estimated to be 829.85 ± 37µM and 226 ± 1.56 µM, respectively (**Figure 2.4C and 2.4D**). Standard deviation was taken from three independent experiments. Enzymatic assays for determination of kinetic parameters were performed at physiological temperature (37 °C) and pH (7.5).

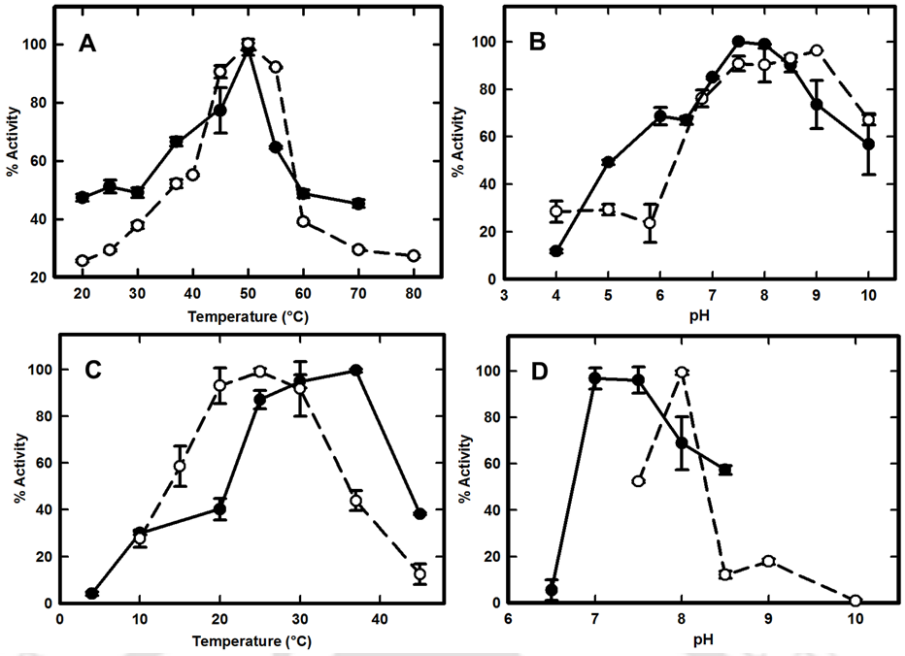

Figure 2.3: Enzymatic properties of *Ld*DLDH variants 1(●) and variant 2 (○). (A) Temperature and **(B)** pH optima in the forward direction. **(C)** Temperature and **(D)** pH optima in the reverse direction.

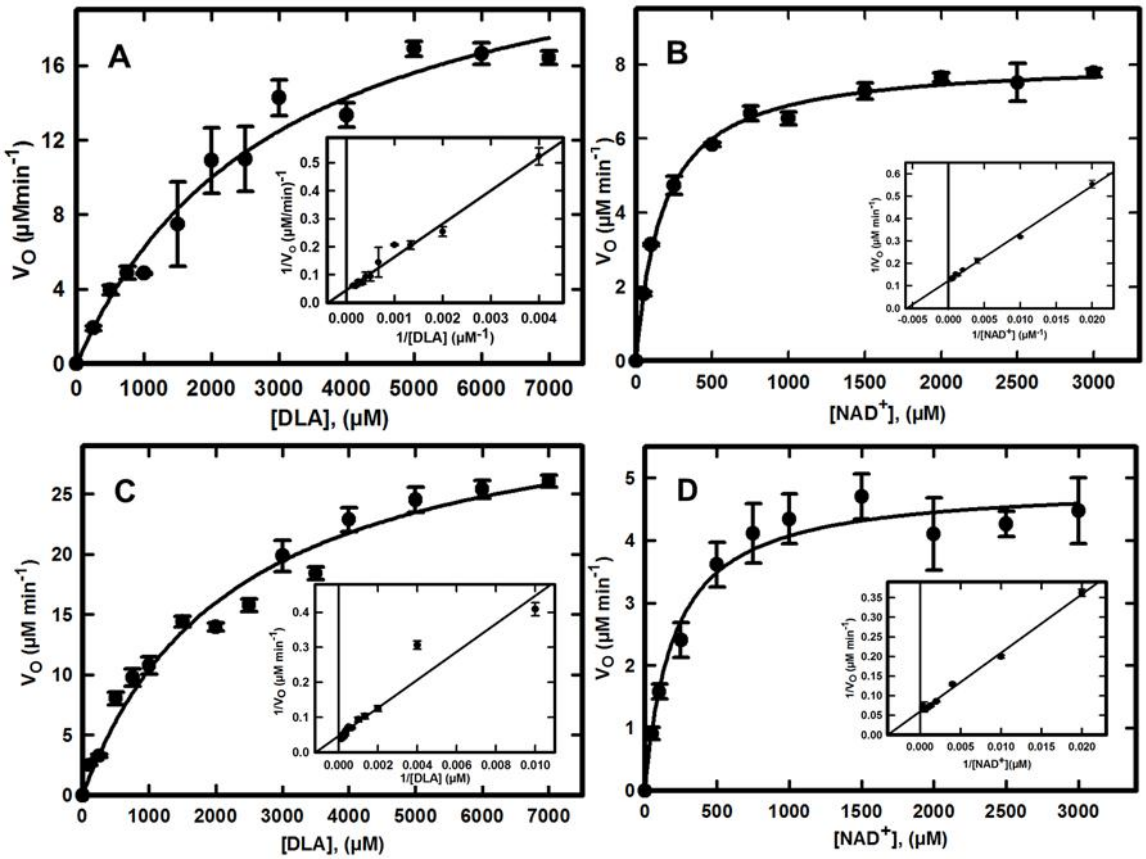

Figure 2.4: End point assay of *Ld*DLDH variant 1 & variant 2 and determination of kinetic constants. Effect of varying concentration on kinetics of *Ld*DLDH variant 1 (**A)** DLA (0.25Mm - 7mM) or **(B)** NAD^+(0.05mM-3mM) at fixed concentration of other substrate (2mM). Likewise, Effect of varying concentration of **(C)** DLA (0.1mM-7mM) or **(D)** NAD^+(0.05mM-3mM) on kinetics of *Ld*DLDH variant 2 at fixed concentration of other substrate (2mM). The inset of all figures shows L-B plot of data for calculation of K_m and V_{max}.

2.4.5 Diaphorase activity assays of LdDLDH variants

Time kinetics was performed with both the variants of *Ld*DLDH. MTT and DCPIP dyes were utilized to analyze diaphorase activities of the variants. Diaphorase activity of variant 1 with DCPIP and MTT was found to be 0.108 units/ml and 0.035 units/ml (**Figure 5A and 5B**). Likewise, for variant 2, diaphorase activity in context with DCPIP and MTT was 0.054 units/ml and 0.00317 units/ml, respectively (**Figure 2.5C and 2.5D**).

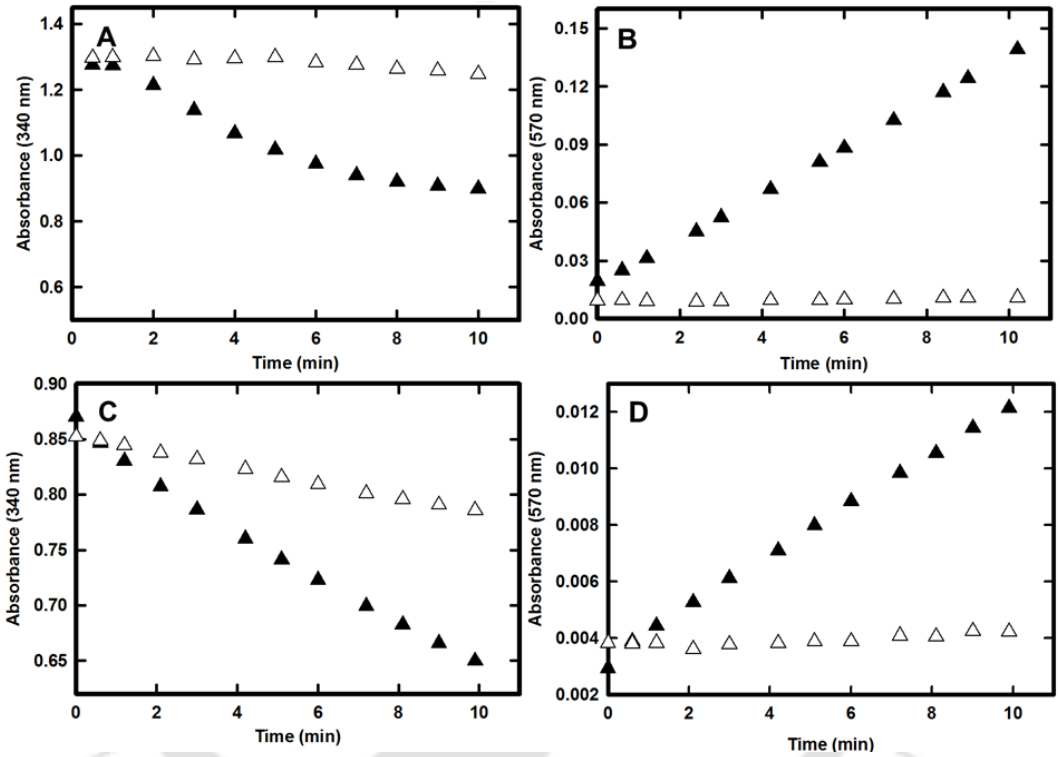

Figure 2.5: Diaphorase activity assays of *Ld*DLDH variants. Time kinetics of variant1 with different dyes. **(A)** DCPIP or **(B)** MTT. Similarly, time kinetics of variant2 with different dyes. **(C)** DCPIP or **(D)** MTT Open triangle (Δ) represents blank (without enzyme) and closed triangle (▲) test (with enzyme).

*2.4.6 Cofactor dependency of variants of Ld*DLDH

In most of the organisms dihydrolipoamide dehydrogenase belongs to flavo enzymes family which means they need FAD as a cofactor for their activity. Hence, we checked whether variant 2 of *Ld*DLDH require FAD for their activity or not. By HPLC based estimation, it was found that *Ld*DLDH requires FAD as a cofactor for their catalysis. Sharp peak was observed at 3.71 min in standard (1.5 nM FAD from Sigma-Aldrich) as well as in test sample indicates the presence of FAD (**Figure 2.6**). The cofactor identification of variant 1 didn't give consistent result; thus it is not reported.

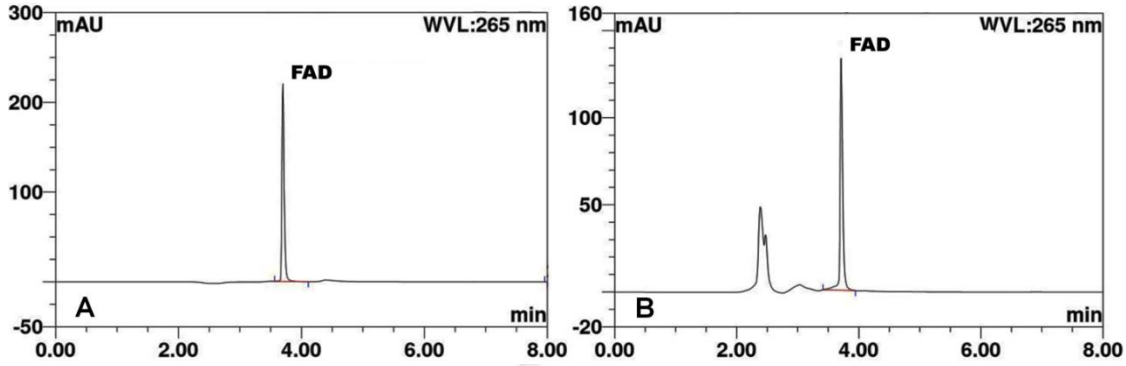

Figure 2.6: FAD identification in variant 2. (A) Standard curve of 1.50 nM FAD (Sigma-Aldrich) through HPLC. **(B)** Chromatogram of test sample. X-axis denotes retention time (min) and y-axis milli-absorbance unit (mAU).

2.5 DISCUSSION

In the present study, we report the presence of two different variants of *Ld*DLDH with significant sequence differences with many gaps during BLAST analysis and C-terminal extension in the variant 1. The sequence analyses by online server indicate that the variant 2 has mitochondrial signal sequence in its N-terminal and likely to be localized in mitochondria of the parasite. The variant 1 do not have such signal sequence and appears to be localized in other cellular compartment. We may relate these differences with some different functions in unique cellular compartment for these two variants. Furthermore, the variant 2 has oxidation reduction mechanism catalyzed through disulfide bond between two cysteine residues at 49 and 54 (hypothesized by BLAST analysis with human DLDH). Role of disulfide bond in catalysis of dihydrolipoamide dehydrogenase is also reported in other organisms (Kim 2002; Arenas et al., 2014) but interestingly we found that variant 1 doesn't have these two consecutive cysteine residues. These cysteine residues are replaced by other amino acid residues aspartate and alanine in variant 1. This also points out towards a possible difference in catalytic mechanism.

In our study, we cloned, expressed, purified and characterized both the variants of *Ld*DLDH. During expression we found that variant 2 had higher expression (0.6 µg/µl) as compared to variant 1 (0.12 µg/µl). Variant 2 is more kinetically active compare to variant 1. It has higher K_m value and V_{max} that achieved at higher substrate concentration. Further, pH optima for these two variants in reverse directions seems to be very different. Both variants have significant activities at lower pH. However, the variant 1 has higher activity at acidic condition hinting toward role of the enzyme in phagolysosomes or other acidic

compartment of the cell. Taken together, the data indicate unique metabolic functions of these variants in their respective cellular compartment.

In previous reports, investigators failed to detect NADH dependent diaphorase activity in *T.cruzi* DLDH (Lohrer and Krauth-Siegel 1990) but there are some reports about drugs (Nitro furan derivatives) that associate with diaphorase mode of action and generate different radicals that damage nucleic acid of the parasite (Maya et al., 2003). First time we are reporting the diaphorase activity associated with *Ld*DLDH variants and showed with two dyes (MTT and DCPIP). Diaphorase activity associated with *Ld*DLDH can be utilized to design new drugs against *Leishmania donovani*, if we could able to make a compound that can accept electrons by NADH. Radical based drug designing will be beneficial over substrate dependent drug development. Substrate dependent drug development may bypass the de novo pathway but radical based drug development cannot be bypassed

CHAPTER III

The role of amino acid C15, C38, A48, D49, and A54 in unexplored variant of *L. donovani* dihydrolipoamide dehydrogenase (LdBPK291950.1)*

3.1 ABSTRACT*

In our current study, five amino acid residues (C15, C38, A48, D49, and A54) from *Ld*BPK291950.1 (*Ld*DLDH_Variant1) has been mutated and expressed mutants were compared with wild type for their role in catalytic activity as well as in the structural stability. As this enzyme belongs to pyridine nucleotide-disulfide oxidoreductase family, Cys-15 is assumed to be one of the members of disulfide bond formation with another partner due to their negligible activity (very high K_m=18 mM for DLD) obtained during the kinetic study. Apart from its high K_m value, no product fluorescence peak was observed during spectral analysis, clearly revealing their role in catalytic as well as in structural stability. Another mutant, Cys-38 showed a similar value of K_m for DLD compare to wild type whereas, 8 times increase in the value of NAD^+, revealing their role in the binding of NAD^+. In other experiments, deviation of fluorescence spectral pattern compare to wild type or product peak obtained during fluorescence spectral studies, clearly indicates their role in catalytic function or doesn't involve in the disulfide bond formation. However, the fluorescence spectral peak of FAD was also found to be shifted compared to wild type, validating its role in FAD binding. Mutants A48I and D49G showed a decrease in K_m value of DLD together with the change in fluorescence spectral pattern compared to wild type indicating their role in catalytic function. All the five mutants showed approximately 3 times increase in K_m value of NAD^+ in comparison to the wild type, revealing its role in NAD^+ binding whereas deviation of the spectral pattern from wild type represented their role in structural stability together with catalytic function.

**** Part of the work is submitted for publication***

3.2 INTRODUCTION

Leishmaniasis, a parasitic disease mainly affecting the tropical and subtropical area is caused by *Leishmania* parasite with diverse clinical manifestations from self-healable cutaneous leishmaniasis (CL) to most fatal visceral leishmaniasis (VL). A disease VL spread by the parasite *Leishmania donovani* and *Leishmania infantum* affect mainly the visceral organs of the human system such as liver, kidney and bone marrow. Different available therapeutics against leishmaniasis have certain levels of resistance issues or toxicity effect and thus innovation in the direction of novel target selection is an instant need for the development of effective therapeutics. Dihydrolipoamide dehydrogenase (DLDH), a crucial enzyme involved in different major metabolic pathways belongs to pyridine nucleotide-disulfide oxidoreductase family. Other members of this family include glutathione reductase (GR), trypanothione reductase (TR) and thioredoxin reductase (TdR) together regulating redox metabolism of the system (Williams 1976). The enzyme belongs to pyridine nucleotide -oxidoreductase, perform the oxidation-reduction process by active site disulfide bridges through FAD as a cofactor with NAD^+ as an electron acceptor. Enzyme DLDH present as an integral part of multienzyme complex in pyruvate dehydrogenase complex (PDH), glycine cleavage complex (GCC) and branched chain amino acid aminotransferase complex (BCAAT) (Reed 1974; Walker and Oliver 1986). DLDH enzyme present in the different organism from bacteria to eukarya possesses most conserved active site residues reported as GG (TV) **C**LN (VX) G**C**IP (Kim 2001). Other residues around two cysteines have also been reported as a key regulator of catalytic activity such as Thr-44, Ile-51, and Lys-54. The mutational substitution of Ile-51 (ATT) into Ala (GCT) in human dihydrolipoamide dehydrogenase (Human DLDH) was performed in order to validate the involvement of the catalytic activity of Ile-51 which was found to be 100 fold decrease in the activity (Kim 2006).

Lysine-54 (K54) and glutamate-192 (E192) in human DLDH stabilize thiolate-FAD intermediate during the catalytic process. Their key role in catalytic reaction or thiolate-FAD stabilization was investigated through substitution of Lys-54 by glutamic acid (K54E) and SK-KS E3s (S53K54-K53S54) showing reduction of 25% bound FAD compared to the wild type, depicting their role in the interaction of FAD-DLDH. These substitutions also significantly reduced the K_m value for dihydrolipoamide (DLD) (forward reaction) and lipoamide (LA) (reverse reaction), representing their role in the catalytic process. Point mutation of Glu192 by glutamine (E192Q) also showed markedly reduced

K_m value for both the substrates (Liu et al, 1999). Human DLDH (homodimeric structure) deficiency due to mutations is always fatal. A point mutation at T148 and R281 represented significant change of the specific activity of the enzyme. However, total FAD content showed significant decrease as compared to the wild type human DLDH. Mutational study suggested that T148 is not important for catalytic function whereas, residue R281 plays a crucial role in catalytic activity (Wang et al, 2008). Other mutants of human DLDH such as N286 and D320 showed a decrease in the specific activity and FAD content, representing their role in the catalytic function (Wang et al, 2007). Mutation at His452 and Glu457 by glutamine showed the corresponding decrease of specific activity and destabilization of the transition state. His-452 substitution by glutamine (Gln-452, Gln-457) showed 0.2% decrease in specific activity and about 6.4 kcal mol^{-1} change in the transition state of human DLDH. Glu-457 to glutamine destabilizes the transition state by 1.7 kcal mol^{-1} and decreases the K_m for dihydrolipoamide by 4.3 fold (Kim and Patel, 1992). Sequence alignment of human DLDH with another organism such as *Sus scrofa domesticus*, *Saccharomyces cerevisiae*, *Escherichia coli*, and *Pseudomonas fluorescens* suggested that Pro-325 and Trp-366 are highly conserved. Their substitution (Pro325Ala) showed a decrease in the catalytic activity. On the other hand, replacement of Trp-366 by Ala-366 doesn't affect the catalytic function, but decrease in the amount of mutant during purification reflecting their role in proper expression or folding of the enzyme (Kim 2013). *Azotobacter vinelandii* DLDH crystal structure suggested that Thr is involved in FAD binding through interaction by adenosine phosphate of FAD. In human, the role of Thr44 in DLDH has been established by substitution through Ala. Although Thr44 doesn't affect the structure and function of DLDH, its conservation throughout different organisms suggested that Thr44 may provide proper microenvironment (hydrophilic) around FAD-binding region, as reported with the three-dimensional structure of *Azotobacter vinelandii* DLDH (Kim 2002). In human DLDH, it has been reported that catalytic center containing disulfide cysteine has an unusual bond which shows relatively shorter C^{α}-C^{α} distance between cysteine residues with unique torsion angle (Mattevi et al, 1991).

Distribution of DLDH enzyme in the different organism is not universal. In *Trypanosoma brucei*, it has been reported that the enzyme DLDH present at the inner leaflet of plasma membrane towards the cytosolic face (Danson et al., 1987; Jackman et al., 1990). In human, the nuclear localization of PDH complex has also been reported. Sub-cellular fraction analysis of T-cells revealed that PDH-E2 is also associated with some nuclear protein (Chueh et al., 2011). Another report suggests that DLDH is also present in

cytoplasmic and mitochondrial fractions of *Paracoccidioides lutzii* fungus (Landgraf et al., 2017). Hence, there are variations present in the subcellular localization of DLDH in different organisms. The enzyme DLDH in *Leishmania donovani* has two variants which are present on two different chromosomes (chromosomes 29 and 32). However, these two variants have very less similarities with each other, even at the active site. Catalytic site sequence in variant 1 (Ala48-Asp49-Phe50- Trp51-Asn52-Ala54-Glu56) is completely different from variant 2 (Thr48-Cys49- Leu50-Asn51-Val52-Cys54-Pro56). Cys-49 and Cys-54 (disulfide bridges -s-s-) active site residues in variant 2 is completely absent in variant 1 (chromosomes 29) as per our previous report (Chiranjivi and Dubey 2018). In our current study, five mutations were performed in *Ld*DLDH_Variant1 which was kinetically as well as structurally compared with wild type protein for their role in catalytic function and structural stability.

3.3 METHODS AND MATERIALS

3.3.1 Parasites, cell lines, and Chemicals

The parasite *Leishmania donovani* (MHOM/IN/2010/BHU1081) was graciously provided by Prof. Shyam Sundar, Banaras Hindu University, India. It was grown in MI99 (Sigma-Aldrich) media supplemented with 15% heat-inactivated fetal bovine serum (FBS) (HiMedia), antibiotic solution (1x) containing penicillin and streptomycin (HiMedia). Genomic DNA isolation kit, PCR Clean-up kit, PCR master mix, and T4 DNA ligase was obtained from Takara (Clonetech). Primers were synthesized by BioServe Biotechnologies, Ltd. All the enzymes for restriction and digestion were obtained from Imperial Life Sciences (NEB). Bacterial media component like yeast extract, tryptone, NaCl and antibiotics (Ampicillin and Chloramphenicol) were purchased from HiMedia. Other buffer components such as Tris-HCl, dithiothreitol (DTT), glycerol and ethylenediaminetetraacetic acid (EDTA) were taken from HiMedia. Substrate (Dihydrolipoamide and Lipoamide) for the kinetic studies were purchased from Sigma-Aldrich. Other substrates like NAD+, NADH, 2, 6-dichlorophenolindophenol sodium salt (DCPIP), and thiazolium blue tetrazolium bromide were obtained from HiMedia. Bio-Rad Ni-NTA beads were utilized for affinity purification of His-tag containing protein. All the kinetic studies were performed in Evolution 201 UV-Visible spectrophotometer, Thermo Scientific. Fluorescence data was generated in FluoroMax®-4, Horiba Scientific.

3.3.2 Sequence Analysis

Sequence of DLDH enzyme from different organism whose PDB structures has been submitted in PDB database were aligned by multiple sequence alignment tools Clustal Omega (Sievers et al., 2011) to analyze the sequence similarity between them. Aligned sequence was represented through ESpript 3 server (Robert and Gouet, 2014). Red highlighted area represented in aligned sequence shows conserved residues throughout the organisms. Protein sequence of *Ld*DLDH_Varainat1 and *Ld*DLDH_Variant2 was aligned together with 1JEH (Yeast E3), 1ZMC (*Homo sapiens*), 2A8X (Mycobacterium tuberculosis), 2QAE (*Trypanosoma cruzi*), 2QAE (*Trypanosoma cruzi*), 1DXL (*Pisum sativum*), 1JEH (Yeast E3), 1LVL (*Pseudomonas putida*), 4JDR (*E.coli*) and 1ZMC (*Homo sapiens*). Conservation of different amino acid residues of active site from different organisms were represented by open broken rectangular area.

3.3.3 Modelling of LdDLDH_Variant1 and LdDLDH_Variant2

Both the variant of *Ld*DLDH was modeled by modeller 9.21 (Webb and Sali, 2016). This software is used for homology or comparative modeling of 3D-protein structure. Modeller utilizes most similar templates for modeling execution. The protein sequence of both the variants was aligned with different known DLDH PDB structure sequence and most top four similar structures were utilized as a template for modeling. During modelling, total four templates were utilized which includes 1JEH (Yeast E3), 1ZMC (*Homo sapiens*), 2A8X (*Mycobacterium tuberculosis*) and 2QAE (*Trypanosoma cruzi*) for *Ld*LDH_Varinat1 or 2QAE (*Trypanosoma cruzi*), 1DXL (*Pisum sativum*), 1JEH (Yeast E3) and 1ZMC (*Homo sapiens*) for *Ld*LDH_Varinat2, respectively.

3.3.4 Site-directed mutagenesis of LdDLDH_Variant1 and cloning of mutant variant in pMAL-p5x vector

Total of five point mutations (C15T, C38G, A48I, D49G, and A54I) were inserted in the coding region by PCR based method (Darshan et al., 2009). Mutations were inserted in two self-complementary primers (MFP: Mutated forward primer; MRP: Mutated reverse primer) manually. Other sets of two primers (NFP: Normal forward primer & NRP: Normal reverse primer, without mutation) were also utilized that was complementary to 5’ and 3’ end of the gene of interest (*Ld*DLDH_Varainat1). These four sets of primer were used to perform mutation simply by two steps of PCR reaction. All the primer sequences having

inserted mutation is listed in **table 3.1** and the process of mutation has been mentioned in **Fig. 3.1**.

In 1st PCR reaction for each mutation, two combinations of primer were taken (N_{FP} & M_{RP}; M_{FP} & N_{RP}) in two PCR tubes. *L. donovani* genomic DNA was used as a template to amplify *Ld*DLDH_Variant1 gene. For each reaction, 50 ng of template, 1x PCR master mix, and 0.25 µM primer were mixed together. Subsequently, the final volume of the reaction mixture was maintained at 20 µl by nuclease-free water. Total 30 cycles of amplification (Denaturation at 95ºC for 0.35 sec; annealing temperature were taken as for primer for 0.35 sec; extension at 72ºC for 1.5 min, respectively) were performed to get ample amount of amplified product. At the end of 1st PCR two fragments were amplified which was run on 1% agarose gel. Further, both the fragments were utilized as a template for second sets of PCR set up to get the mutated fragment.

In 2nd PCR reaction, two fragments from 1st PCR were taken in equal concentration. Initially for the first step, 5 min Initialization was performed for the end extension to make full length fragment followed by normal primer (N_{FP} & N_{RP} containing 10xHIS-tag) was added for 30 cycles to make amplified product of mutated gene (Initialization at 95 ºC for 35 sec, annealing at 59º for 35 sec and extension at 72ºC for 1.50 min). All the mutated amplified fragments were cloned in pMAL-p5X vector (NEB cat No. N8109S). For that, vector and insert (mutated fragment) were digested with *Bam*HI and *Hind*III at 37ºC for 3 hrs. Finally, ligation was performed at 25ºC for 2 hrs by T4 DNA ligase. The ligated mixture was transformed in *E. coli* DH5α (DE3 strain) to screen positive clone which was selected in ampicillin (+) agarose plate. Finally, the clone was confirmed by amplification and digestion.

Table 3.1: List of primers of all the mutants and *Ld*DLDH_Variant1 for mutation.

S.No.	Sequence Name	Sequence
1.	*Ld*DLDH_Variant1_A48I_FP	CGTATCGGCGGTATTGACTTTTGGAATGGCGCGCTGCAG
2.	*Ld*DLDH_Variant1_A48I_RP	CTGCAGCGCGCCATTCCAAAAGTCAATACCGCCGATACG
3.	*Ld*DLDH_Variant1_D49G_FP	CGTATCGGCGGTGCTGGTTTTTGGAATGGCGCGCTGCAG
4.	*Ld*DLDH_Variant1_D49G_RP	CTGCAGCGCGCCATTCCAAAAACCAGCACCGCCGATACG
5.	*Ld*DLDH_Variant1_A54I_FP	CGTATCGGCGGTGCTGACTTTTGGAATGGCATTCTGCA
6.	*Ld*DLDH_Variant1_A54I_RP	TGCAGAATGCCATTCCAAAAGTCAGCACCGCCGATACG
7.	*Ld*DLDH_Variant1_C38G_FP	CTAGGGAAAAAGGCCGGCATTATTGAAGAGTCC
8.	*Ld*DLDH_Variant1_C38G_RP	GGACTCTTCAATAATGCCGGCCTTTTTCCCTAG
9.	*Ld*DLDH_Variant1_C15T_FP	AGGAAATTCGATGTTACAGTGCTAGGCGGTGGT
10.	*Ld*DLDH_Variant1_C15T_RP	ACCACCGCCTAGCACTGTAACATCGAATTTCCT
11.	*Ld*DLDH_Variant1_FP	TTGGATCCATGAAGCGCACTATCTTTGCATGGA
12.	*Ld*DLDH_Variant1_10HIS_RP	AAGCTTTTAATGGTGATGGTGATGGTGATGGTGATGGT GTTTATTGTGCGCGTACGCGCGCCCGTGCTCGAAATGA GGTGGATTCCATT **(10 His-tag sequence included)**

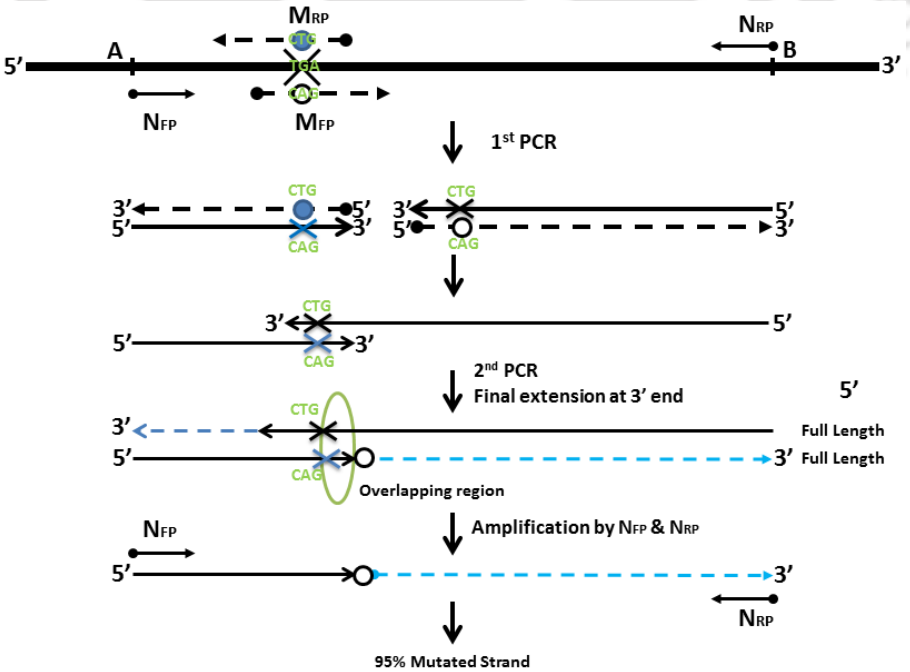

Figure. 3.1. Schematic illustration of site directed mutagenesis (SDM) procedure. Site of mutation in the sequence has been shown in crossed sign. Three letter nucleotide sequence like TGA, CTC, and CAG shown in figure to make the procedure easily understandable. NFP, Wild type forward primer (without mutation); NRP, Wild type reverse primer (without mutation); MFP, (Mutated forward primer); MRP (mutated reverse primer). Region A to B represents gene sequence of LdDLDH_Variant1.

3.3.5 Protein expression and purification

Positive clone of *Ld*DLDH_Variant1 mutants was transformed in Rosetta-gami strain (DE3) for protein expression. A single colony of mutants was inoculated in 5 ml LB tubes (Luria-Bertani broth) containing dual antibiotics (chloramphenicol & ampicillin) for selection at 37ºC for overnight in the incubator which was used as an inoculum for secondary culture. This primary culture (1%) was inoculated in 3 liters LB media in respective antibiotic at 37ºC for 3-4 hrs, till to O.D 0.4-0.6. Afterward, secondary culture was induced by 0.25mM IPTG and kept for overnight at 16 ºC. Next day, culture was centrifuged at 10,000 rpm for 10 mins. Afterward, supernatant was discarded and pellet was suspended in lysis buffer (50mM Tris-HCl, 500mM NaCl, 0.05% NaN3, 5% glycerol, 0.5mg/ml lysozyme pH 8.5). Further solubilized pellet was sonicated with 3 secs on cycle and 25 secs off cycle for 45 mins followed by sample was centrifuged at 10,000 rpm for 30 mins. Pellet was discarded and the supernatant was filtered through a 0.2 µm filter. Desired protein was purified from crude protein by Ni-NTA (nitriloacetic acid) affinity purification. Finally, the purified protein was eluted at 500mM imidazole which was dialyzed in 3 liters 50mM potassium phosphate buffer (pH 7.5) with 300mM NaCl to remove imidazole. Protein concentration was measured by Bradford from the standard graph of BSA.

3.3.6 Enzymatic assays of E3 mutants

Mutants and wild type *Ld*DLDH_Variant1 were enzymatically characterized to confirm the role of mutated amino acid residues in catalysis and FAD binding. Procedure for calculation of kinetic parameters (K_m & V_{max}) were followed from previous articles (Laine et al, 2015; Håkansson and Smith 2007; Dos et al, 2016) with modification in range of substrate concentration. K_m and V_{max} of DLD for each mutant were determined by taking the range of concentration (0.50-8 mM), at the same time another substrate NAD^+ (2 mM) was kept constant. Similarly, for NAD^+ concentration range was taken 0.25-4 mM for calculating kinetic parameters by fixing the DLD concentration (2 mM). All the reactions were performed in 50 mM potassium phosphate buffer with 10 µg of enzyme concentration. Physiological pH (7.5) and temperature (37ºC) were utilized for all the kinetic parameter study. Temperature and pH optima for *Ld*DLDH_Variant1 has been reported in our earlier publication (Chiranjivi and Dubey, 2018). Each experiment was performed in duplicate and all the graphs were plotted by Sigma-Plot software.

3.3.7 Fluorescence spectroscopy

All the fluorescence experiment were performed in FluoroMax®-4, Horiba Scientific, spectrofluorometer. Initially, proteins were excited at 296 nm and emission spectra were recorded between 300 and 600 nm (Liu et al., 1999). Effect of NAD^+ and DLD on fluorescence emission spectra of enzyme and their mutants were analyzed. Reading were recorded in 50mM potassium phosphate buffer with 750 µM NAD^+, 2 mM DLD and 100 µg of proteins. Data was transferred on ASCII file and finally, spectra were drawn through Sigma-plot.

3.4 RESULTS

3.4.1 Sequence Comparison of both the variants of LdDLDH with different organism of DLDH represents devoid of key catalytic residues

Active site residues of DLDH from different organisms were aligned with *Ld*DLDH variants (**Fig.3.2**). In all aligned organisms, the sequences GGTCLNVGCIP is conserved which has been represented as a broken black color rectangular box in **Fig. 3.2**. Previous studies as well as in aligned sequences in our study, two cysteine residues are conserved throughout the organism. Previous reports tells that disulfide (C-**S**-**S**-C) bridge take part in the catalytic process of flavo-enzyme whereas in *Ld*DLDH_Varaint1 is devoid of such conserved cysteines. However, other active site residues in *Ld*DLDH_Varaint1, GGTCLNVGCIP (present in all other organisms along with *Ld*DLDH_Varaint2) are replaced by GGADFWNGALQ (*Ld*DLDH_Variant2).

3.4.2 Structural comparison of known PDB structure of Trypanosoma cruzi lipoamide dehydrogenase (PDB ID: 2QAE_A) with modelled structure of LdDLDH variants shows devoid of key residues

*Ld*DLDH variants were modeled by modeller 9.21 which was further analyzed by Ramachandran plot to confirm their structural stability. Ramachandran plot for *Ld*DLDH_Variant1 and variant 2 has been shown in **Fig. 3.3**. Both the variant's active site were compared with known PDB structure of *T. cruzi* lipoamide dehydrogenase **(***T. cruzi* LADH**)** and all the interactions were analyzed for the difference of their activity. All the reported PDB structure of family pyridine oxidoreductase in PDB database have similar conserved residues at an active site like that of *Ld*DLDH_Variant2, whereas *Ld*DLDH_Variant1 have completely different conserved residues at the active center even at the structural level. It has been reported that cysteine-cysteine disulfide bridge (C-**S**-**S**-

C) involved in catalytic process in DLDH enzyme whereas even in the modeled structure of *Ld*DLDH variant1, we found devoid of disulfide bridge at the catalytic center. However, *Ld*DLDH_variant2 have similar disulfide structure as present in other reported PDB structure of pyridine oxidoreductase enzyme. In **Fig. 3.4A**, key catalytic residue in *T.cruzi* LADH Cys-41 and Cys-46 is replaced by Asp-49 and Ala-54 in *Ld*DLDH_Variant1, respectively. Similarly, other residues at the catalytic center such as Thr-40, Leu-42, Asn-43, Val-44, and Ile-47 of *T.cruzi* LADH are replaced by Ala-48, Phe-50, Trp-51, Asn52, and Leu-55, respectively. Other variants (**Fig. 3.4B**) have exactly similar residues as present in *T.cruzi* LADH even at the structural level, which shows a very high degree of similarity (76.77%).

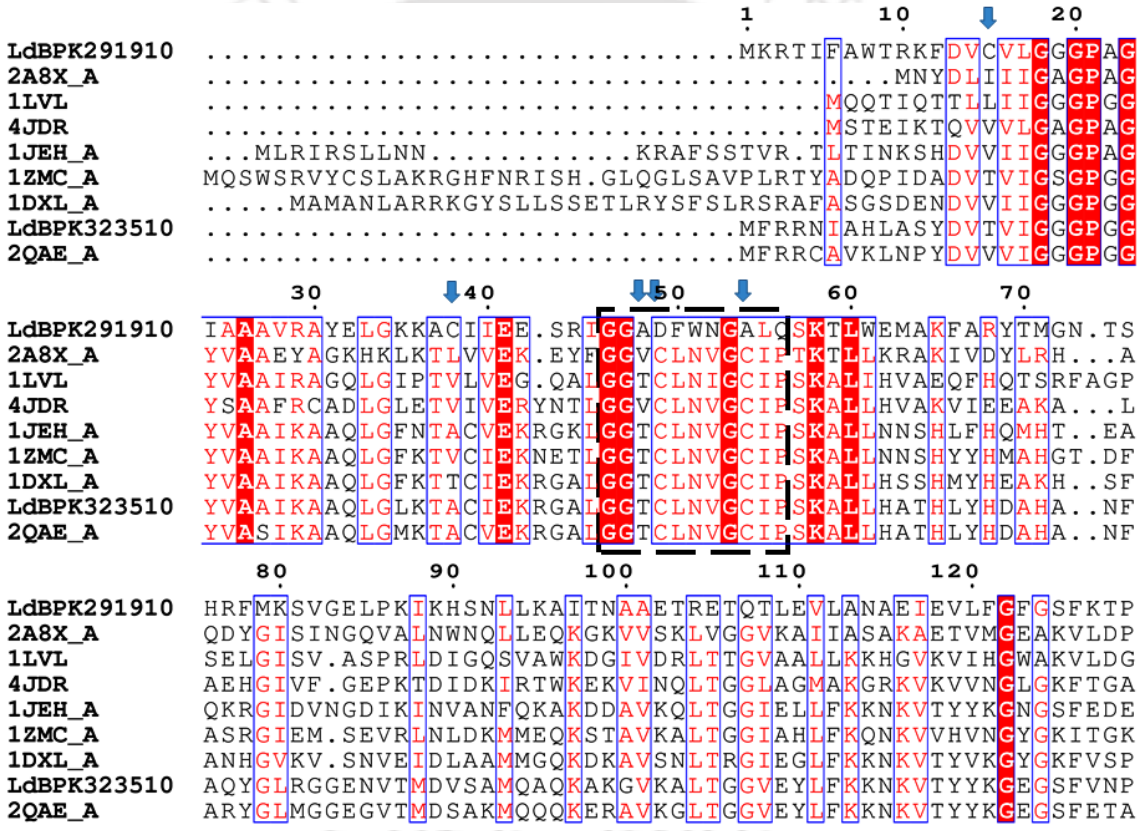

Figure. 3.2. N-terminal sequence alignment of dihydrolipoamide dehydrogenase from different organism. LdBPK291910 (*Ld*DLDH_Varaint1), *Mycobacterium pneumoniae* (PDB ID: 2A8X_A), *Pseudomonas putida* (PDB ID: 1LVL), *Escherichia coli* (PDB ID: 4JDR), *Saccharomyces cerevisiae* (PDB ID: 1JEH_A), *Homo sapiens* (PDB ID: 1ZMC_A), *Pisum sativum* (PDB ID: 1DXL_A), LdBPK323510 (*Ld*DLDH_Variant2), *Trypanosoma cruzi* (PDB ID: 2QAE_A). Open broken black color rectangular area (46-54) represents active site residues throughout the organism. Blue color arrow represent residue of interest. Cys-49 and Cys-54 absent in *Ld*DLDH_Varaint1 but present in other shown organism. These two cysteine amino acid play major key role in flavo-enzyme catalytic activity. Red highlighted residue depicts identical residues. Blue rectangular area represent similar amino acid residues.

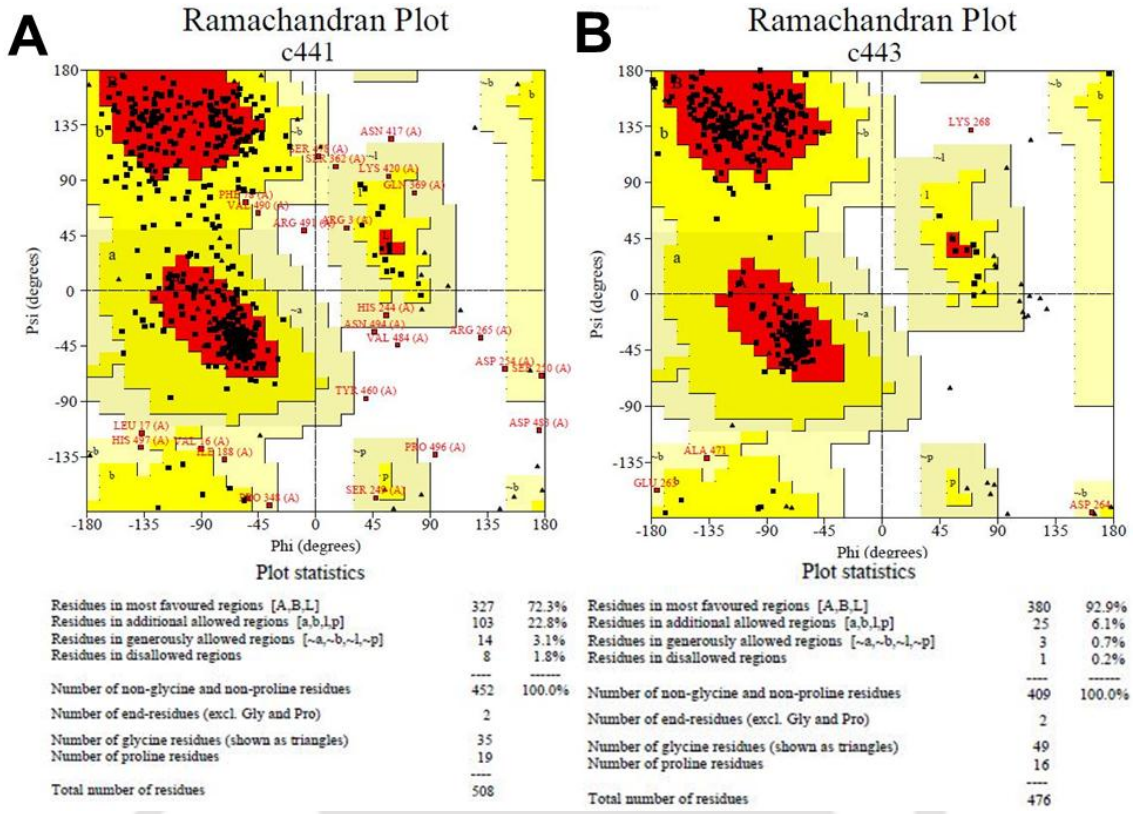

Figure. 3.3. Ramachandran plot of *Ld*DLDH_Variant1 (A) and *Ld*DLDH_Variant2 (B).

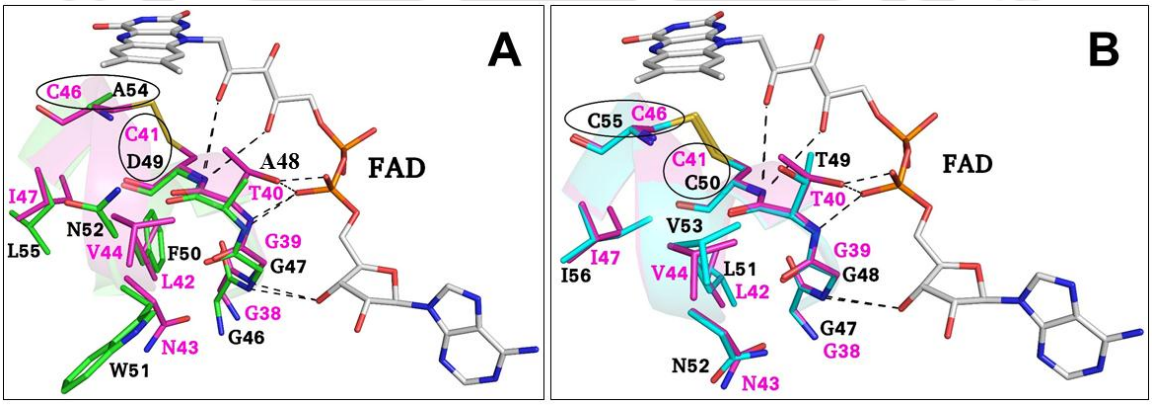

Figure. 3.4. Overlaid structure of known PDB structure of *T.cruzi* LADH (PDB ID: 2QAE) with *Ld*DLDH variants. (A) Overlaid structure of *Ld*DLDH_Variant1 on *T.cruzi* LADH. Green color stick structure represent variant 1 active site residues (predicted from BLAST analysis of variant 1 with variant 2). Green and black color labelling depict active site residues of *T.cruzi* LADH and *Ld*DLDH_Variant1, respectively. (B) Overlaid structure of *Ld*DLDH_Variant2 on *T.cruzi* LADH. Pink color stick structure shows variant 2. Pink and cyan color labelling represent catalytic site residues of *T.cruzi* LADH and *Ld*DLDH_Variant2, respectively. FAD structure in both the figures shown in cyan color. Some of the back bone of the protein and side chains has been deleted in both the figures for clear representation and visibility. Black circled residues are the key residue involved in catalytic process that completely absent in variant 1 whereas present in variant 2.

3.4.3 Cloning and protein expression confirmation of LdDLDH_Variant1 mutants

Five key mutations (A48I, D49G, A54I, C15T, and C38G) were performed in *Ld*DLDH_Variant1. To perform a mutation, two PCR reactions were performed. Amplified fragments of the first PCR reaction is shown in **Fig 3.5A**. In case of mutation of A48I, D49G and A54I, the larger fragment is shown amplified at 1,398 bp and smaller fragment at 178 bp. Other mutants like C15T and C38G showed amplification of larger fragment at 1,472 bp and 1,409 bp, smaller fragment at 54 bp and 117 bp, respectively. Second PCR reaction gave amplified mutated fragment at 1,526 bp with all mutated residues (**Fig. 3.5B**). The amplified fragment was cloned in pMAL-p5X vector between *Bam*HI and *Hind*III site. A positive clone was confirmed by amplification (**Fig. 3.5C**) and restriction digestion (**Fig. 3.5D**). Mutated proteins were expressed in Rosetta-gami strain (DE3) and expression was confirmed by a band of 99 kDa on 12% SDS-PAGE (**Fig. 3.5E**). Wild type *Ld*DLDH_Variant1 was amplified from genomic DNA and cloned in pMAL-p5X vector. A positive clone was similarly expressed in Rosetta-gami strain (DE3) as other mutant and expression are represented in **Fig 3.5E**. Clone confirmation of wild type *Ld*DLDH_Variant1 didn't shown in **Fig. 3**.5. However, insert (wild type gene, *Ld*DLDH_Variant1) cloned in pET28a_*Ld*DLDH_Variant1 (cloning reported in our earlier publications (Chiranjivi and Dubey 2018) was digested by *Bam*HI and *Hind*III. Subsequently, released insert after digestion was cloned in pMAL-p5X vector. Expression of pMAL-p5x_*Ld*DLDH_Variant1 (wild type) has been shown in **Fig. 3.5E** which was confirmed by the band size of 99 kDa on SDS-PAGE.

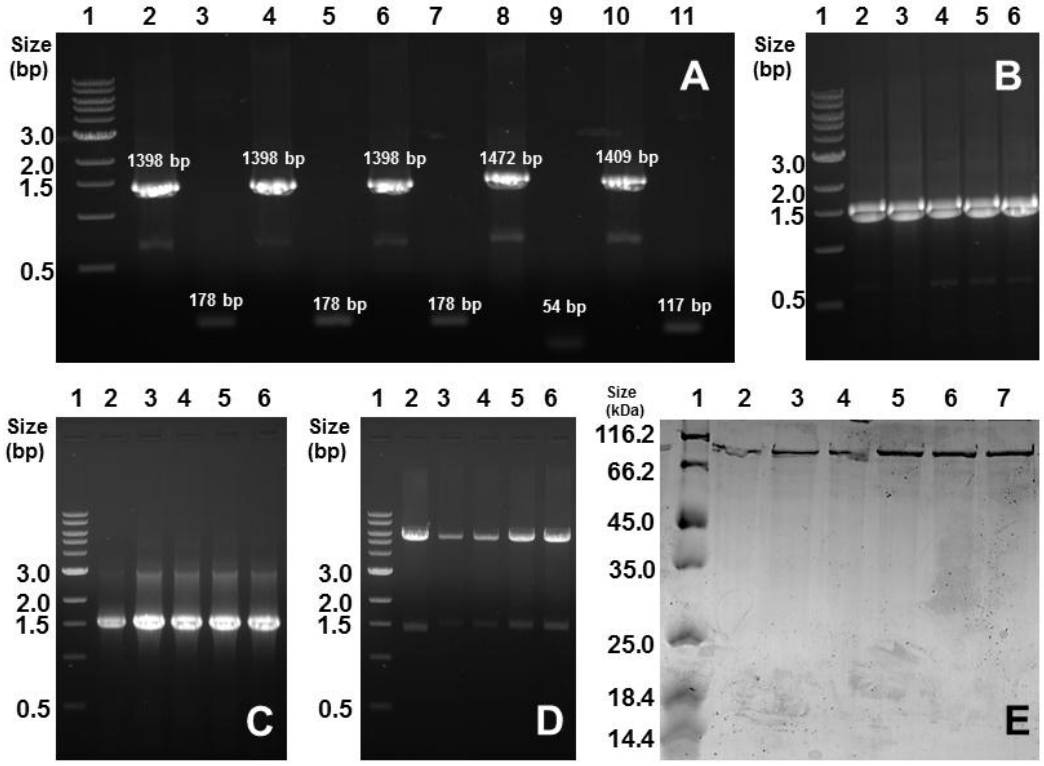

Figure. 3.5. Site directed mutagenesis and expression of *Ld*DLDH_Variant1. (A) Amplified product of 1st PCR reaction. Lane 2 (A48I), 4 (D49G), 6 (A54I), 8 (C15T) and 10 (C38G) represent amplified product by NFP and MRP. Lane 3 (A48I), 5 (D49G), 7 (A54I), 9 (C15T) and 11 (C38G) depict amplified fragment by MFP and NRP. (B) PCR amplification (1,526 bp) by 2nd PCR. (C) And (D) Clone confirmation by PCR and restriction digestion by *Bam*HI and *Hind*III (1,526 bp). In figure A, B, C and D; Lane 1, 1 kb DNA Ladder. (B), (C), (D) and (E) Lane 2, 3, 4, 5 and 6 is respective mutants such as A48I, D49G and A54I, C15T, C38G,. Cloning was performed in pMAL-p5x NEB vector (periplasmic expression vector). (E) Expression of wild type and mutants on 12 % SDS-PAGE. Lane 1-7 represents protein marker, Variant1 (Wild type), A48I, D49G, A54I, C15T and C38G.

3.4.4 Kinetic Parameters analysis of different mutants of LdDLDH_Variant1 and wild type

DLDH enzyme performs oxidation-reduction reaction by catalyzing the reversible conversion of dihydrolipoamide (DLD) into lipoamide (LA) by FAD as an electron carrier and NAD^+ as a co-substrate. The kinetic parameters (K_m and V_{max}) of five different mutants and wild type *Ld*DLDH_Variant1 were determined in forward direction for substrate DLD and NAD^+. Mutant's activity was compared with wild type protein to check their importance in the catalytic activity, FAD binding, and protein structural stability. The estimated K_m values for wild type *Ld*DLDH_Variant1 were found to be 3.56 ± 0.32 mM (DLD) and 439.81 ± 15 µM S-1 (NAD^+), respectively. Other mutants A54I and C15T showed a significantly higher value of K_m for DLD supporting the involvement in catalytic as well as binding around the active site region. However, A48I and D49G showed a significant decrease in K_m value for DLD which clearly indicates their role in the catalytic process. C38G substitution didn't show any change in K_m value for DLD. All the mutants showed significantly higher values of K_m for NAD^+ clearly indicating their role in NAD^+ binding around FAD-binding region. Out of five mutants, C15T represented an extremely high value of K_m (18 ± 0.32 mM) for DLD as well as for NAD^+ which means almost negligible activity was observed that indicate Cys-15 may involve in disulfide bond formation with other cysteine partner. It was further confirmed by fluorescence spectral pattern analysis. Comparative Michaelis-Menton (MM) plot together with LB-plot and table of kinetic parameters of different mutants with wild type are shown in **Fig. 3.6** and **Table 3.2,** respectively.

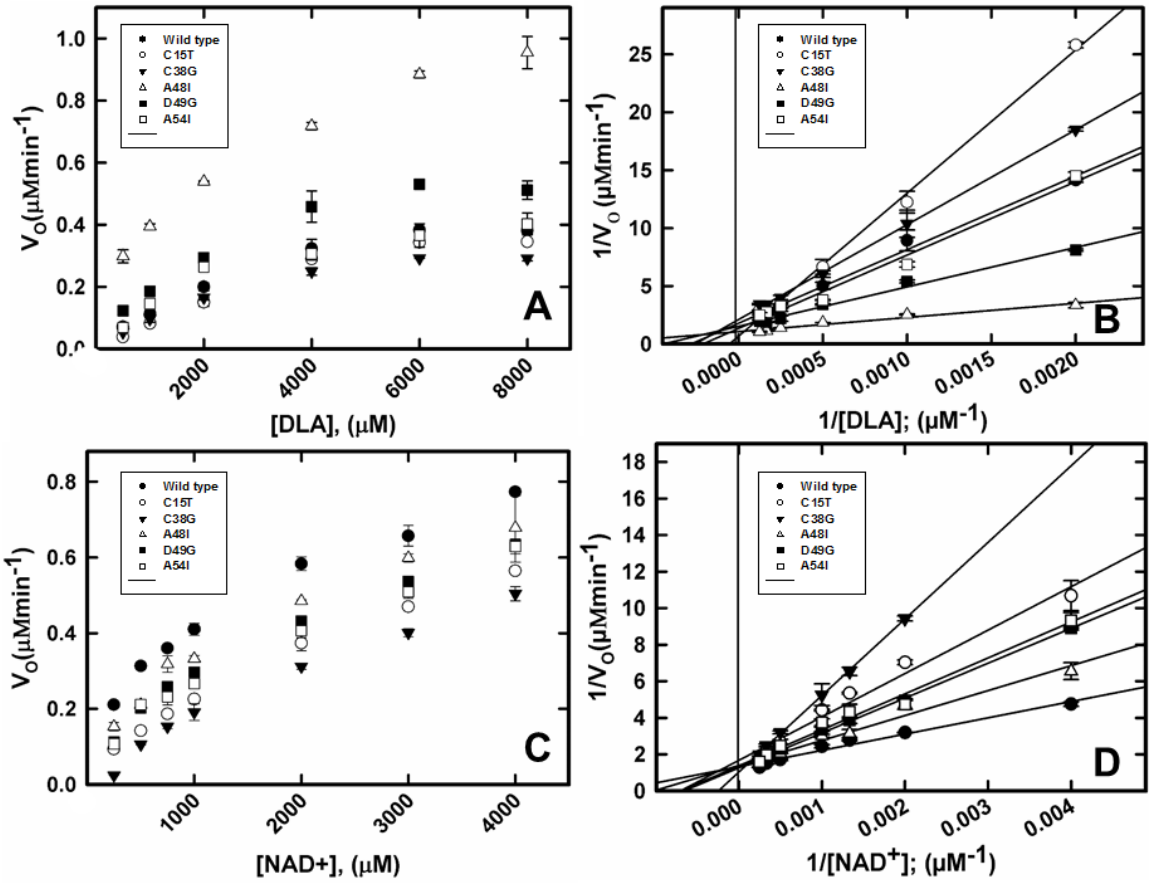

Figure. 3.6. Comparative kinetic study of *Ld*DLDH_Variant1 mutants and wild type. Effect of varying concentration on kinetics of *Ld*DLDH_Variant1 mutants and wild types. (A) DLA (0.5 – 8 mM) or (C) NAD^+ (0.1 – 4 mM) at fixed concentration of other substrate (2 mM). Kinetic parameters (K_m and V_{max}) of the wild types and variants for the substrate DLA and NAD^+ were determined from L-B plot (B) and (D).

Table 3.2: Kinetic parameters of wild type and *Ld*DLDH_Variant1 mutants

Mutation		K_m (mM)	V_{max} (μM S^{-1})
Wild type	DLD	3.56 ± 0.32	561.45 ± 60.5
	NAD^+	439.81 ± 0.015	638.80 ± 6
C15T	DLD	18.4 ± 0.20	1.49 ± 0.011
	NAD^+	1.436 ± 0.31	601.76 ± 78
C38G	DLD	3.891 ± 0.24	474 ± 31
	NAD^+	4.105 ± 0.90	977 ± 182
A48I	DLD	1.15 ± 0.18	941.72 ± 55.776
	NAD^+	981.96 ± 0.20	713.95 ± 59.3
D49G	DLD	2.2 ± 0.062	652.64 ± 6
	NAD^+	1.50 ± 0.105	789 ± 41
A54I	DLD	4.7 ± 0.031	743 ± 14
	NAD^+	1.318 ± 0.290	680 ± 109.5

3.4.5 Fluorescence analysis of wild type and mutants

The tryptophan residue in DLDH enzyme emits energy at 330 nm upon excitation at 296nm. These energies are absorbed by FAD cofactor which leads to release of energy at 570 nm. Wild type DLDH and its cofactor are reduced by DLD that affect both the peak at 330 nm and 570 nm. When NAD^+ is added with the enzyme, peak at 570 nm reduced slightly but upon addition of DLD reduced significantly as the FAD is reduced, with concomitant appearance of product peak of NADH at 460 nm. The product NADH forms upon reduction of NAD^+ by DLDH enzyme with the oxidation of DLD. The fluorescence spectral change of *Ld*DLDH_Variant1 (wild type enzyme) is illustrated in **Fig. 3.7A** upon addition of 750 µM of NAD^+ and 2 mM DLD together as well as separately. Similar conditions were employed to record fluorescence spectra of all the mutants.

In **Fig. 3.7B**. mutant C15T showed the characteristic curve of DLDH but shifting in the peak of 330 nm and 570 nm was observed. Addition of DLD doesn't affect the structure of the protein whereas NAD^+ addition reduced the FAD peak significantly either alone or together with the DLD. Interestingly, in this case upon reduction of FAD peak, product peak (NADH) was not observed. It indicates that probably this mutation affects the protein stability upon binding of NAD^+ near FAD-binding region which may lead to FAD dissociation from the protein. The role of Cys-15 in the protein seems to be involved in disulfide bond formation with the other partners.

The fluorescence spectra of mutation C38G is shown in **Fig. 3.7C**.This mutation represented deviation from characteristic spectra which gave shifted peak of FAD from 570 nm. Shifting of FAD peak indicates that this mutation affect the environment around FAD. Addition of NAD^+ and DLD doesn't which was observed in case of wild type representing their role in catalytic function. In this mutation, product peak was observed validating Cys-38 is not the other partner of Cys-15 for disulfide bond former.

Next mutant A48I, is illustrated in **Fig. 3.7D** representing different fluorescence spectral pattern from wild type protein clearly indicating their role in catalytic function as well as protein structural stability. Similarly, other mutants such as D49G (**Fig. 3.7E**) and A54I (**Fig. 3.7F**) also depicted different spectral pattern from wild type revealed their role in structural stability and catalytic function. However, all the mutants showed a characteristic fluorescence spectral peak as another DLDH enzyme

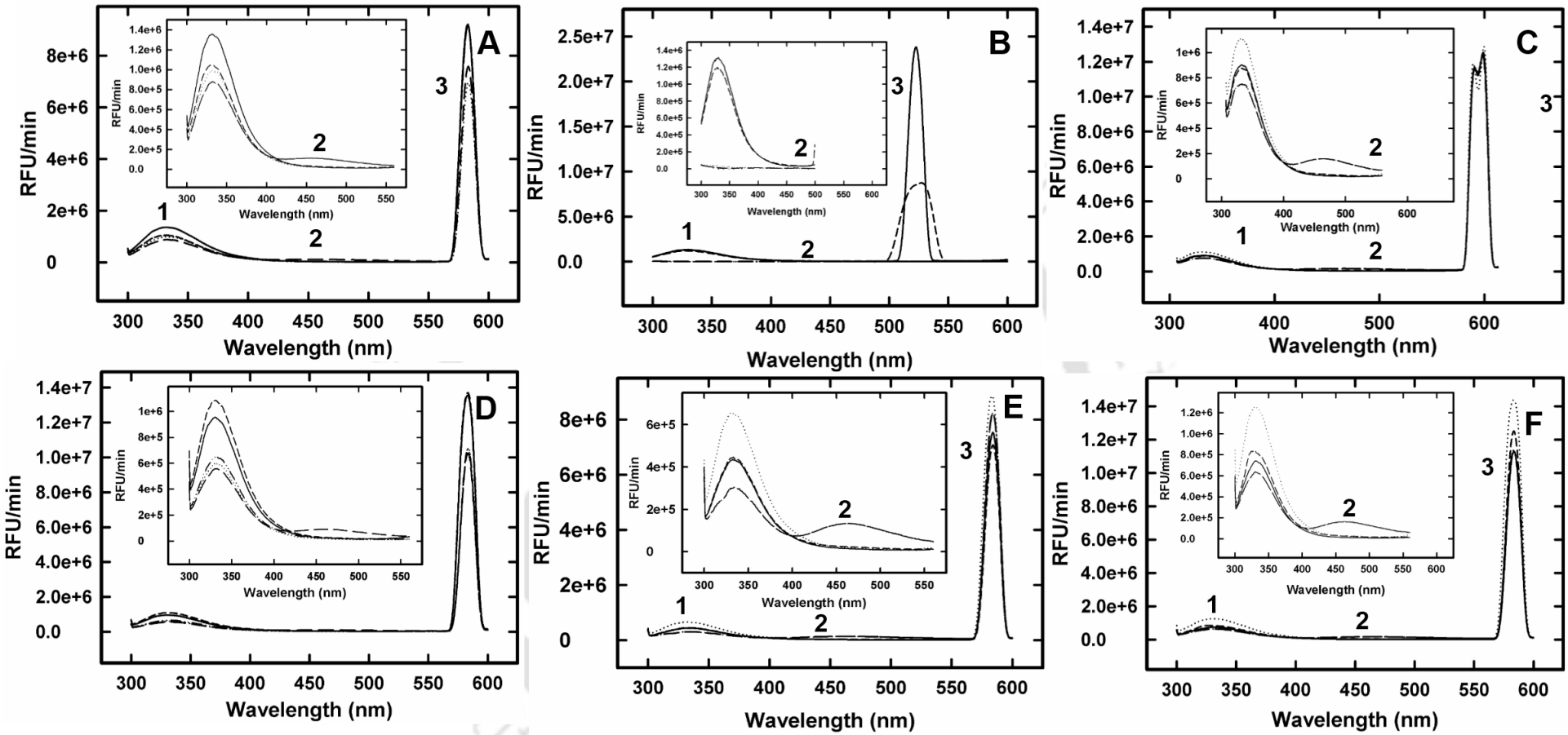

Figure. 3.7. Fluorescence spectra of mutants and LdDLDH_Variant1. Fluorescence spectral changes of wild type *Ld*DLDH_Variant1 (A), C15T (B), C38G (C), A48I (D), D49G (E), A54I (F) upon reduction by substrate DLA (2 mM) and NAD^+ (750 µM). Spectral pattern was also recorded upon addition of DLA (2 mM) or NAD^+ (750 µM) alone. Peak 1, 2, and 3 represents fluorescence spectral peak of protein, product (NADH), and FAD, respectively. Peak 2 shown in enlarge form in the inset of each figures.

3.5 Discussion

*Ld*DLDH enzyme have two variants which are present on two different chromosomes (Chromosome 19 and 32). Previously we observed for the first time that the sequence dissimilarities between *Ld*DLDH variants are very less (less than 30%) (Chiranjivi and Dubey 2018). Fewer sequence similarities between variants clearly indicate their distinct compartmental localization and some different functions together with a common one. We have also modelled the structure of both the variants (structures are validated through Ramachandran-plot) which was compared with known PDB structure of *T. cruzi* LADH to confirm their structural homology to known DLDH structure. Variant 2 showed very high homology to *T. cruzi* LADH even at active site whereas, variant 1 represented distinct structure with very fewer sequence similarities at catalytic center. We have observed that most of the enzymes belonging to pyridine nucleotide-disulfide oxido-reductase family have similar active site residues as present in *Ld*DLDH_Variant2. All the submitted PDB structures of DLDH enzyme from the different organisms in PDB database have similar active site residues as variant 2 (GGTCLNVGCIP), but not as variant 1 (GGADFWNGALQ). In one of the studies, it has been shown that Thr residue is highly conserved at the active site disulfide bond regions of DLDH enzyme throughout the organisms. The X-ray crystallographic studies of *Azotobacter vinelandii* DLDH suggested that hydroxyl group associated to Thr makes interaction with the FAD adenosine phosphate group (Kim 2002**).** Interestingly, we found that this Thr residue is completely absent in *Ld*DLDH_Variant1, whereas present in variant 2. Similarly, Ile-51 present at human DLDH present at the catalytic center is highly conserved in most of the DLDH of different organisms (Kim 2006). However, this conservation was found to be completely absent in *Ld*DLDH_Variant1 but present in variant 2 (In variant 1 'Ile' is replaced by 'Leu'). Most active and essential catalytic residue Cys-Cys disulfide (C-**S**-**S**-C) is completely absent at the active center in *Ld*DLDH_Variant1 which are replaced by Asp and Ala, respectively. In previous work, we observed that variant 1 have very high K_m value compared to variant 2 showing less catalytic activity (Chiranjivi and Dubey, 2018). Our structural studies suggested that *Ld*DLDH_Variant1 makes less number of interactions with cofactor FAD as compared to *Ld*DLDH_Variant2 which may be the plausible cause of very high K_m values for variant 1. Mutational studies were performed with key residues of variant 1 at active sites by PCR based approach. Total five mutations (C15T, C38G, A48I, D49G, and A54I) were performed in variant 1 which were compared

with the activity of wild type to confirm their importance in FAD binding or protein structural stability. Out of five mutants, C15T showed very high K_m value for DLD (18 ± 0.32 mM) which is approximately 5 fold more than the wild type. Large variation of fluorescence spectra from wild type also suggested the structural change in the protein. During fluorescence study, it was interestingly found that addition of NAD^+ largely affected the structure with concomitant reduction of FAD peak. However, the addition of DLD showed no effect on protein and FAD peak, which conclude that DLD has no effect on protein structural stability but NAD^+ may change the FAD microenvironment that quenches the FAD fluorescence significantly. Increase in the K_m value of C15T mutants may be the result of change in microenvironment around the binding site of NAD^+ and FAD. Absence of product formation during fluorescence spectral study and negligible protein activity might clearly indicate about their involvement in disulfide bridge formation. Other mutants C38G also showed an increase in the K_m value for NAD^+ whereas DLD represented similar K_m value as of wild type. Deviation of protein spectra and FAD peak pattern from wild type may be the possible reason for increase in the K_m value of NAD^+. Product peak observed with C38G mutation clearly represents Cys-38 is not involved in disulfide formation in variant 1. Mutation in Cys-15 and Cys-38 were performed to investigate about the disulfide bond forming candidate in *Ld*DLDH_Variant1. Next mutants A48I, showed a three-fold decrease in K_m value of DLD with two-fold increase of NAD^+. Fluorescence spectral study suggested deviation of protein and FAD peak from the wild type. Change of peaks may be due to change in the binding condition on NAD^+ that may subsequently affected the protein and FAD peak. Deviation of K_m value of DLD and NAD^+ from wild type represents their role in the catalytic process. In the other two mutants, D49G and A54I showed an almost similar pattern of fluorescence spectra, but different from wild type. D49G mutation decreases the K_m value from wild type for DLD but increase in K_m value was also observed for NAD^+. However, A54I represented an increase in K_m value for DLD and NAD^+ but both the mutants showed a large deviation in K_m value from wild types. Increase in K_m value in both the mutants for NAD^+ might modulate the environment around FAD and NAD^+ binding region at the active site which can be hypothesized in inhibiting the proper orientation of NAD^+ at catalytic center. Our mutational studies suggest *Ld*DLDH_Variant1 have different key active site residues which is completely different from *Ld*DLDH_Variant2.

CHAPTER IV

Subcellular localization of *Leishmania donovani* dihydrolipoamide dehydrogenase variants*

4.1 ABSTRACT*

Dihydrolipoamide dehydrogenase (DLDH) is one of the member of multienzyme complex that take part in many crucial metabolic pathways includes tricarboxylic acid cycle (TCA), folic acid metabolism, and branched change amino acid degradation pathways. In *Leishmania donovani*, DLDH have two variants which present on two different chromosomes (Chromosomes no. 19 and 32). However, these two variants having very less similarities between each other. The enzyme DLDH in *L.donovani* is not completely characterized till now. In our current study, subcellular localization of *Ld*DLDH variant were performed by GFP-fluorescence based approach. For that, GFP was cloned together with different variants of *Ld*DLDH in *Leishmania* specific vector (B3324 pXGPhleo). Positive construct, pXGPhleo_variant1-GFP and pXGPhleo_variant2-GFP was electroporated in *L.donovani* whose GFP expression was confirmed by western blot as well as flow cytometry. During localization studies, *Ld*DLDH_Variant1 was found to be localized in mitochondria, nucleus and kinetoplast whereas, *Ld*DLDH_Variant2 localize in inner leaflet of plasma membrane. Further studies may reveal the some common and different functions of the variants.

**** Part of the work is submitted for publication***

4.2 INTRODUCTION

Leishmaniasis, a parasitic disease that is caused by different species of *Leishmania* which spread by the bite of several sand-flies. *Phlebotomus* spread this disease in the old world and *Lutzomyia* in the new world countries. The disease leishmaniasis have mainly three clinical manifestations which includes less severe cutaneous leishmaniasis (CL) to most severe visceral leishmaniasis (VL). *Leishmania donovani* and *Leishmania infantum* are the main causative agents of VL. In the Indian subcontinent VL is most commonly known as kala-azar (black fever). Efforts to cure this deadly disease have mostly unsuccessful may be due to emerging drug resistance by the parasite. The currently available second line treatment drugs miltefosine and amphotericin B possess high toxic effect. However, in order to find out new drug targets, study of various key metabolic pathways of the *Leishmania* parasite would be interesting.

Dihydrolipoamide dehydrogenase (EC: 1.8.1.4) (DLDH), an enzyme that belongs to pyridine nucleotide-disulphide oxidoreductases family which perform oxidation-reduction process by utilizing FAD as a cofactor. It converts a substrate dihydrolipoamide (DLA) into lipoamide (LA) by utilizing another coenzyme NAD^+ in a reversible way. This enzyme present in several organisms as a member of many multi-enzyme complex such as pyruvate dehydrogenase complex (PDH), glycine cleavage complex (GCC), α-ketoglutarate dehydrogenase complex (α-KGDH), and branched chain amino acid amino transferase complex (BCAAT). Most of the studies suggested that DLDH mainly localize in the mitochondria where it involved in many bioenergetics pathways. However, their role in transport of some sugar (raffinose) has also been reported with *Streptococcus pneumoniae* where DLDH was found to be associated with regulatory domain of Rafk (raffinose ATP-binding protein) (Tyx et al., 2011). In *Pseudomonas aeruginosa,* enzyme DLDH is associated with the plasma membrane where it interacts with different serum proteins (four human plasma proteins, Factor H, Factor H-like protein-1 (FHL-1), complement Factor H-related protein 1 (CFHR1), and plasminogen) to make them inactive for evading of host immune response (Hallström et al., 2012). However, membrane association of DLDH has also been reported with *T. brucei* where it is associated with whole inner surface of the plasma membrane together with the flagellar pocket region (Jackman et al., 1990). The disease paracoccidioidomycosis (PCM) is caused by fungi *Paracoccidioides brasiliensis* and *Paracoccidioides lutzii* found in Latin America. These fungi contain many molecule of DLD, one of them that interacts with the host. Different

techniques like transmission electron microscopy and immune gold labelling revealed that DLDH is also localized in cytoplasm and mitochondria of *P. brasiliensis* (Landgraf et al., 2017).

4.3 MATERIAL AND METHODS

4.3.1 Materials

Leishmania donovani strain (BHU 1081) was kindly gifted by Prof, Shyam Sundar, Banaras Hindu University, India. *L. donovani* culture condition are established in our lab which include M199 medium (Sigma-Aldrich) with 15% fetal bovine serum (HiMedia), and antibiotics (penicillin and streptomycin, HiMedia**)** (Saudagar 2011). Green fluorescent protein **(**GFP) coding sequence was amplified from pGL1686 vector was gifted by Prof. David Mottram (University of Glasgow, Scotland, UK). All the enzymes for Gibson based cloning were purchased from Imperial life sciences (ILS) with high purity grades. All the buffer constituents for electroporation were purchased from HiMedia with high purity. Protocols for parasite electroporation were also optimized in our lab (Ruchika et al., 2017; Prakash et al. 2018). Stain (Hoechst 33342, Alexa fluor, and Mitotracker) used for localization studies were from Invitrogen.

4.3.2 Cloning of LdDLDH_Variant1 and LdDLDH_Variant2 gene with GFP in B3324 pXGPhleo (Phleomycin) vector

The coding sequence of *Ld*DLDH_Variant1 and *Ld*DLDH_Variant2 with GFP were cloned in pXGPhleo vector, (*Leishmania*- specific vector) by Gibson chew back and anneal assembly (Gibson et al, 2009). This method can able to ligate any fragments (4-5 insert + vector) without the use of restriction enzyme. Initially, all the coding sequences were amplified by using overlapping primers (**Table 4.1**). Whereas, the coding sequence of GFP was amplified from pGL1686 vector. Total 4 overlapped primers were designed, two for variants and remaining two for GFP. Forward primers (FP) of variants were made with the overlapping sequence with pXGPhleo vector at *Xma*I site and reverse primer (RP) with GFP 5' overhanging part. Similarly for GFP-FP were prepared with over hanged region of 3' end of variant and RP with the overlapping region with pXGPhleo vector at *Bam*HI site. Two amplified fragments (coding sequence of variants and GFP) with vector (pXGPhleo) digested with *Xma*I and *Bam*HI in Gibson master mix (5x Isothermal buffer, Taq Ligase, T5 exonuclease, Phusion polymerase) were incubated at 50 ºC for 60 min in PCR to make complete construct. Subsequently, the ligated construct was transformed in

E.coli DH5α strain which was selected on ampicillin-containing LB plate. Finally, positive clones were confirmed through amplification of both the fragments by gene-specific primer through colony PCR.

Table 4.1: List of primers for cloning of *Ld*DLDH_Variant1 and *Ld*DLDH_Variant2 with GFP in pXGPhleo vector.

S.No	Sequence Name	Sequence
1.	*Ld*DLDH_Variant1_FP_Localzn	GCCCTCCCCCTGTCCCCGGGATGAAGCGCACTATCTTTGC
2.	*Ld*DLDH_Variant1_RP_ Localzn	AACAGTTCCTCGCCCTTGCTCATTTTATTGTGCGCGTACGCGC
3.	*Ld*DLDH_Variant2_FP_ Localzn	GCCCTCCCCCTGTCCCCGGGATGTTCCGCAGGAACATAGC
4.	*Ld*DLDH_Variant2_RP_ Localzn	AACAGTTCCTCGCCCTTGCTCATGAAGTTGATCGTCTGCGCAAA
5.	*Ld*DLDH_Variant1_FP_ Localzn	GCGCGTACGCGCACAATAAAATGAGCAAGGGCGAGGAACTGTT
6.	*Ld*DLDH_Variant1/Variant2_RP_ Localzn	GAGGATCTGCTAGTGGATCCTCACTTGTACAGCTCGTCCATGCC
7.	*Ld*DLDH_Variant2_FP_ Localzn	TTTGCGCAGACGATCAACTTCATGAGCAAGGGCGAGGAACTGTT

4.3.3 Generation of L. donovani expressing GFP tagged LdDLDH variants

Log phage *L.donovani* promastigote cells were electroporated with pXGPhleo_*Ld*DLDH_Variant1-GFP/pXGPhleo_*Ld*DLDH_Variant2-GFP. Protocol for electroporation was established in our lab (Tiwari and Dubey, 2018; Bhardwaj et al, 2017). Briefly, one million promastigote cells were centrifuged at 2500 rpm for 5 min to remove dead cell debris. Media above the cell pellet were discarded and cells were washed with two times by 2 ml PBSG buffer (10 mM NaH_2PO_4, 10 mM Na_2HPO_4, 145 mM NaCl and 2% glucose). After each washing, the cells were centrifuged at low rpm (2500 rpm, 5 min). Subsequently, the supernatant was discarded and the pellet was processed for further washing with electroporation buffer (21 mM HEPES, 137 mM NaCl, 5 mM KCl, 0.7 mM Na_2HPO_4, 6 mM glucose). Finally, the pellet was suspended in 1 ml electroporation buffer and distributed in three electroporation cuvette (Control, Test 1 and Test 2). In control cells, no plasmid was added whereas, in test 1 and 2, pXGPhleo_*Ld*DLDH_Variant1-GFP and pXGPhleo_*Ld*DLDH_Variant2-GFP were added, respectively. Thereafter, cells were incubated in ice for 15 min followed by electroporation by application of exponential protocol (450 V, 400 µF capacitance, 50 Ω resistance for 2 mm cuvette) in Gene Pulsar Xcell™ Electroporation system (Bio-Rad). After electroporation cells were further incubated at 4 ºC for 15 min which was finally transferred in M199 media. Next day, cells

were transferred in antibiotic (Phleomycin, Sigma-Aldrich) containing M199 media for selection. Positively selected all sets of cells were used to visualize green fluorescence.

4.3.4 Western blot analysis to confirm the expression of LdDLDH_Variant1-GFP and LdDLDH_Variant2-GFP

Initially, GFP tagged *Ld*DLDH variant expressing cells were washed with two times by 1 x PBS and lysed in RIPA buffer (1x Protease Inhibitor cocktail, 1 mM PMSF and 10 mM EDTA). Total cell lysates were utilized for GFP detection by western blot (Towbin et al, 1979). Briefly, Cell lysate of both the variants with the control cell was run on 12% SDS-PAGE followed by protein were transferred on methanol charged polyvinylidene fluoride (PVDF) membrane. Protein containing PVDF membrane was blocked with 5% skimmed milk for 2 hr at room temperature. Further, the membrane was washed with 1 x TBST buffer three times followed membrane was incubated with primary anti-GFP primary antibody (1:1000 dilution) (Sigma-Aldrich, cat no. AB10145) overnight at 4 ºC. Afterward, the membrane was again washed with 1x TBST buffer (thrice) and further incubated for 60 min at room temperature with secondary anti-rabbit IgG antibody (1:10,000 dilution). The band was detected in chemiluminescent HRP substrate (Bio-Rad) under Chemi-Doc, BioRad. *L. donovani* anti-α-tubulin (1:1000 dilution) used as endogenous control and anti-rabbit IgG conjugated with HRP (1:10,000) was used as a secondary antibody against tubulin.

4.3.5 Cellular imaging through fluorescence microscope

The phleomycin positive *L. donovani* promastigotes cells were visualized for GFP tagged protein under a Nikon inverted microscope (Eclipse Ti-U). The cells were washed with 1 x PBS (pH 7.4) (twice) to remove residual media and dead cells followed by cells were fixed by 2 % formaldehyde by keeping at 25 ºC for 30 min. Further, the cells were permeabilized by application of 0.1 % Triton X 100 which was kept for 10 min at 25 ºC. After, permeabilization, cells were washed two times with PBS and counterstained with different organelle specific stain (Mitotracker, Hoechst, and Alexa fluor). Again, the cells were washed with PBS followed by mounted with anti-fade reagent (n-propyl gallate). Finally, mounted cells were imaged under 100 x oil immersion of Nikon inverted microscope (Eclipse Ti-U) with an excitation wavelength of 488 nm for GFP. The plasma membrane was stained with Alexa Fluor 594 (excitation wavelength 594 nm), nucleus by

Hoechst 3342 (excitation at 350 nm) and mitochondria by Mito-Tracker (excitation at 579 nm).

4.4 RESULTS

4.4.1 Cloning and expression confirmation of LdDLDH_Variant1 and Variant 2 with GFP

*Ld*DLDH variants together with GFP were cloned in B3324 pXGPhleo vector. Initially, all the fragments were amplified by gene-specific primers and the size of the fragments was confirmed on 1% agarose gel. Different *Ld*DLDH variants were amplified from *L. donovani* genomic DNA and GFP from pGL1686 vector. The size of the fragment of variant 1 (1,527 bp + 40 bp overlapping region), variant 2 (1,431 bp + 40 bp overlapping region), and GFP (717 bp + 40 bp overlapping region) were confirmed by comparing with 1 kb DNA ladder (**Fig. 4.1A**). Thereafter, all the amplified fragments were cloned in double digested *Leishmania*-specific vector B3324 pXGPhleo. Positive clones for variant 1 + GFP and variant 2 + GFP were confirmed through gene-specific primers. The whole frame of the construct was checked by amplification using variant_FP and GFP_RP as well as they were also confirmed individually through variants and GFP specific forward (FP) and reverse primer (RP), respectively. Further, each amplification size was confirmed by running 1% agarose gel. The whole frame size (variant + GFP) were confirmed by the amplification band of 2,284 bp for variant 1 + GFP and 2,188 bp for variant 2 + GFP, respectively. Separate amplification of variant 1 and GFP1 were too confirmed by amplification band of 1,567 bp and 757 bp, respectively. Likewise, variant 2 and GFP2 were confirmed from the amplified fragment of 1,471 bp and 757 bp, respectively (**Fig. 4.1B**). Frame of expression of variants with GFP was confirmed through western blot analysis (**Fig. 4.1C**). Size of bands at 83.3 kDa (56.3 kDa- Variant 1 + 27 kDa-GFP) and 77.6 kDa (50.6 kDa-Variant 2 + 27 kDa-GFP) on nitrocellulose paper were confirmed the expression of *Ld*DLDH_Variant1-GFP and *Ld*DLDH_Variant2-GFP, respectively. However, expression of variants with GFP were also validated through absence of band in control sample comprising cell lysate devoid of GFP transform vector-pXGPhleo_Variant1 or Variant 2.

GFP expression and transformation efficiency of promastigote cells was confirmed by flow cytometry. Formaldehyde-fixed control (without transform pXGPhleo_variant1-GFP and pXGPhleo_Variant2-GFP) and test cells (transformed with pXGPhleo_Variant1-GFP and pXGPhleo_Variant2-GFP) were run through FACS. Histogram were recorded in

the green channel (FL-1 in FACS caliber, BD Biosciences). The pXGPhleo_Variant1-GFP and pXGPhleo_Variant2-GFP expressed cells were depicted as histogram plot in **Fig. 4.1D and 4.1E**. Shifting of GFP expressed population with control cells in histogram plot confirm the GFP expressed cells.

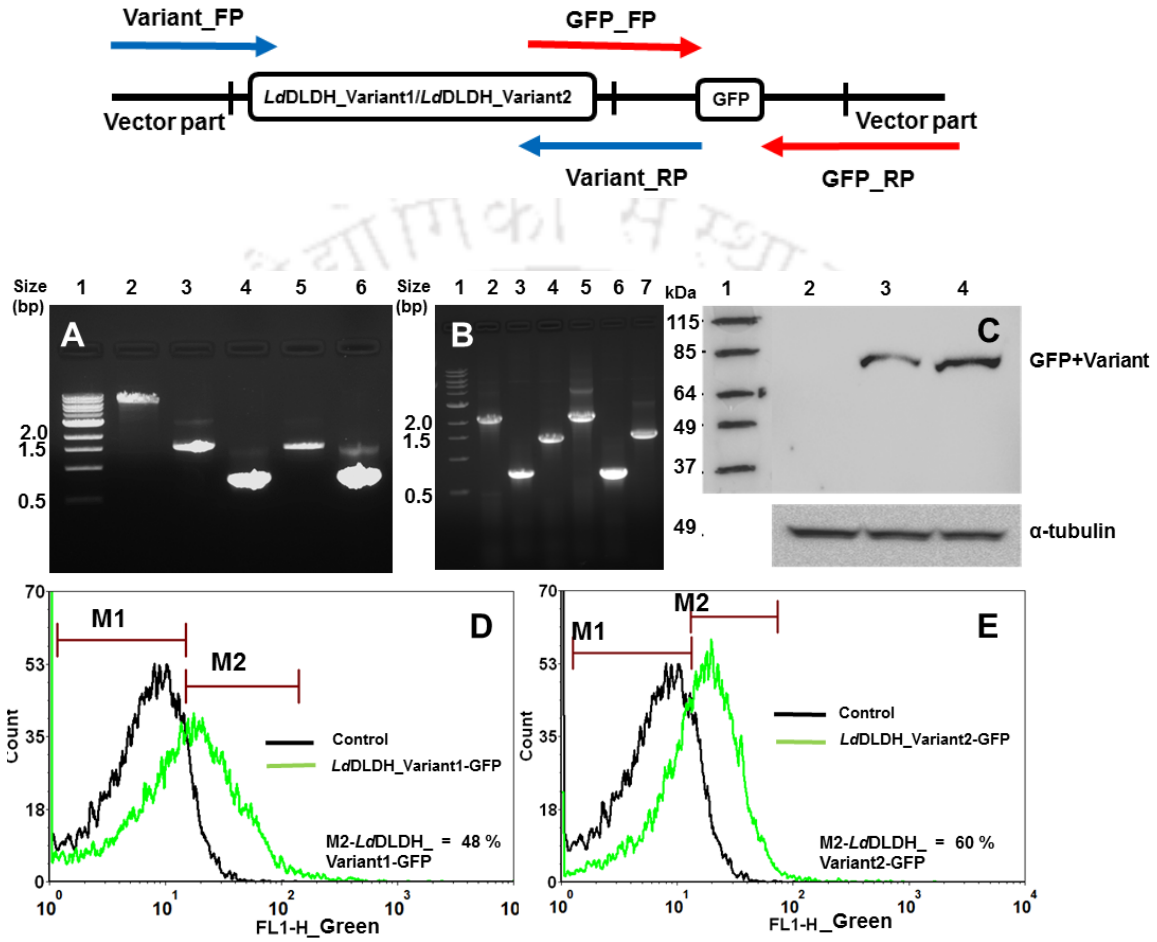

Figure 4.1. Cloning and expression of pXGPhleo_*Ld*DLDH_Variant1-GFP and pXGPhleo_ *Ld*DLDH_Variant2-GFP. In figure (A) Lane 2, double digested pXGPhleo vector (6,317 bp) by *Bam*HI and *Xma*I; lane 3 and 4, amplified fragment of variant 1 (1,527 bp + 40 bp overlapping region) and GFP1 (717 bp + 40 bp overlapping region) by variant 1 specific overlapping primers; lane 5 and 6, amplified product of variant 2 (1,431 bp + 40 bp overlapping region) and GFP2 (717 bp + 40 bp overlapping region) by variant 2 specific overlapping primers. (B) Clone confirmation of the variants with GFP by gene specific primers. Lane 2, amplified fragment of size 2,284 bp [Variant 1 (1,527 bp) + GFP (717 bp) + overlapping region of vector (40 bp)] of variant 1 with GFP by primers variant 1_FP and GFP_RP; lane 3 and 4, amplified product of GFP (717 bp) and variant 1 (1,527 bp) by gene specific primers; Lane 5 amplified fragment of size 2,188 bp [Variant 2 (1,431 bp) + GFP (717 bp) + overlapping region of vector (40 bp)] of variant 2 with GFP by primers variant 2_FP and GFP_RP; lane 3 and 4, amplified product of GFP (717 bp) and variant 2 (1,431 bp) by gene specific primers. Lane 1, 1kb DNA ladder in both the figures. (C)Expression confirmation of complete cassette of *Ld*DLDH_Variant1-GFP and *Ld*DLDH_Variant2-GFP by anti-GFP antibody. Lane 1, prestained protein marker; lane 2, 3 and 4 are control, *Ld*DLDH_Variant1-GFP, and *Ld*DLDH_Variant1-GFP, respectively. α-tubulin (49 kDa) used as housekeeping. (D) and (E) GFP expression confirmed by flow cytometry. Black color histogram in both the figures represent control cells and green color GFP expressed cells. M1 and M2 are the total percentage population of control and GFP expressed cells.

4.4.2 Localization study of LdDLDH_Variant1 and LdDLDH_Variant2 showed different compartmental distribution

*Ld*DLDH variants codes by two different genes present on two different chromosomes 19 and 32. Both the genes having very less sequence similarities that leads to the structural difference between them. Difference in structural dissimilarities gave the hint about different compartmental localization. Hence, subcellular localization of these two variants was performed by visualizing GFP fluorescence. Similar populations of GFP expressed cells were counterstained with Mito Tracker and Hoechst 33342 in one set (Variant 1) and in other sets (Variant 2) by Phalloidin Alexa Fluor 594 and Hoechst 33342, respectively. Subsequently, merged image of GFP with Mito Tracker and Hoechst 33342 of variant 1 revealed their mitochondrial localization (**Fig. 4.2**). However, overlaid image of *Ld*DLDH_Variant1 also indicate their localization in nucleus and kinetoplast which require further validation (**Fig. 4.2**). Similarly, overlaid image of Phalloidin Alexa Fluor 594 and Hoechst 33342 with GFP of variant 2 showed their localization in cytosolic face of the plasma membrane (**Fig. 4.2**).

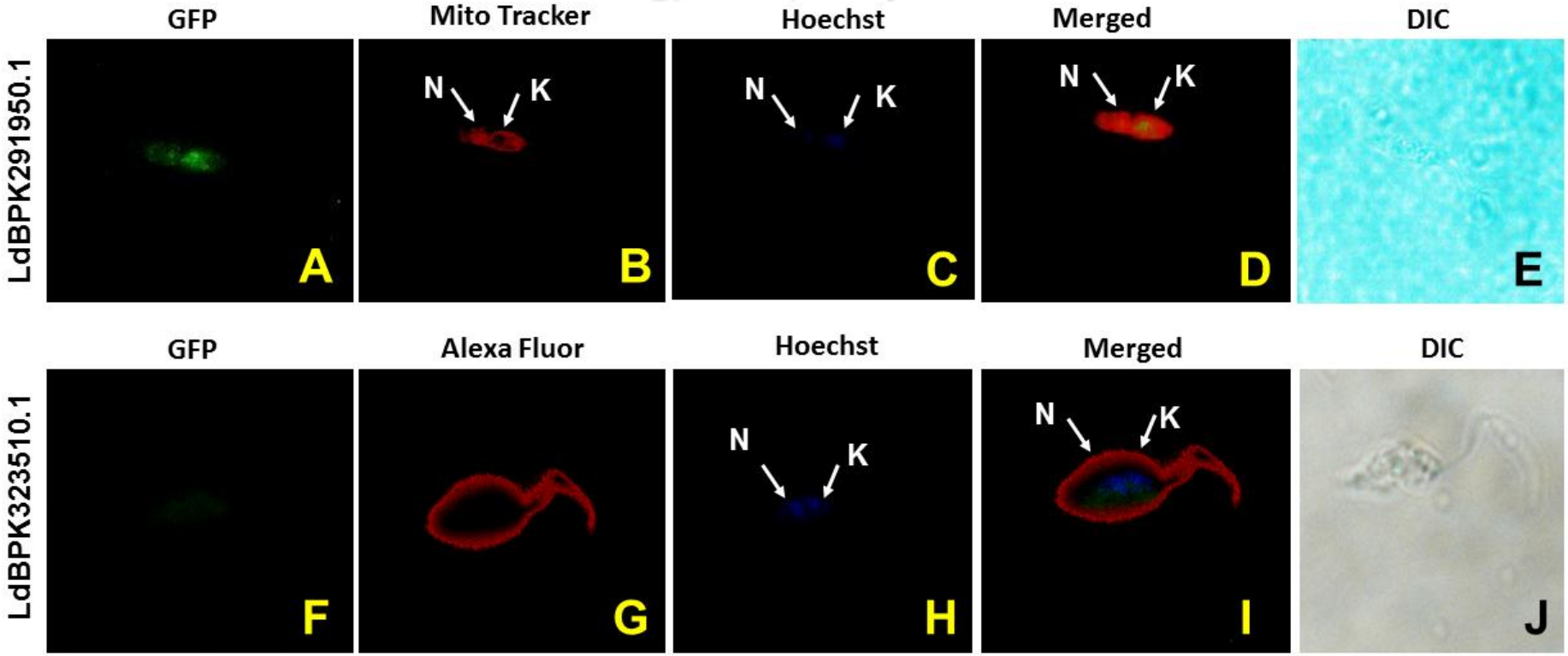

Figure 4.2. Subcellular Localization of *Ld*DLDH variants. (A) Green fluorescence image of *Ld*DLDH_Variant1 (LdBPK291950.1). (B) *L. donovani* mitochondria stained with Mito Tracker stain (Invitrogen cat No. M7512). (C) & (G) Nucleus (N) and kinetoplast (K) stained by Hoechst 33342 stain (Invitrogen cat No. 134406). (D) Merged image of A, B, and C shows localization in nucleus, kinetoplast and mitochondria, respectively. (F) Green fluorescence image of *Ld*DLDH_Variant2 (LdBPK323510.1). (F) Plasma membrane stained by Alexa Fluor (Invitrogen cat no. 134406). (H) Overlay image of E, F, and G represent plasma membrane localization (at cytoplasmic face). (E) And (J) depicts bright field image of *Ld*DLDH_Variant1 and variant 2, respectively.

4.5 DISCUSSION

In most of the organisms, localization of DLDH enzyme is not universal which shows variation in their position. Some of the studies suggested that DLDH enzyme has been localizing in mitochondria (Landgraf et al., 2017), cytoplasm (Landgraf et al., 2017), inner (Jackman et al., 1990) and outer leaflet (Hallstrom et al., 2012) of the plasma membrane. In the present study, we are the first group to report the localization of two variants of *Ld*DLDH in a different compartment of the cell. *Ld*DLDH_Variant1 localizes in mitochondria whereas *Ld*DLDH_Variant2 at the inner leaflet (cytoplasmic face) of the plasma membrane. However, overlaid image of *Ld*DLDH_Variant1 also indicate their localization in nucleus and kinetoplast but further validation via different techniques is required to confirm the actual localization state.

CHAPTER V

Summary of research performed*

5.1 ABSTRACT*

Our whole work provides clear evidence about the existence of two different variants of *Ld*DLDH enzyme which has a difference in catalytic activity. *Ld*DLDH_Variant1 showed high physiological catalytic activity compare to *Ld*DLDH_Variant2 during biochemical studies. These enzymes belong to the flavo group that was confirmed by estimation of FAD (flavo compound) cofactor by HPLC analysis. Other than a physiological activity such as the conversion of DLD into LA (natural substrate), it also performs a function like diaphorases. *Ld*DLDH enzyme has also the ability to transfer an electron to any electro accepting compound which forms radical. *Ld*DLDH_Variant1 showed greater diaphorase activity upon *Ld*LDH_Variant2. In the search of the reason behind less activity of *Ld*DLDH _Variant1, mutational studies were performed. Out of five mutations (C15T, C38G, A48I, D49G, and A54I), Cys-15 may be one of the members of disulfide bridge former. In flavo group of enzyme, disulfide bridge at the active site utilized in the catalytic process. All other mutated amino acids including Cys-15 having a role in the catalytic activity which was also confirmed by fluorescence study. GFP-based localization study of *Ld*DLDH variants revealed that *Ld*DLDH_Variant1 present in more than one compartment includes the nucleus, kinetoplast, and mitochondria whereas another variant localizes in cytoplasmic face of the plasma membrane.

5.2 Biochemical characterization of two *Ld*DLDH variants

Conclusion: DLDH is having two variants in *Leishmania* parasite and both have only 30% similarities. Active site BLAST analysis showed dissimilarities between both the variants. Catalytic domain reported in other organisms is 75% dissimilar in one of the variants. This structural distinctness in addition to the active site difference within the variants led us to investigate their biochemical role *Leishmania* parasite. Biochemical characterization was performed in physiological direction for both the variants (LdBPK291950.1-Variant 1, LdBPK323510.1-Variant 2). *Leishmania donovani* dihydrolipoamide dehydrogenase (*Ld*DLDH) variants catalyze forward reaction at pH of 7.5 and protein is even active at higher temperature (50°C). Kinetic parameter K_m and specific activity were also analyzed for both the variants which revealed *Ld*DLDH_Variant1 having greater activity compare to *Ld*DLDH_Variant1. We found in literature, the enzyme DLDH have one unique function called "Diaphorase" means it has ability to transfer an electron to any electron accepting dyes other than physiological substrate, so diaphorase activity of *Ld*DLDH was also evaluated and we found that both the variants showed activity with MTT (Thiazolium blue bromide) and DCPIP (2, 6-dichlorophenolindophenol) dyes. However, Variant 1 showed better diaphorase activity compare to variant 2.

5.3 Mutational study of five amino acid residues on and around active site of *Ld*LDH_Variant1

Conclusion: BLAST analysis of catalytic region together with homology modelling suggested that Variant 2 is sequencely as well as structurally similar to already reported crystal structure of DLDH from different organism in PDB database. Thereby, Reason behind difference in biochemical activity (Activity: Variant 1< Variant 2) was also evaluated by site directed mutagenesis approach. Total five mutations (C15T, C38G, A48I, D49G, and A54I) were created in Variant 1 on or around active site region and activity of those mutant proteins were compared with wild type *Ld*DLDH. Interestingly, it was found that all the mutated residues effects the catalytic activity of the protein which was revealed from deviation of spectral pattern of mutants proteins from wild type. Out of five mutants, C15T showed very high K_m (18 µM) value compare to wild type *Ld*DLDH. Hence, this mutation represented negligible activity that also confirmed by fluorescent spectral studies. In spectra of C15T mutation, no product peak was obtained revealed Cys-15 may one of the member of disulfide bond former in *Ld*DLDH. Thereafter, in search of other disulfide bond former, Cys-38 was mutated but it showed product peak during

fluorescence spectral study. Biochemical studies revealed that Cys-38 helps in proper binding NAD^+ (Very high K_m value compare to wild type) but no other member of disulfide bond former.

5.4 Subcellular localization of *Ld*DLDH variants

Conclusion: Localization study of these variants were also performed through immunofluorescence (GFP based approach) study to check whether these variants localize in same compartment or different. Studies showed that *Ld*DLDH_Variant1 localize in multiple compartment of the cells include nucleus, kinetoplast and mitochondria whereas, *Ld*DLDH_Variant2 localize in inner leaflet of the plasma membrane. Our studies opened a new door of the research towards variants of the enzyme.

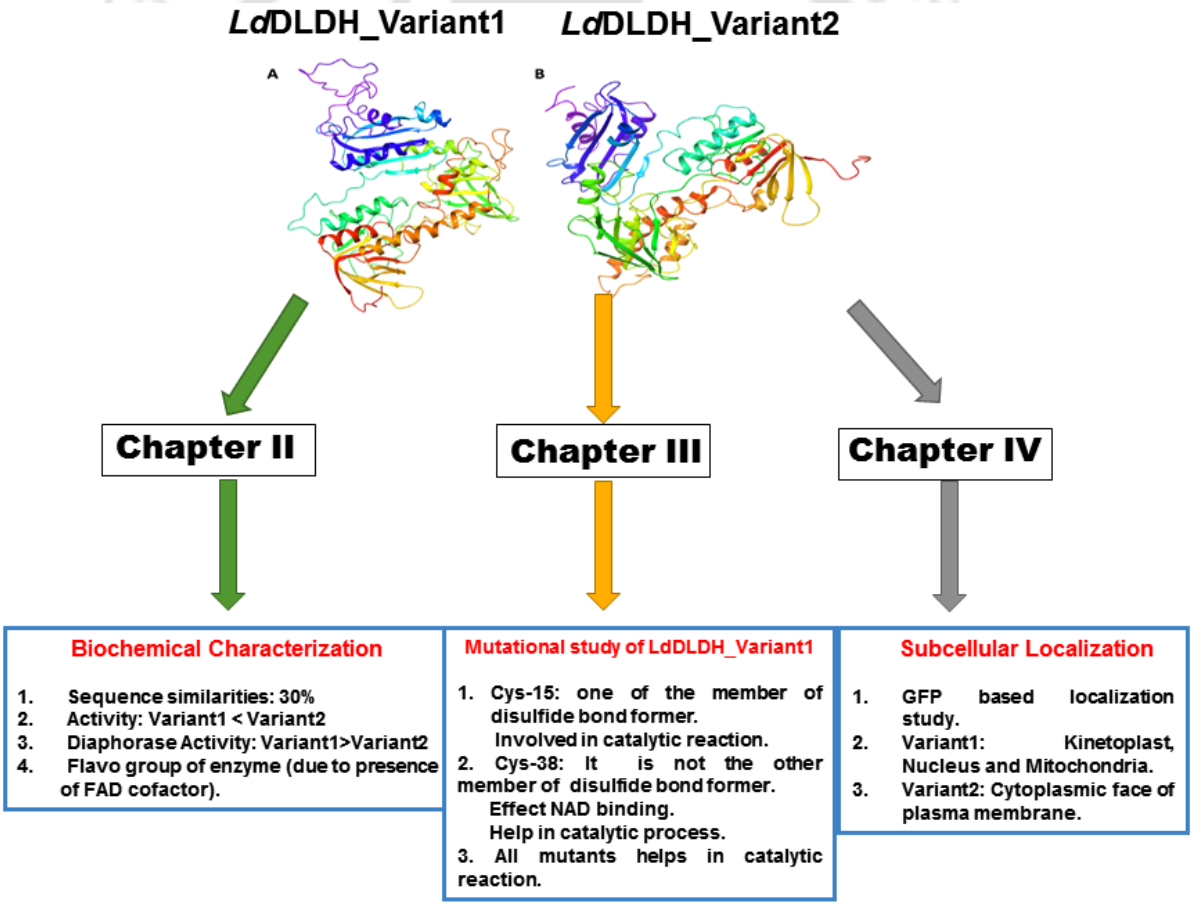

Figure 5.1: The figure represents overall outcome of the PhD work**.**

5.5 Future Perspective

Dihydrolipoamide dehydrogenase in *L. donovani* (*Ld*DLDH) has two variants present on two different chromosomes. Both the variant having very fewer sequence similarities (30 %) with each other. Our finding suggested that both the variants catalyzed similar reaction but the rate of catalysis is different between them. *Ld*DLDH_Variant1 is less efficient in catalyzing a similar substrate upon *Ld*DLDH_Variant2. In another parameter like diaphorase activity, *Ld*DLDH_Variant1 was found to be more efficient. As diaphorase family enzyme having the ability to generate radical which is toxic to any organism. Hence, this activity can be utilized for the discovery of new drug having anti-leishmanial effect in coming future. All the PDB structure of DLDH from any organism available in PDB database is similar to *Ld*DLDH_Variant2 whereas, *Ld*DLDH_Variant1 was found to be completely different. Therefore, many amino acid residues at or around the active site were mutated in *Ld*DLDH_Variant1 and defined some key catalytic residues involved in the catalytic process. Our finding opened the new door for the research in the variants of the enzyme. For future studies synthesis of the crystal structure of *Ld*DLDH_Variant1 is very important, to check their structural organization. Our mutational studies will give some support in future research to solve their crystal structure together with the mechanism of catalyzing the reaction. Localization studies of the variants were suggested that *Ld*DLDH_Variant1 present in multiple compartments includes nucleus, kinetoplast, and mitochondria. As for future perspective, it is important to the functions of this variant in comportment in *Leishmania* parasite. Another variant, *Ld*DLDH_Variant2 present on the cytoplasmic side of the plasma membrane. Similarly, for future studies of *Ld*DLDH_Variant2, important to check the role of this variant in the inner side of the plasma membrane. Our finding has been suggested that *Ld*DLDH_Variants is even active without the other multi-enzyme complex partners. Ultimately, our studies on *Ld*DLDH variants were given some clues regarding the existence of different rate of catalytic activity together with different localization of the variants of the enzyme.

Bibliography

Abdallah KA, Nour BY, Schallig HD, Mergani A, Hamid Z, Elkarim AA, *et al*. Evaluation of the direct agglutination test based on freeze-dried *Leishmania donovani* promastigotes for the serodiagnosis of visceral leishmaniasis in Sudanese patients. ***Trop Med Int Health***. (2004), 9: 1127-1131.

Adams PD, Afonine PV, Bunko´czi G, Chen VB, Davis IW, Echols N, Headd JJ, Hung LW, Kapral GJ, Grosse-Kunstleve RW, Mc- Coy AJ, Moriarty NW, Oeffner R, Read RJ, Richardson DC, Richardson JS., Terwilliger TC, and Zwart PH. PHENIX: a comprehensive Python-based system for macromolecular structure solution. ***Acta Crystallogr. D Biol. Crystallogr.*** (2010), 66:213–221.

Aebischer T, Wolfram M, Patzer SI, Ilg T, Wiese M, Overath P. Subunit vaccination of mice against new world cutaneous leishmaniasis: comparison of three proteins expressed in amastigotes and six adjuvants. ***Infect Immun***. (2000), 68:1328-1336.

Aikat BK, Sahaya S, Pathania et al. Clinical profile of cases of kala-azar in Bihar. ***Indian Journal of Medical Research***. (1979), 70:563–570.

Alexander J, Christine Carter K, Al-Fasi N, Atoskar A, and Brombacher F. Endogenous IL-4 is necessary for effective drug therapy against visceral leishmaniasis. ***European Journal of Immunology.*** (2000), 30:2935–2943.

Aliverti A, Curti B, Vanoni MA. Identifying and quantitating FAD and FMN in simple and in iron-sulfur-containing flavoproteins. ***Methods Mol Biol***. (1999), 131: 9-23.

Alvar J, Aparicio P, Aseffa A, Den Boer M, Cañavate C, Dedet JP, et al. The relationship between leishmaniasis and AIDS: The second 10 years. ***Clin Microbiol Rev***. (2008), 21:334-359.

Alvar J, Yactayo S, Bern C. Leishmaniasis and poverty. ***Trends Parasitol***. (2006), 22:552-557.4.

Andrade-Neto VV, Cunha-Junior EF, Dos Santos Faioes V, Pereira TM, Silva RL, Leon LL, Torres-Santos EC. Leishmaniasis treatment: update of possibilities for drug repurposing. ***Front Biosci***. (2018), 23:967-996.

Antillón A, de Vries AH, Espinosa-Caballero M, Falcón-González JM, Flores Romero D, González-Damián J, Jiménez-Montejo FE, León-Buitimea A, López-Ortiz M, Magaña R, Marrink SJ, Morales-Nava R, Periole X, Reyes-Esparza J, Rodríguez Lozada J, Santiago-Angelino TM, Vargas González MC, Regla I, Carrillo-Tripp M, Fernández-Zertuche M, Rodríguez-Fragoso L, Ortega-Blake I. An Amphotericin B Derivative Equally Potent to Amphotericin B and with Increased Safety. ***PLoS One***. (2016), 11:e0162171.

Arenas FA, Leal CA, Pinto CA, Arenas-Salinas MA, Morales WA, Cornejo FA, Díaz-Vásquez WA, Vásquez CC. On the mechanism underlying tellurite reduction by *Aeromonas caviae* ST dihydrolipoamide dehydrogenase. ***Biochimie.*** (2014), 102:174-182.

Arjunan P, Nemeria N, Brunskill A, Chandrasekhar K, Sax M, Yan Y, Jordan F, Guest JR, Furey W. Structure of the pyruvate dehydrogenase multienzyme complex E1 component from *Escherichia coli* at 1.85 A resolution. ***Biochemistry***. (2002), 41, 5213-5221.

Armijos RX, Weigel MM, Aviles H, Maldonado R, Racines J. Field trial of a vaccine against New World cutaneous leishmaniasis in an at-risk child population: safety, immunogenicity, and efficacy during the first 12 months of follow-up. ***J Infect Dis***. (1998), 177:1352-1357.

Ashford RW, Bates PA. Leishmaniasis in the Old World. Topley & Wilson's microbiology and microbial infections. ***Parasitology***. (1998), 9:215-240.

Bando Y and Aki K. Mechanisms of generation of oxygen radicals and reductive mobilization of ferritin iron by lipoamide dehydrogenase. ***J. Biochem***. (1991), 109:450–454.

Basu JM, Mookerjee A, Sen et al. Sodium antimony gluconate induces generation of reactive oxygen species and nitric oxide via phosphoinositide 3-kinase and mitogen activated protein kinase activation in *Leishmania Donovani* infected macrophages. ***Antimicrobial Agents and Chemotherapy***. (2006), 50, 1788–1797.

Batista AP, Kletzin A, Pereira MM. The dihydrolipoamide dehydrogenase from the crenarchaeon Acidianus ambivalens. ***FEMS Microbiol Lett***. (2008), 281:147-154.

Bhardwaj R, Das M, Singh S, Chiranjivi AK, Prabhu SV, Singh SK, Dubey VK. Evaluation of CAAX prenyl protease II of Leishmania donovani as potential drug target: Infectivity and growth of the parasite is significantly lowered after the gene knockout. ***Eur J Pharm Sci***. (2017), 102:156-160.

Bhatia A, Daifalla NS, Jen S, Badaro R, Reed SG, Skeiky YA. Cloning, characterization and serological evaluation of K9 and K26: two related hydrophilic antigens of *Leishmania chagasi*. ***Mol Biochem Parasitol.*** (1999), 102:249-261.

Bisswanger H. Regulatroy properties of the pyruvate-dehydrogenase complex from *Escherichia coli*. Thiamine pyrophosphate as an effector. ***Eur J Biochem***. (1974), 48:377-387.

Bleile DM, Munk P, Oliver RM, and Reed LJ. Subunit structure of dihydrolipoyl transacetylase component of pyruvate dehydrogenase complex from *Escherichia coli*. ***Proc. Natl. Acad. Sci. U.S.A.*** (1979), 76:4385–4389.

Blumenstiel K, Schöneck R, Yardley V, Croft SL, Krauth-Siegel RL. Nitrofuran drugs as common subversive substrates of *Trypanosoma cruzi* lipoamide dehydrogenase and trypanothione reductase. ***Biochem Pharmacol***. (1999), 58:1791-1799.

Boelaert M, Rijal S, Regmi S, *et al*. Comparative study of the effectiveness of diagnostic tests for visceral leishmaniasis. ***Am J Trop Med Hyg***. (2004), 70:72-77.

Brautigam CA, Wynn RM, Chuang JL, Machius M, Tomchick DR, and Chuang DT. Structural insight into interactions between dihydrolipoamide dehydrogenase (E3) and E3 binding protein of human pyruvate dehydrogenase complex. ***Structure***. (2006), 14:611–621.

Brochu C, Wang GJ, Roy et al. Antimony uptake systems in the protozoan parasite *Leishmania* and accumulation differences in antimony-resistant parasites. ***Antimicrobial Agents and Chemotherapy***. (2003), 47:3073–3079.

Bulos BA, Thomas BJ and Sacktor B. Calcium inhibition of the NADC-linked isocitrate dehydrogenase from blowfly flight muscle mitochondria. ***J. Biol. Chem***. (1984), 259:10232–10 237.

Cabrera M, Blackwell JM, Castes M, Trujillo D, Convit J, Shaw MA. Immunotherapy with live BCG plus heat killed *Leishmania* induces a T helper 1-like response in American cutaneous leishmaniasis patients. ***Parasite Immunol***. (2000), 22:73-79.

Castés M, Blackwell J, Trujillo D, Formica S, Cabrera M, Zorrilla G, Rodas A, Castellanos PL, Convit J. Immune response in healthy volunteers vaccinated with killed leishmanial promastigotes plus BCG. I: Skin-test reactivity, T-cell proliferation and interferon-gamma production. ***Vaccine***. (1994), 12:1041-1051.

Castes M, Moros Z, Martinez A, Trujillo D, Castellanos PL, Rondon AJ, Convit J. Cell-mediated immunity in localized cutaneous leishmaniasis patients before and after treatment with immunotherapy or chemotherapy. ***Parasite Immunol.*** (1989), 11:211-222.

Chakraborty S, Sakka M, Kimura T, Sakka K. Characterization of a dihydrolipoyl dehydrogenase having diaphorase activity of ***Clostridium kluyveri***. ***Biosci Biotechnol Biochem***. (2008), 72: 982-8.

Chappuis F, Sundar S, Hailu A, Ghalib H, Rijal S, Peeling RW, Alvar J, Boelaert M. Visceral leishmaniasis: what are the needs for diagnosis, treatment and control? ***Nat Rev Microbiol***. (2007), 5:873-882.

Chiranjivi AK, Dubey VK. Dihydrolipoamide dehydrogenase from *Leishmania donovani*: New insights through biochemical characterization. ***Int J Biol Macromol***. (2018), 112:1241-1247.

Chrusciak-Talhari A, Dietze R, Chrusciak-Talhari C, da Silva RM, Gadelha Yamashita EP, de Oliveira Penna G, et al. Randomized controlled clinical trial to access efficacy and safety of miltefosine in the treatment of cutaneous leishmaniasis caused by *Leishmania* (Viannia) *guyanensisin* Manaus. ***Brazil. Am. J. Trop. Med. Hyg***. (2011), 84:255–260.

Chueh FY, Leong KF, Cronk RJ, Venkitachalam S, Pabich S, Yu CL. Nuclear localization of pyruvate dehydrogenase complex-E2 (PDC-E2), a mitochondrial enzyme, and

its role in signal transducer and activator of transcription 5 (STAT5)-dependent gene transcription. ***Cell Signal***. (2011), 23:1170-1178.

Ciszak EM, Makal A, Hong YS, Vettaikkorumakankauv, A. K., Korotchkina, L. G., and Patel, M. S. How dihydrolipoamide dehydrogenase- binding protein binds dihydrolipoamide dehydrogenase in the human pyruvate dehydrogenase complex. ***J. Biol. Chem***. (2006), 281:648–655.

Coimbra ES, Libong D, Cojean S, Saint-Pierre-Chazalet M, Solgadi A, Le Moyec L, Duenas-Romero AM, Chaminade P, Loiseau PM. Mechanism of interaction of sitamaquine with Leishmania donovani. ***J Antimicrob Chemother***. (2010), 65:2548-2555.

Constant P, Davodeau F, Peyrat MA, Poquet Y, Puzo G, Bonneville M, Fournié JJ. Stimulation of human gamma delta T cells by nonpeptidic mycobacterial ligands. ***Science***. (1994), 264:267-270.

Croft SL, Engel J. Miltefosine-discovery of the antileishmanial activity of phospholipid derivatives. ***Trans. R. Soc. Trop. Med. Hyg***. (2006), 100:S4–S8.

Cunningham DD. On the presence of peculiar parasitic organisms in the tissue of a specimen of Delhi Boil. ***Sci Mem Med Offic Army India***. (1885), 1:21–31.

Danson MJ, Conroy K, McQuattie A, Stevenson KJ. Dihydrolipoamide dehydrogenase from *Trypanosoma brucei*. Characterization and cellular location. ***Biochem J***. (1987), 243: 661-5.

Darshan HP, Seung GW and Hyeun J. Modification of overlap extension PCR: A mutagenic approach. ***Indian Journal of Biotechnology***. (2009), 8:183-186.

Dasgupta B, Roychoudhury K, Ganguly et al. Antileishmanial drugs cause up-regulation of interferon-gamma receptor 1, not only in the monocytes of visceral leishmaniasis cases but also in cultured THP1 cells. ***Annals of Tropical Medicine and Parasitology***. (2003), 97:245–257.

Davis BD, Chen L and Tai PC. Misread protein creates membrane channels: an essential step in the bactericidal action of aminoglycosides. Proc. Natl. Acad. Sci. U. S. A. (1986), 83:6164–6168.

De Luca PM, Mayrink W, Alves CR, Coutinho SG, Oliveira MP, Bertho AL, Toledo VP, Costa CA, Genaro O, Mendonça SC. Evaluation of the stability and immunogenicity of autoclaved and non autoclaved preparations of a vaccine against American tegumentary leishmaniasis. ***Vaccine***. (1999), 17:1179-1185.

Delgado J, Pineda JA, Macías J, Regordán C, Gallardo JA, Leal M, *et al*. Low sensitivity of peripheral blood smear for diagnosis of subclinical visceral leishmaniasis in human immunodeficiency virus type 1-infected patients. ***J Clin Microbiol***. (1998), 36:315-316.

Denton H, McGregor JC, and Coombs GH. Reduction of anti-leishmanial pentavalent antimonial drugs by a parasite-specific thiol-dependent reductase, TDR1. ***Biochemical Journal***. (2004), 381:405–412.

Denton RM, Randle PJ and Martin BR. Stimulation by calcium ions of pyruvate dehydrogenase phosphate phosphatase. ***Biochem. J.*** (1972), 128:161–163.

Denton RM, Richards DA and Chin JG. Calcium ions and the regulation of NADC-linked isocitrate dehydrogenase from the mitochondria of rat heart and other tissues. ***Biochem. J.*** (1978), 176:899–906.

Donovan C. On the possibility of the occurrence of trypanosomiasis in India. ***Br Med J***. (1903), 2:79.

Dörsam B, Fahrer J. The disulfide compound α-lipoic acid and its derivatives: A novel class of anticancer agents targeting mitochondria. ***Cancer Lett.*** (2016), 371:12-19.

Dos Santos Ferreira C, Silveira Martins P, Demicheli C, Brochu C, Ouellette M, and Fr´ezard F. Thiol-induced reduction of antimony (V) into antimony (III): a comparative study with trypanothione, cysteinyl-glycine, cysteine and glutathione. ***BioMetals.*** (2003), 16, 441–446.

Dos Santos PF, Moreira DS, Baba EH, Volpe CMO, Ruiz JC, Romanha AJ, Murta SMF. Molecular characterization of lipoamide dehydrogenase gene in *Trypanosoma cruzi* populations susceptible and resistant to benznidazole. ***Exp Parasitol***. (2016), 170:1-9.

Duchen MR. Ca (2C)-dependent changes in the mitochondrial energetics in single dissociated mouse sensory neurons. ***Biochem. J.*** (1992), 283:41–50.

Duenas-Romero AM, Loiseau PM, Saint-Pierre-Chazalet M. Interaction of sitamaquine with membrane lipids of Leishmania donovani promastigotes. ***Biochim Biophys Acta***. (2007), 1768: 246–252.

Esterbauer H, Schaur RJ and Zollner H. Chemistry and biochemistry of 4-hydroxynonenal, malonaldehyde and related aldehydes. ***Free Radic. Biol. Med***. (1991), 11:81–128.

Fairlamb AH and Cerami A. Metabolism and functions of trypanothione in the kinetoplastida," ***Annual Review of Microbiology***. (1992), 46:695–729.

Fr´ezard F, Demicheli C and Ribeiro RR. Pentavalent antimonials: new perspectives for old drugs. ***Molecules***. (2009), 14:2317–2336.

Fr´ezard F, Demicheli C, Ferreira CS and Costa MAP. Glutathione-induced conversion of pentavalent antimony to trivalent antimony in meglumine antimoniate. ***Antimicrobial Agents and Chemotherapy***. (2001), 45:913–916.

Fujiwara K, Okamura K and Motokawa Y. Hydrogen carrier protein from chicken liver. Purification, characterization, and role of its prosthetic group, lipoic acid, in the glycine cleavage reaction. ***Arch. Biochem. Biophys***. (1979), 197:454–462.

Fujiwara K, Okamura-Ikeda K and Motokawa Y. Chicken liver H-protein, a component of the glycine cleavage system. Amino acid sequence and identification of the Ne-lipoyllysine residue. ***J. Biol. Chem***. (1986), 261:8836–8841.

Fujiwara K, Okamura-Ikeda K and Motokawa Y. Mechanism of the glycine cleavage reaction. Further characterization of the intermediate attached to H-protein and of the reaction catalyzed by T-protein. ***J. Biol. Chem***. (1984), 259:10664–10668.

Fujiwara K, Takeuchi S, Okamura-Ikeda K and Motokawa Y. Purification, characterization, and cDNA cloning of lipoate-activating enzyme from bovine liver. ***J. Biol. Chem***. (2001), 276:28819–28823.

Fujiwara K, Toma S, Okamura-Ikeda K, Motokawa Y, Nakagawa A and Taniguchi H. Crystal structure of lipoate-protein ligase A from Escherichia coli: determination of the lipoic acid-binding site. ***J. Biol. Chem***. (2005), 280:33645–33651.

Gagnon D, Foucher A, Girard I, Ouellette M. Stage specific gene expression and cellular localization of two isoforms of the serine hydroxymethyltransferase in the protozoan parasite *Leishmania*. ***Mol. Biochem. Parasitol.*** (2006), 150:63–71.

Garnier T, Brown MB, Lawrence MJ et al. In vitro and in vivo studies on a topical formulation of sitamaquine dihydrochloride for cutaneous leishmaniasis. ***J Pharm Pharmacol***. (2006), 58: 1043–1054.

Gazaryan IG, Krasnikov BF, Ashby GA, Thorneley RN, Kristal BS and Brown AM. Zinc is a potent inhibitor of thiol oxidoreductase activity and stimulates reactive oxygen species production by lipoamide dehydrogenase. ***J. Biol. Chem.*** (2002), 277:10064–10072.

Gibson DG, Young L, Chuang RY, Venter JC, Hutchison CA 3rd, Smith HO. Enzymatic assembly of DNA molecules up to several hundred kilobases. ***Nat Methods***. (2009), 6:343-345.

Gibson ME. The identification of kala azar and the discovery of *Leishmania donovani*. ***Med Hist***. (1983), 27:203–213.

Goyard S, Segawa H, Gordon et al. An *in vitro* system for developmental and genetic studies of *Leishmania donovani* phosphoglycans. ***Molecular and Biochemical Parasitology***. (2003), 130:31–42.

Goyard S, Segawa H, Gordon J et al. An *in vitro* system for developmental and genetic studies of *Leishmania donovani* phosphoglycans. ***Molecular and Biochemical Parasitology***. (2003), 130:31–42.

Green DE, Morris TW, Green J, Cronan JE, Guest JR. Purification and properties of the lipoate protein ligase of *Escherichia coli*. ***Biochem. J.*** (1995), 309:853–862.

Gurunathan S, Sacks DL, Brown DR, Reiner SL, Charest H, Glaichenhaus N, Seder RA. Vaccination with DNA encoding the immune dominant LACK parasite antigen

confers protective immunity to mice infected with *Leishmania major*. ***J Exp Med***. (1997), 186:1137-1147.

Gurunathan S, Wu CY, Freidag BL, Seder RA. DNA vaccines: a key for inducing long-term cellular immunity. ***Curr Opin Immunol***. (2000), 12:442-447.

Hag IA, Hashim FA, el Toum IA, Homeida M, el Kalifa M, el Hassan AM. Liver morphology and function in visceral leishmaniasis (Kala-azar). ***J Clin Pathol.*** (1994); 47:547-551.

Håkansson AP, Smith AW. Enzymatic characterization of dihydrolipoamide dehydrogenase from *Streptococcus pneumoniae* harboring its own substrate. ***J Biol Chem***. (2007), 282:29521-29530.

Hallström T, Mörgelin M, Barthel D, Raguse M, Kunert A, Hoffmann R, Skerka C, Zipfel PF. Dihydrolipoamide dehydrogenase of *Pseudomonas aeruginosa* is a surface-exposed immune evasion protein that binds three members of the factor H family and plasminogen. ***J Immunol***. (2012), 189:4939-4944

Handman E, Hocking RE, Mitchell GF, Spithill TW. Isolation and characterization of infective and non-infective clones of Leishmania tropica. ***Mol Biochem Parasitol***. (1983), 7:111-126.

Hansford RG. Control of mitochondrial substrate oxidation. ***Curr. Top. Bioenerg***. (1980), 10:217–278.

Harris, R. A., Bowker-Kinley, M. M., Huang, B., and Wu, P. Regulation of the activity of the pyruvate dehydrogenase complex. ***Adv. Enzyme Regul***. (2002), 42, 249–259.

Hasan UA, Abai AM, Harper DR, Wren BW, Morrow WJ. Nucleic acid immunization: concepts and techniques associated with third generation vaccines. ***J Immunol Methods***. (1999), 229:1-22.

Herbrecht R, Natarajan-Amé S, Nivoix Y, Letscher-Bru V. The lipid formulations of amphotericin B. ***Expert Opin Pharmacother***. (2003), 4:1277-1287.

Hoare CA. Early discoveries regarding the parasites of Oriental sore. ***Trans R Soc Trop Med Hyg.*** (1938), 32:66–92.

Howard JC. Restrictions on the use of antigenic peptides by the immune system. ***Proc Natl Acad Sci U S A.*** (1993), 90:3777-3779.

Huang F, Qu F, Peng Q, Xia Y, Peng L. Synthesis and characterization of photo labeling probes of miltefosine. ***J. Fluorine Chem***. (2005), 126:739–743.

Humphries KM and Szweda LI. Selective inactivation of alpha-ketoglutarate dehydrogenase and pyruvate dehydrogenase: reaction of lipoic acid with 4-hydroxy-2-nonenal. ***Biochemistry***. (1998):15835–15841.

Imbard A, Boutron A, Vequaud C, Zater M, de Lonlay P, de Baulny HO, Barnerias C, Miné M, Marsac C, Saudubray JM, Brivet M. Molecular characterization of 82

patients with pyruvate dehydrogenase complex deficiency. Structural implications of novel amino acid substitutions in E1 protein. ***Mol Genet Metab***. (2011), 104:507-516.

Iqbal J, Hira PR, Saroj G, Philip R, Al-Ali F, Madda PJ, *et al*. Imported visceral leishmaniasis: diagnostic dilemmas and comparative analysis of three assays. ***J Clin Microbiol***. (2002), 40:475-479.

Jackman SA, Hough DW, Danson MJ, Stevenson KJ, Opperdoes FR. Subcellular localization of dihydrolipoamide dehydrogenase and detection of lipoic acid in bloodstream forms of *Trypanosoma brucei*. ***Eur J Biochem***. (1990), 193:91-95.

Jardim A, Alexander J, Teh HS, Ou D, Olafson RW. Immunoprotective *Leishmania major* synthetic T cell epitopes. ***J Exp Med***. (1990), 172:645-648.

Jarvis JN, Lockwood DN. Clinical aspects of visceral leishmaniasis in HIV infection. ***Curr Opin Infect Dis***. (2013), 26:1-9.26.

Jensen AT, Gasim S, Moller T, Ismail A, Gaafar A, Kemp M, *et al*. Serodiagnosis of *Leishmania donovani* infections: assessment of enzyme-linked immunosorbent assays using recombinant *L. donovani* gene B protein (GBP) and a peptide sequence of *L. donovani* GBP. ***Trans R Soc Trop Med Hyg***. (1999), *93*:157-160.

Jeoung NH, Harris CR, Harris RA. Regulation of pyruvate metabolism in metabolic-related diseases. Rev ***Endocr Metab Disord***. (2014), 15:99-110.

Jha TK, Sundar S, Thakur CP et al. 2005. A phase II dose-ranging study of sitamaquine for the treatment of visceral leishmaniasis in India. ***Am J Trop Med Hyg***. (2005), 73: 1005–1011.

Kale S, Arjunan P, Furey W, and Jordan F. A dynamic loop at the active center of the *Escherichia coli* pyruvate dehydrogenase complex E1 component modulates substrate utilization and chemical communication with the E2 component. ***J. Biol. Chem***. (2007), 282:28106–28116.

Kaplon J, Zheng L, Meissl K, Chaneton B, Selivanov VA, Mackay G, van der Burg SH, Verdegaal EM, Cascante M, Shlomi T, Gottlieb E, Peeper DS. A key role for mitochondrial gatekeeper pyruvate dehydrogenase in oncogene-induced senescence. ***Nature***. (2013), 498:109-112.

Kato M, Wynn RM, Chuang JL, Tso SC, Machius M, Li J, Chuang DT. Structural basis for inactivation of the human pyruvate dehydrogenase complex by phosphorylation: role of disordered phosphorylation loops. ***Structure.*** (2008), 16, 1849-1859.

Kawasaki H, Sato T and Kikuchi G. A new reaction for glycine biosynthesis. ***Biochem. Biophys. Res. Commun***. (1966), 23:227–233.

Killick-Kendrick R. The life-cycle of *Leishmania* in the sand-fly with special reference to the form infective to the vertebrate host. ***Ann Parasitol Hum Comp***. (1990), 1, 7-42.

Kim H, Patel MS. Characterization of two site-specifically mutated human dihydrolipoamide dehydrogenases (His-452----Gln and Glu-457----Gln). ***J Biol Chem***. (1992), 267:5128-5132.

Kim H. Activity of human dihydrolipoamide dehydrogenase is largely reduced by mutation at isoleucine-51 to alanine. ***J Biochem Mol Biol***. (2006), 39:223-227.

Kim H. Activity of human dihydrolipoamide dehydrogenase is reduced by mutation at threonine-44 of FAD-binding region to valine. ***J Biochem Mol Biol***. (2002), 35:437-41.

Kim H. Characterization of Two Site-specific Mutations in Human Dihydrolipoamide dehydrogenase. ***Bull. Korean Chem. Soc***. (2013), 34, 1621.

Kim, H. Consensus sequence for the active site disulfide bond region of dihydrolipoamide dehydrogenases with known primary structures. ***J. Nat. Sci***. (2001), 18:23-29.

Kleiger G, Perry J, and Eisenberg D. 3D structure and significance of the GPhiXXG helix packing motif in tetramers of the E1beta subunit of pyruvate dehydrogenase from the archeon *Pyrobaculum aerophilum*. ***Biochemistry***. (2001), 40, 14484-14492.

Koike M and Koike K. Structure, assembly and function of mammalian alpha-keto acid dehydrogenase complexes. **Adv. Biophys**. (1976), 9:182–227.

Kolobova, E, Tuganova A, Boulatnikov I, and Popov KM. Regulation of pyruvate dehydrogenase activity through phosphorylation at multiple sites. ***Biochem. J***. (2001), 358:69–77.

Korotchkina LG and Patel MS. Mutagenesis studies of the phosphorylation sites of recombinant human pyruvate dehydrogenase. Site specific regulation. ***J. Biol. Chem***. (1995), 270:14297–14304.

Korotchkina LG, and Patel MS. (2001a). Probing the mechanism of inactivation of human pyruvate dehydrogenase by phosphorylation of three sites. ***J. Biol. Chem***. (2001a), 276:5731–5738.

Kraulis P. MOLSCRIPT: a program to produce both detailed and schematic plots of protein structures. ***J. Appl. Crystallogr***. (1991), 24:946-950.

Kumar R, Tiwari K, Dubey VK. Methionine aminopeptidase 2 is a key regulator of apoptotic like cell death in *Leishmania donovani*. ***Sci Rep***. (2017), 7:95.

Kume A, Koyata H, Sakakibara T, Ishiguro Y, Kure S and Hiraga K. The glycine cleavage system. Molecular cloning of the chicken and human glycine decarboxylase cDNAs and some characteristics involved in the deduced protein structures. ***J. Biol. Chem***. (1991), 266:3323–3329.

Lai JC and Cooper AJ. Brain alpha-ketoglutarate dehydrogenase complex: kinetic properties, regional distribution and effects of inhibitors. ***J. Neurochem***. (1986), 47:1376–1386.

Lai JC, Walsh JM, Dennis SC and Clark JB. Synaptic and non-synaptic mitochondria from rat brain: isolation and characterization. ***J. Neurochem***. (1977), 28:625–631.

Laine LM, Biddau M, Byron O, Müller S. Biochemical and structural characterization of the apicoplast dihydrolipoamide dehydrogenase of *Plasmodium falciparum*. ***Biosci Rep.*** (2015), 35: pii: e00171.

Lainson R. The neotropical Leishmania species: a brief historical review of their discovery, ecology and taxonomy. ***Rev Pan-Amaz Saude***. (2010), 1:13–32.

Landgraf TN, Costa MV, Oliveira AF, Ribeiro WC, Panunto-Castelo A, Fernandes FF. Involvement of Dihydrolipoyl Dehydrogenase in the Phagocytosis and Killing of *Paracoccidioides brasiliensis* by Macrophages. ***Front Microbiol***. (2017), 8:1803.

Lee HH, Kim DJ, Ahn HJ, Ha JY and Shu SW. Crystal structure of T-protein of the glycine cleavage system. Cofactor binding, insights into H-protein recognition, and molecular basis for understanding nonketotic hyperglycinemia. ***J. Biol. Chem***. (2004), 279:50514–50523.

Leishman WB. On the possibility of the occurrence of trypanosomiasis in India. ***Br Med J.*** (1903), 1:1252–1254.

Lindsay H, Beaumont E, Richards SD, Kelly SM, Sanderson SJ, Price NC, Lindsay JG. FAD insertion is essential for attaining the assembly competence of the dihydrolipoamide dehydrogenase (E3) monomer from *Escherichia coli*. ***J Biol Chem***. (2000), 275:36665-36670.

Liu TC, Hong YS, Korotchkina LG, Vettakkorumakankav NN, Patel MS. Site-directed mutagenesis of human dihydrolipoamide dehydrogenase: role of lysine-54 and glutamate-192 in stabilizing the thiolate-FAD intermediate. ***Protein Expr Purif***. (1999), 16:27-39.

Logan-Klumpler FJ, De Silva N, Boehme U, Rogers MB, Velarde G, McQuillan JA, Carver T, Aslett M, Olsen C, Subramanian S, Phan I, Farris C, Mitra S, Ramasamy G, Wang H, Tivey A, Jackson A, Houston R, Parkhill J, Holden M, Harb OS, Brunk BP, Myler PJ, Roos D, Carrington M, Smith DF, Hertz-Fowler C, Berriman M. GeneDB--an annotation database for pathogens. ***Nucleic Acids Res***. (2012), 40:D98-108.

Lohrer H, Krauth-Siegel RL. Purification and characterization of lipoamide dehydrogenase from *Trypanosoma cruzi*. ***Eur J Biochem***. (1990), 194: 863-869.

Lokanath NK, Kuroishi C, Okazaki N and Kunishima N. Crystal structure of a component of glycine cleavage system. T-protein from *Pyrococcus horikoshii* OT3 at 1.5A˚ resolution. ***Proteins: Struct. Funct. Genet***. (2004), 58:769–773.

Maalej IA, Chenik M, Louzir H, *et al*. Comparative evaluation of ELISAs based on ten recombinant or purified *Leishmania* antigens for the serodiagnosis of Mediterranean visceral leishmaniasis. ***Am J Trop Med Hyg***. (2003), 68:312-20.

Machado PR, Ampuero J, Guimarães LH, Villasboas L., Rocha AT. Schriefer AT, et al. Miltefosine in the treatment of cutaneous leishmaniasis caused by *Leishmania braziliensis* in Brazil: a randomized and controlled trial. ***PloS Negl. Trop. Dis***. (2010), 4:1–6.

Marco C, Jimenez-Lopez JM, Rios-Marco P. Hexadecylphosphocholine alters non-vesicular cholesterol traffic from the plasma membrane to the endoplasmic reticulum and inhibits the synthesis of sphingomyelin in HepG2cells. ***Int. J. Biochem. Cell Biol***. (2009), 41:1296–1303.

Maroli M, Feliciangeli MD, Bichaud L, Charrel RN, Gradoni L. Phlebotomine sandflies and the spreading of leishmaniasis and other diseases of public health concern. ***Med Vet Entomol***. (2013), 27:123–147.

Marquis N, B. Gourbal, B. P. Rosen, R. Mukhopadhyay, and M. Ouellette. Modulation in aquaglyceroporin AQP1 gene transcript levels in drug-resistant *Leishmania*. ***Molecular Microbiology***. (2005), 57:1690–1699.

Marr JJ. Purine analogs as chemotherapeutic agents in leishmaniasis and American trypanosomiasis. ***Journal of Laboratory and Clinical Medicine***. (1991), 118:111–119.

Martins AL, Barreto JA, Lauris JR, Martins AC. American tegumentary leishmaniasis: correlations among immunological, histopathological and clinical parameters. ***An Bras Dermatol***. (2014), 89:52–58.

Marzochi KB, Marzochi MA, Silva AF, Grativol N, Duarte R, Confort EM, Modabber F. Phase 1 study of an inactivated vaccine against American tegumentary leishmaniasis in normal volunteers in Brazil. ***Mem Inst Oswaldo Cruz.*** (1998), 93:205-212.

Mattevi A, Obmolova G, Kalk KH, van Berkel WJ, and Hol WG. Three-dimensional structure of lipoamide dehydrogenase from *Pseudomonas fluorescens* at 2.8 Å resolution. Analysis of redox and thermostability properties. ***J. Mol. Biol***. (1993), 230:1200–1215.

Mattevi A, Schierbeek AJ, and Hol WG. Refined crystal structure of lipoamide dehydrogenase from *Azotobacter vinelandii* at 2.2 Å resolution. A comparison with the structure of glutathione reductase. ***J. Mol. Biol***. (1991), 220:975–994.

Mattevi A, Schierbeek AJ, Hol WGJ. The refined crystal structure of *Azotobacter vinelandii* lipoamide dehydrogenase at 2.2 Å resolution. ***J. Mol. Biol***. (1991), 220:975-994.

Matzinger P. An innate sense of danger. ***Semin. Immunol***. (1998), 10:399–415.

Maya JD, Bollo S, Nuñez-Vergara LJ, Squella JA, Repetto Y, Morello A, Périé J, Chauvière G. *Trypanosoma cruzi*: effect and mode of action of nitroimidazole and nitrofuran derivatives. ***Biochem Pharmacol***. (2003), 65: 999-1006.

McConville MJ, Bacic A, Mitchell GF, Handman E. Lipophosphoglycan of *Leishmania major* that vaccinates against cutaneous leishmaniasis contains an alkyl glycerophosphoinositol lipid anchor. ***Proc Natl Acad Sci U S A***. (1987), 84:8941-8945.

McDonough MA, Loenarz C, Chowdhury R, Clifton IJ, Schofield CJ. Structural studies on human 2-oxoglutarate dependent oxygenases. ***Curr Opin Struct Biol***. (2010), 20:659-672.

McWilliam H, Li W, Uludag M, Squizzato S, Park YM, Buso N, Cowley AP, Lopez R. Analysis Tool Web Services from the EMBL-EBI. ***Nucleic Acids Res***. (2013), 41:W597-600.

Mendonca SC, De Luca PM, Mayrink W, Restom TG, Conceicao-Silva F, Da-Cruz AM, Bertho AL, Da Costa CA, Genaro O, Toledo VP, et al. Characterization of human T lymphocyte-mediated immune responses induced by a vaccine against American tegumentary leishmaniasis. ***Am J Trop Med Hyg***. (1995), 53:195-201.

Mimori T, Matsumoto T, Calvopina MH, Gomez EA, SayaH, Katakura K, *et al*. Usefulness of sampling with cotton swab for PCR-diagnosis of cutaneous leishmaniasis in the New World. ***Acta Trop***. (2002), 81:197-202.

Mishra J, Saxena A, Singh S. Chemotherapy of leishmaniasis: past, present and future. ***Curr Med Chem***. (2007), 14:1153-1169.

Momeni AZ, Jalayer T, Emamjomeh M, Khamesipour A, Zicker F, Ghassemi RL, Dowlati Y, Sharifi I, Aminjavaheri M, Shafiei A, Alimohammadian MH, Hashemi-Fesharki R, Nasseri K, Godal T, Smith PG, Modabber F. A randomised, double-blind, controlled trial of a killed *L. major* vaccine plus BCG against zoonotic cutaneous leishmaniasis in Iran. ***Vaccine***. (1999), 17:466-72.

Mondal D, Nasrin KN, Huda MM, Kabir M, Hossain MS, Kroeger A, Thomas T, Haque R. Enhanced case detection and improved diagnosis of PKDL in a Kala-azar-endemic area of Bangladesh. ***PLoS Negl Trop Dis***. (2010), 4, pii: e832.

Moody DB, Ulrichs T, Mühlecker W, Young DC, Gurcha SS, Grant E, Rosat JP, Brenner MB, Costello CE, Besra GS, Porcelli SA. CD1c-mediated T-cell recognition of isoprenoid glycolipids in Mycobacterium tuberculosis infection. ***Nature***. (2000), 404:884-888.

More B, Bhatt H, Kukreja V, Ainapure SS. Miltefosine great expectations against visceral leishmaniasis. ***J. Postgrad. Med***. (2003), 49:101–103.

Motokawa Y and Kikuchi G. Glycine metabolism by rat liver mitochondria. IV. Isolation and characterization of hydrogen carrier protein, an essential factor for glycine metabolism. ***Arch. Biochem. Biophys.*** (1969), 135:402–409.

Mukherjee SB, Das M, Sudhandiran G and Shaha C. Increase in cytosolic Ca2+ levels through the activation of non-selective cation channels induced by oxidative stress causes mitochondrial depolarization leading to apoptosis like death in *Leishmania donovani* promastigotes. ***Journal of Biological Chemistry***. (2002), 277:24717–24727.

Muller M, Papadopoulou B. Stage-specific expression of the glycine cleavage complex subunits in *Leishmania infantum*. ***Mol. Biochem. Parasitol***. (2010), 170:17–27.

Muller YA, Lindqvist Y, Furey W, Schulz GE, Jordan F, Schneider G. A thiamin diphosphate binding fold revealed by comparison of the crystal structures of transketolase, pyruvate oxidase and pyruvate decarboxylase. ***Structure***. (1993), 1:95-103.

Murray HW, Montelibano C, Peterson R, and Sypek JP. Interleukin-12 regulates the response to chemotherapy in experimental visceral leishmaniasis. ***Journal of Infectious Diseases.*** (2000), 182, 1497–1502.

Murta SM, Nogueira FB, Dos Santos PF, Campos FM, Volpe C, Liarte DB, Nirdé P, Probst CM, Krieger MA, Goldenberg S, Romanha AJ. Differential gene expression in ***Trypanosoma cruzi*** populations susceptible and resistant to benznidazole. ***Acta Trop***. 2008; 107: 59-65.

Nemeria N, Volkov A, Brown A, Yi J, Zipper L, Guest JR, and Jordan F. Systematic study of the six cysteines of the E1 subunit of the pyruvate dehydrogenase multienzyme complex from *Escherichia coli*: none is essential for activity. ***Biochemistry***. (1998), 37:911–922.

Okamura-Ikeda K, Fujiwara K and Motokawa Y. Mechanism of the glycine cleavage reaction. Properties of the reverse reaction catalyzed by T-protein. ***J. Biol. Chem***. (1987), 262:6746–6749.

Okamura-Ikeda K, Fujiwara K and Motokawa Y. The amino-terminal region of the *Escherichia coli* T-protein of the glycine cleavage system is essential for proper association with H-protein. Eur. ***J. Biochem***. (1999), 264, 446–452.

Okamura-Ikeda K, Hosaka H, Yoshimura M, Yamashita E, Toma S, Nakagawa A, Fujiwara K, Motokawa Y and Taniguchi H. Crystal structure of human T-protein of glycine cleavage system at 2.0A˚ resolution and its implication for understanding non-ketotic hyperglycinemia. ***J. Mol. Biol***. (2005), 351:1146–1159.

Okamura-Ikeda K, Kameoka N, Fujiwara K and Motokawa Y. Probing the H-protein induced conformational change and the function of the N-terminal region of Escherichia coli T-protein of the glycine cleavage system by limited proteolysis. ***J. Biol. Chem.*** (2003), 278:10067–10072.

Okamura-Ikeda K, Ohmura Y, Fujiwara K and Motokawa Y. Cloning and nucleotide sequence of the gcv operon encoding the Escherichia coli glycine-cleavage system. ***Eur. J. Biochem.*** (1993), 216:539–548.

Okamura-Ikeda, K., Fujiwara, K. and Motokawa, Y. Purification and characterization of chicken liver T-protein, a component of the glycine cleavage system. ***J. Biol. Chem***. (1982), 257:135–139.

Olanow CW. A radical hypothesis for neurodegeneration. ***Trends Neurosci.*** (1993), 16:439–444.

Overath P, Aebischer T. Antigen presentation by macrophages harboring intra vesicular pathogens. ***Parasitol Today***. (1999), 15:325-332.

Palatnik-de-Sousa CB, Gomes EM, Paraguai-de-Souza E, Palatnik M, Luz K, Borojevic R. *Leishmania donovani*: titration of antibodies to the fucose-mannose ligand as an aid in diagnosis and prognosis of visceral leishmaniasis. ***Trans R Soc Trop Med Hyg***. (1995); 89:390-393.

Palumbo E. Treatment strategies for mucocutaneous leishmaniasis. ***J Glob Infect Dis***. (2010), 2:147-150.

Pardoll DM, and Beckerleg AM. Exposing the immunology of naked DNA vaccines. ***Immunity***. (1995), 3:165–169.

Park YH, and Patel M S. Characterization of interactions of dihydrolipoamide dehydrogenase with its binding protein in the human pyruvate dehydrogenase complex. ***Biochem. Biophys***. (2010), 395:416–419.

Park YH. (2008) *Protein-Protein Interactions in the Pyruvate Dehydrogenase Complex from Escherichia coli.* Ph.D. thesis, Rutgers University

Patel KP, O'Brien TW, Subramony SH, Shuster J, Stacpoole PW. The spectrum of pyruvate dehydrogenase complex deficiency: clinical, biochemical and genetic features in 371 patients. ***Mol Genet Metab***. (2012), 106:385-94.

Patel MS, Korotchkina LG, and Sidhu S. Interaction of E1 and E3 components with the core proteins of the human pyruvate dehydrogenase complex. ***J. Mol. Catal. B Enzym.*** (2009), 61:2–6.

Perez-Victoria JM, Cortés-Selva F, Parodi-Talice A, Bavchvarov BI, Pérez-Victoria FJ, Mu˜noz-Martínez F, et al. Combination of suboptimal doses ofinhibitors targeting different domains of LtrMDR1 efficiently over comes resistance of *Leishmania spp* to miltefosine by inhibiting drug efflux. ***Antimicrob. Agents Chemother.*** (2006), 50:3102–3110.

Perham RN. Swinging arms and swinging domains in multifunctional enzymes: catalytic machines for multistep reactions. ***Annu. Rev. Biochem***. (2000), 69:961–1004.

Peters W. The treatment of kala-azar: new approaches to an old problem. ***Indian Journal of Medical Research.*** (1981), 73:1–18.

Petiz LL, Pires ADRA, Echevarria A, Rodrigues-Santos CE, Eliane Merlin Rocha M, Acco A, Cadena SMSC. Effects of a new antiprotozoal drug, N, N'-diphenyl-4-

methoxy-benzamidine, on energy-linked functions of rat liver mitochondria. ***ChemBiol Interact***. (2017), S0009-2797:130436-130437.

Pettit FH, Roche TE and Reed LJ. Function of calcium ions in pyruvate dehydrogenase phosphatase activity. ***Biochem. Biophys. Res. Commun***. (1972), 49:563–571.

Pfeffer K, Schoel B, Gulle H, Kaufmann SH, Wagner H. Primary responses of human T cells to mycobacteria: a frequent set of gamma/delta T cells are stimulated by protease-resistant ligands. ***Eur J Immunol***. (1990), 20:1175-1179.

Poinar Jr G, Poinar R. Paleoleishmania proterus n. gen., n. sp., (Trypanosomatidae: Kinetoplastida) from Cretaceous Burmese amber. ***Protist***. (2004), 155:305–310.

Poinar Jr G. Lutzomyia adiketis sp. n. (Diptera: Phlebotomidae), a vector of Paleoleishmania neotropicum sp. n. (Kinetoplastida: Trypanosomatidae) in Dominican amber. ***Parasit Vectors.*** (2008), 1:22.

Rais S, Perianin A, Lenoir M. et al. Sodium stibogluconate (Pentostam) potentiates oxidant production in murine visceral leishmaniasis and in human blood. ***Antimicrobial Agents and Chemotherapy*.** (2000), 44:2406–2410.

Rakotomanga M, Loiseau PM, Saint-Pierre-Chazalet M. Hexadecylphosphocholine interaction with lipid monolayers. ***Biochim. Biophys. Acta***. (2004), 1661:212–218.

Ramalho-Ortigao M, Saraiva EM, Traub-Csekö YM. Sand fly-*Leishmania* interactions: long relationships are not necessarily easy. ***Open Parasitol J***. (2010), 4:195-204.

Reed LJ and Hackert ML. Structure-function relationships in dihydrolipoamide acyltransferases. ***J. Biol. Chem***. (1990), 265, 8971–8974.

Reed LJ. Multienzyme complexes. ***Acc. Chem. Res***. (1974), 7:40-46.

Richert DA, Amberg R and Wilson M. Metabolism of glycine by avian liver. ***J. Biol. Chem***. (1962), 237:99–103.

Rivier D, Bovay P, Shah R, Didisheim S, Mauël J. Vaccination against Leishmania major in a CBA mouse model of infection: role of adjuvants and mechanism of protection. ***Parasite Immunol***. (1999), 21:461-473.

Robert X, Gouet P. Deciphering key features in protein structures with the new ENDscript server. ***Nucleic Acids Res***. (2014), 42:W320-324.

Roberts WL, Berman JD and Rainey PM. *in vitro* antileishmanial properties of tri- and pentavalent antimonial preparations. ***Antimicrobial Agents and Chemotherapy***. (1995), 39:1234–1239.

Roche TE, Baker JC, Yan X, Hiromasa Y, Gong X, Peng T, Dong J, Turkan A, Kasten SA. Distinct regulatory properties of pyruvate dehydrogenase kinase and phosphatase isoforms. ***Prog Nucleic Acid Res Mol Biol.*** (2001), 70:33-75.

Roche TE, Hiromasa Y, Turkan A, Gong X, Peng T, Yan X, Kasten SA, Bao H, Dong J. Essential roles of lipoyl domains in the activated function and control of pyruvate dehydrogenase kinases and phosphatase isoform 1. ***Eur J Biochem***. (2003), 270:1050-1056.

Roldán A, Comini MA, Crispo M, Krauth-Siegel RL. Lipoamide dehydrogenase is essential for both bloodstream and procyclic *Trypanosoma brucei*. ***Mol Microbiol***. (2011), 81:623-39.

Romero GAS, Sampaio RNR, Macêdo VO, Marsden PD. Sensitivity of lymph node aspiration in localized cutaneous leishmaniasis due to *Leishmania* (*Viannia*) *braziliensis*. ***Mem Inst Oswaldo Cruz, Rio de Janeiro***. (1999), 94:509-511.

Rosen BP. Transport and detoxification systems for transition metals, heavy metals and metalloids in eukaryotic and prokaryotic microbes. ***Comparative Biochemistry and Physiology***. (2002), 133:689–693.

Russell DG, and Alexander J. Effective immunization against cutaneous leishmaniasis with defined membrane antigens reconstituted into liposomes. ***J. Immunol***. (1988), 140:1274–1279.

Russo DM, Jardim A, Carvalho EM, Sleath PR, Armitage RJ, Olafson RW, Reed SG. Mapping human T cell epitopes in *Leishmania* gp63: identification of cross-reactive and species-specific epitopes. ***J Immunol***. (1993), 150:4713.

Sagers RD and Gunsalus IC. Intermediary metabolism of *Diplococcus glycinophilus*. I. Glycine cleavage and one carbon interconversions. ***J. Bacteriol***. (1961), 81:541–549.

Sale GJ, Randle PJ. Analysis of site occupancies in [32P] phosphorylated pyruvate dehydrogenase complexes by aspartyl-prolyl cleavage of tryptic phosphopeptides. ***Eur J Biochem***. (1981), 120:535-540.

Santos DCMD, de Souza MLS, Teixeira EM, Alves LL, Vilela JMC, Andrade M,Carvalho MDG, Fernandes AP, Ferreira LAM, Aguiar MMG. A new nanoemulsion formulation improves antileishmanial activity and reduces toxicity of amphotericin B. ***J Drug Target***. (2018), 26:357-364.

Saudagar P, Dubey VK. Cloning, expression, characterization and inhibition studies on trypanothione synthetase, a drug target enzyme, from *Leishmania donovani*. ***Biol Chem***. (2011), 392:1113-1122.

Savage N. Preparation and properties of highly purified diaphorase. ***Biochem J***. (1957), 67: 146-155.

Schallig HD, Schoone GJ, Kroon CC, Hailu A, Chappuis F, Veeken H. Development and application of 'simple' diagnostic tools for visceral leishmaniasis. ***Med Microbiol Immunol (Berl)*** (2001), 190:69-71.

Schoone GJ, Hailu A, Kroon CC, Nieuwenhuys JL, Schallig HD, Oskam L. A fast agglutination-screening test (FAST) for the detection of anti-*Leishmania* antibodies. ***Trans R Soc Trop Med Hyg***. (2001), 95:400-401.

Scott DA, Hickerson SM, Vickers TJ, Beverley SM. The role of the mitochondrial glycine cleavage complex in the metabolism and virulence of the protozoan parasite *Leishmania major*. ***J. Biol. Chem*.** (2008), 283:155–165.

Sensi SL, Yin HZ, Carriedo SG, Rao SS and Weiss JH. Preferential Zn2C influx through Ca2C- permeable AMPA/kainate channels triggers prolonged mitochondrial superoxide production. ***Proc. Natl Acad. Sci. USA.*** (1999), 96:2414–2419.

Shaked-Mishant P, Ulrich N, Ephros M and Zilberstein D. Novel intracellular Sb reducing activity correlates with antimony susceptibility in *Leishmania donovani*. ***Journal of Biological Chemistry***, (2001), 276, 3971–3976.

Shaked-Mishant P, Ulrich N, Ephros M, and Zilberstein D. Novel intracellular Sb reducing activity correlates with antimony susceptibility in *Leishmania donovani*. ***Journal of Biological Chemistry*.** (2001), 276:3971–3976.

Sharifi I, FeKri AR, Aflatonian MR, Khamesipour A, Nadim A, Mousavi MR, Momeni AZ, Dowlati Y, Godal T, Zicker F, Smith PG, Modabber F. Randomised vaccine trial of single dose of killed *Leishmania major* plus BCG against anthroponotic cutaneous leishmaniasis in Bam, Iran. ***Lancet***. (1998), 351:1540-1543.

Shatry AM, Oster CN, Mebrahtu YB, Perkins PV, Hendricks LD. Mouse foot-pad inoculation as an aid to the isolation of *Leishmania* spp. from patients. ***Trans R Soc Trop Med Hyg*.** (1988), 82: 701-703.

Sheu KF, Kim YT, Blass JP and Weksler ME. An immunochemical study of the pyruvate dehydrogenase deficit in Alzheimer's disease brain. ***Ann. Neurol***. (1985), 17:444–449.

Sieling PA, Ochoa MT, Jullien D, Leslie DS, Sabet S, Rosat JP, Burdick AE, Rea TH, Brenner MB, Porcelli SA, Modlin RL. Evidence for human CD4+ T cells in the CD1-restricted repertoire: derivation of mycobacteria-reactive T cells from leprosy lesions. ***J Immunol***. (2000), 164:4790-4796.

Siesjo BK, Zhao Q, Pahlmark K, Siesjo P, Katsura K and Folbergrova J. Glutamate, calcium and free radicals as mediators of ischemic brain damage. ***Ann. Thorac. Surg***. (1995), 59:1316–1320.

Sievers F, Wilm A, Dineen D, Gibson TJ, Karplus K, Li W, Lopez R, McWilliam H, Remmert M, Söding J, Thompson JD, Higgins DG. Fast, scalable generation of high-quality protein multiple sequence alignments using Clustal Omega. ***Mol Syst Biol***. (2011), 7:539.

Singh S, Dey A, Sivakumar R. Applications of molecular methods for *Leishmania* control. ***Rev Expert Rev Mol Diagn***. (2005), 5:251-265.

Singh S, Kumari V, Singh N. Predicting kala-azar disease manifestations in asymptomatic patients with latent *Leishmania donovani* infection by detection of antibody against recombinant K39 antigen. ***Clin Diagn Lab Immunol***. (2002), 9:568-572.

Singh S, Mohapatra DP, Sivakumar R. Successful replacement of foetal calf serum with human urine for *in vitro* culture of *Leishmania donovani*. ***J Commun Dis***. (2000), 32:289-94.

Singh S, Siva kumar R. Recent advances in the diagnosis of leishmaniasis. ***J Postgrad Med***. (2003), 49:55-60.

Singh S. and Sivakumar R. Challenges and new discoveries in the treatment of leishmaniasis. ***Journal of Infection and Chemotherapy***. (2004), 10:307–315.

Sjölander A, Baldwin TM, Curtis JM, Handman E. Induction of a Th1 immune response and simultaneous lack of activation of a Th2 response are required for generation of immunity to leishmaniasis. ***J Immunol***. (1998), 160:3949-3957.

Smith LE, Rodrigues M, and Russell DG. The interaction between CD8+ cytotoxic T cells and Leishmania-infected macrophages. ***Journal of Experimental Medicine***. (1991), 174:499–505.

Soto J, Arana BA, Toledo J, Rizzo N, Vega JC, Diaz et al. Miltefosine for new world cutaneous leishmaniasis. ***Clin. Infect. Dis.*** (2004), 38:1266–1272.

Spitzer N, Jardim A, Lippert D, Olafson RW. Long-term protection of mice against Leishmania major with a synthetic peptide vaccine. ***Vaccine***. (1999), 17:1298-1300.

Stacpoole PW. Therapeutic Targeting of the Pyruvate Dehydrogenase Complex/Pyruvate Dehydrogenase Kinase (PDC/PDK) Axis in Cancer. ***J Natl CancerInst***. (2017), 111:109.

Starkov AA and Fiskum G. Myxothiazol induces H_2O_2 production from mitochondrial respiratory chain. ***Biochem. Biophys. Res. Commun.*** (2001), 281:645–650.

Starkov AA, Fiskum G, Chinopoulos C, Lorenzo BJ, Browne SE, Patel MS and Beal MF. Mitochondrial alpha-ketoglutarate dehydrogenase complex generates reactive oxygen species. ***J. Neurosci***. (2004), 24:7779–7788.

Stephens PE, Darlison, MG, Lewis HM, and Guest, J. R. The pyruvate dehydrogenase complex of *Escherichia coli* K12. Nucleotide sequence encoding the dihydrolipoamide acetyltransferase component. ***Eur. J. Biochem***. (1983), 133:481–489.

Steverding D. The history of leishmaniasis. ***Parasit Vectors***. (2017), 10, 82.

Stover P, Schirch V. The metabolic role of leucovorin. ***Trends Biochem. Sci***. (1993), 18:102–106.

Sudhandiran G and Shaha C. Antimonial-induced increase in intracellular Ca2+ through non-selective cation channels in the host and the parasite is responsible for

apoptosis of intracellular *Leishmania donovani* amastigotes. ***Journal of Biological Chemistry***. (2003), 278:25120–25132.

Sugita M, Moody DB, Jackman RM, Grant EP, Rosat JP, Behar SM, Peters PJ, Porcelli SA, Brenner MB. CD1--a new paradigm for antigen presentation and T cell activation. ***Clin Immunol Immunopathol***. (1998), 87:8-14.

Sümegi B, Alkonyi I. Elementary steps in the reaction of the pyruvate dehydrogenase complex from pig heart. Kinetics of thiamine diphosphate binding to the complex. ***Eur J Biochem***. (1983), 136:347-353.

Sundar S, Jha TK, Thakur CP, Sinha PK and Bhattacharya SK. Injectable paromomycin for visceral leishmaniasis in India. ***N. Engl. J. Med***. (2007), 356:2571–2581.

Sundar S, Rai M. Laboratory Diagnosis of Visceral Leishmaniasis. ***Clinical and diagnostic laboratory immunology***. (2002), 9:951–958.

Tan TH, Bochud-Allemann N, Horn EK, Schneider A. Eukaryotic-type elongator tRNAMet of Trypanosoma brucei becomes formylated after import into mitochondria. ***Proc Natl Acad Sci U S A***. (2002), 99:1152-1157.

Thakur CP, Olliaro P, Gothoskar S, Bhowmick S, Choudhury BK, Prasad S, Kumar M, Verma BB. Treatment of visceral leishmaniasis (kala-azar) with aminosidine (=paromomycin)-antimonial combinations, a pilot study in Bihar, India. ***Trans R Soc Trop Med Hyg.*** (1992), 86:615-616.

Thomas MC, Macias F, Alonso C, López MC. The biology and evolution of transposable elements in parasites. ***Trends Parasitol***. (2010), 26:350-356.

Titus RG, Gueiros-Filho FJ, de Freitas LA, Beverley SM. Development of a safe live *Leishmania* vaccine line by gene replacement. ***Proc Natl Acad Sci U S A***. (1995), 92:10267-10271.

Tiuman TS, Santos AO, Ueda-Nakamura T, Filho BP, Nakamura CV. Recent advances in leishmaniasis treatment. ***Int J Infect Dis***. (2011), 15:e525-532.

Tiwari K, Dubey VK. *Leishmania donovani* asparaginase variants exhibit cytosolic localization. ***Int J Biol Macromol***. (2018), 114:35-39.

Towbin H, Staehelin T, Gordon J. Electrophoretic transfer of proteins from polyacrylamide gels to nitrocellulose sheets: procedure and some applications. ***Proc Natl Acad Sci U S A***. (1979), 76:4350-4354.

Toyoda T, Suzuki K, Sekiguchi T, Reed LJ, and Takenaka A. Crystal structure of eukaryotic E3, lipoamide dehydrogenase from yeast. ***J. Biochem***. (1998), 123:668–674.

Tretter L and Adam-Vizi V. Generation of reactive oxygen species in the reaction catalyzed by alphaketoglutarate dehydrogenase***. J. Neurosci.*** (2004), 24:7771–7778.

Tretter L, Adam-Vizi V. Alpha-ketoglutarate dehydrogenase: a target and generator of oxidative stress. ***Philos Trans R Soc Lond B Biol Sci.*** (2005), 360:2335-45.

Turner SR, Ireland R and Rawsthorne S. Cloning and characterization of the P subunit of glycine decarboxylase from pea (*Pisum sativum*). ***J. Biol. Chem***. (1992), 267:5355–5360.

Turrens JF and Boveris A. Generation of superoxide anion by the NADH dehydrogenase of bovine heart mitochondria. ***Biochem. J***. (1980), 191:421–427.

Twining W. Observations on diseases of the spleen particularly on the vascular engorgement of that organ common in Bengal. ***Trans Med Phys Soc Bengal***. (1827), 3:351–412.

Veras P, Brodskyn C, Balestieri F, Freitas Ld, Ramos A, Queiroz A, Barral A, Beverley S, Barral-Netto M. A dhfr-ts- *Leishmania major* knockout mutant cross-protects against *Leishmania amazonensis*. ***Mem Inst Oswaldo Cruz.*** (1999), 94:491-496.

Vickers TJ, Beverley SM. Folate metabolic pathways in Leishmania. ***Essays Biochem***. (2011), 51:63-80.

Walker JL, Oliver DJ. Glycine decarboxylase multienzyme complex. Purification and partial characterization from leaf mitochondria. ***J. Biol. Chem***. (1986), 261:2214-2221.

Walker PS, Scharton-Kersten T, Rowton ED, Hengge U, Bouloc A, Udey MC, Vogel JC. Genetic immunization with glycoprotein 63 cDNA results in a helper T cell type 1 immune response and protection in a murine model of leishmaniasis. ***Hum Gene Ther***. (1998), 9:1899-1907.

Wang YC, Wang ST, Li C, Chen LY, Liu WH, Chen PR, Chou MC, Liu TC. The role of amino acids T148 and R281 in human dihydrolipoamide dehydrogenase. ***J Biomed Sci***. (2008), 15:37-46.

Wang YC, Wang ST, Li C, Liu WH, Chen PR, Chen LY, Liu TC. The role of N286 and D320 in the reaction mechanism of human dihydrolipoamide dehydrogenase (E3) center domain. ***J Biomed Sci.*** (2007), 14:203-210.

Webb B, Sali A. Comparative Protein Structure Modeling Using MODELLER. CurrProtoc ***Bioinformatics***. (2016), 54:5.6.1-5.6.37.

Weigle KA, de Davalos M, Heredia P, Molineros R, Saravia NG, D'Alessandro A. Diagnosis of cutaneous and mucocutaneous leishmaniasis in Colombia: a comparison of seven methods. ***Am J Trop Med Hyg***. (1987), 36:489-496.

Williams CH, Jr. Flavin containing dehydrogenases: in Enzymes (Boyer, P., ed.), 3rd ed., (1976), 13:89-173, Academic Press, New York, New York.

Wyllie S and Fairlamb AH. Differential toxicity of antimonial compounds and their effects on glutathione homeostasis in a human leukaemia monocyte cell line. ***Biochemical Pharmacology***. (2006), 71:257–267.

Wyllie S, Cunningham ML, and Fairlamb AH. Dual action of antimonial drugs on thiol redox metabolism in the human pathogen *Leishmania donovani*. ***Journal of Biological Chemistry***. (2004), 279:39925–39932.

Xu M, Kitaura Y, Ishikawa T, Kadota Y, Terai C, Shindo D, Morioka T, Ota M, Morishita Y, Ishihara K, Shimomura Y. Endurance performance and energy metabolism during exercise in mice with a muscle-specific defect in the control of branched-chain amino acid catabolism. ***PLoS One***. (2017), 18, 12:e0180989.

Yan S, Li F, Ding K, and Sun H. Reduction of pentavalent antimony by trypanothione and formation of a binary and ternary complex of antimony (III) and trypanothione. ***Journal of Biological Inorganic Chemistry***. (2003), 8:689–697.

Yeaman SJ, Hutcheson ET, Roche TE, Pettit FH, Brown JR, Reed LJ, Watson DC and Dixon GH. Sites of phosphorylation on pyruvate dehydrogenase from bovine kidney and heart. ***Biochemistry.*** (1978), 17:2364–2370.

Yi J, Nemeria N, McNally A, Jordan F, Machado R, and Guest JR. Effect of substitutions in the thiamin diphosphate-magnesium fold on the activation of the pyruvate dehydrogenase complex from Escherichia coli by cofactors and substrate. ***J. Biol. Chem.*** (1996), *271*:33192-33200.

Yoshida T and Kikuchi G. Major Pathways of glycine and serine catabolism in various organs of the rat and cock. ***J. Biochem***. (1973), 73:1013–1022.

Zhou Y, Messier N, Ouellette M, Rosen BP, and Mukhopadhyay R. *Leishmania major* LmACR2 is a pentavalent antimony reductase that confers sensitivity to the drug Pentostam. ***Journal of Biological Chemistry***. (2004), 279:37445–37451.

PUBLICATIONS

1. **Chiranjivi AK**, Dubey VK. Dihydrolipoamide dehydrogenase from *Leishmania donovani*: New insights through biochemical characterization. ***Int J Biol Macromol.*** (2018); 112: 1241-1247. **(*IF*: 4.78)**

2. **Chiranjivi AK**, Saha G, Chandra P, Dubey VK. Mutational study of *Leishmania donovani* Dihydrolipoamide dehydrogenase (LdBPK291950.1): To Investigate their role in catalytic process. **(Communicated).**

3. Bhardwaj R, Das M, Singh S, **Chiranjivi AK**, Prabhu SV, Singh SK, Dubey VK. Evaluation of CAAX prenyl protease II of *Leishmania donovani* as potential drug target: Infectivity and growth of the parasite is significantly lowered after the gene knockout. ***Eur J Pharm Sci.*** (2017); 102:156-160. **(*IF*: 3.53)**

4. Bhalla P, Sultana S, **Chiranjivi AK**, Saikia AK, Dubey VK. Synthesis and Evaluation of Methyl 4-(7-Hydroxy-4, 4, 8-Trimethyl-3-Oxabicyclo [3.3.1] Nonan-2-yl) Benzoate as an Antileishmanial Agent and Its Synergistic Effect with Miltefosine. ***Antimicrob Agents Chemother.*** (2018); 62, pii: e01810-0181017. **(*IF*: 4.71)**

5. Prakash J, Yadav S, Saha G, **Chiranjivi AK**, Kumar S, Sasidharan S, Saudagar P, Dubey VK. Episomal expression of human glutathione reductase (HuGR) in *Leishmania* sheds light on evolutionary pressure for unique redox metabolism pathway: Impaired stress tolerance ability of *Leishmania donovani.* ***Int J Biol Macromol***. (2019), 121:498-507. **(*IF*: 4.78)**

6. Baranwal A, **Chiranjivi AK**, Kumar A, Dubey VK, Chandra P. Design of commercially comparable nanotherapeutic agent against human disease-causing parasite, *Leishmania*. ***Sci Rep.*** (2018), 8:8814. **(Nature Publishing Group) (*IF*: 4.01)**

7. Saha G, **Chiranjivi AK**, Khamar MB, Kumar M, Dubey VK**.** BLIMP-1 dependent downregulation of TAK1 and P^{53} molecules is responsible for resisting pathogen clearance during *Leishmania* infection. (**Communicated**)

CONFERENCE PROCEEDINGS AND WORKSHOP

1. **Adarsh Kumar Chiranjivi,** Vikash Kumar Dubey. Role of Dihydrolipoamide dehydrogenase (LdBPK323510.1, LdBPK291950.1) in growth and survival of *Leishmania donovani*. 1st International Conference on Biotechnology and Biological Sciences (BIOSPECTRUM 2017) held at University of Engineering and Management Kolkata, India, 25th -26th August 2017.

2. **Adarsh Kumar Chiranjivi,** Vikash Kumar Dubey. Variants of Dihydrolipoamide dehydrogenase: Investigating their kinetic behavior and their role in physiology of *Leishmania donovani.* 58th Annual Conference of Association of Microbiology of India (AMI 2017) held at Babasaheb Bhimrao

Ambedkar University Lucknow, Uttar Pradesh, India, 16th-19th November 2017.

3. **Adarsh Kumar Chiranjivi,** Vikash Kumar Dubey. Site directed mutagenesis of *Leishmania donovani* dihydrlipoamide dehydrogenase (*Ld*DLDH29): To investigate the role of Cys-15, Cys-38, Ala-48, Asp-49 and Ala-54 in regulation of catalytic activity.RABEB2019 held at School of Biochemical Engineering IIT-BHU, Varanasi, Uttar Pradesh, India, 15th - 16th March 2019.

4. **Adarsh Kumar Chiranjivi.** Actively participatedin9th TCS Annual Event & Flow Cytometry Workshop on "Flow Application in Basics, Applied and Clinical Biology" organized by Department of Biosciences and Bioengineering, IIT Guwahati, Guwahati, Assam, India, 3rd-5th November 2016.

5. **Adarsh Kumar Chiranjivi.** Actively participated "Training Program on Confocal Laser Scanning Microscopy" organized by Guwahati Biotech Park, Guwahati, Assam, India.

6. **Adarsh Kumar Chiranjivi.** Actively participated in "Advances in Computational Biology and Computer Aided Drug Design" organized by Bioinformatics Infrastructure Facility (BIF), Department of Biosciences and Bioengineering, IIT Guwahati, Guwahati, Assam, India, 24th-26th June 2015.

7. **Adarsh Kumar Chiranjivi**, Vikash Kumar Dubey*.Role of Dihydrolipoamide dehydrogenase (LdBPK 323510.1, LdBPK 291950.1) in growth and survival of *Leishmania donovani.* Research conclave'17 held at IIT Guwahati. Assam, India. March 16-19, 2017.

8. **Adarsh Kumar Chiranjivi**, Vikash Kumar Dubey*. Cloning, expression, purification and characterization of Dihydrolipoamide dehydrogenase (DLDH) from *Leishmania donovni*. Research conclave'16 held at IIT Guwahati. Assam, India. March 17-20, 2016.